

ETCHING AND CHARACTERIZATION OF MICROELECTRONIC FILMS
AND INTEGRATED CIRCUITS

THESIS

Presented to the Graduate Council of
Southwest Texas State University
in Partial Fulfillment of
the Requirements

For the Degree

Master of Science

By

Matthew L. Langendorf, B.S.B.A.

San Marcos, Texas
May, 2001

COPYRIGHT

by

Matthew L. Langendorf

2001

I would like to dedicate this thesis to my wife, Stasi Gaveras, for encouraging me and convincing me to believe in myself; to my mother Virginia who always believed in me and; to my father Lew who sees this was my true calling.

ACKNOWLEDGEMENTS

I would like to thank Dr. Carlos J. Gutierrez, for his support and direction throughout this effort. His flexibility around subject matter and his ideas have been of inestimable value. I would like to thank Drs. Crawford and Galloway, for had it not been for that first fateful meeting I never would have become a physicist. Their confidence in my abilities will always be remembered. I'd like to thank my fellow students particularly Albert Tijerina who helped me work through some of the most difficult material one could encounter. I'd like to thank Dr. Daniel Chesire (Lucent Technologies Inc.) and Dr. Steven Hughes (Motorola Inc.) for thin film materials and other materials, supplies and equipment provided; Mr. Kent Erington and Dr. Lecia Khor (Cirrus Logic, Inc.) for materials, guidance and support; and Drs. Jim Crawford and Greg Spencer for being on my thesis committee and for their comments and suggestions regarding this effort. I want to thank my daughter Katy, for giving up so many things over the last four years and for thinking it was cool that her dad was going to be a scientist. Finally I'd like to thank my wife Stasi, for her love and her undying support of my academic efforts. Without both I surely would not be here. She has been a positive force in my life throughout and deserves much of the credit for this work.

TABLE OF CONTENTS

LIST OF TABLES	viii
LIST OF FIGURES	ix
1 INTRODUCTION	1
1.1 THE IMPORTANCE OF THE ETCHING PROCESS IN THE MICROELECTRONICS INDUSTRY	1
1.2 OVERVIEW OF EXPERIMENTS, WORK AND PHYSICAL CHARACTERIZATION METHODS USED	7
1.3 THESIS PROJECT GOALS	9
2 ETCHING THEORY, TECHNIQUES AND APPLICATIONS	11
2.1 ETCHING APPLICATIONS	11
2.1.1 DEVICE FABRICATION OVERVIEW	11
2.1.2 DEVICE DEPROCESSING	15
2.1.3 ETCH CHARACTERISTICS	17
2.2 CHEMICAL ETCHING THEORY	19
2.2.1 REACTION THERMODYNAMICS	21
2.2.2 REACTION KINETICS	23
2.2.3 WET ETCHING	27
2.3 PHYSICAL ETCHING THEORY	29
2.3.1 PLASMAS AND GLOW DISCHARGES	30
2.3.2 HALOGEN CHEMISTRIES	37
2.3.3 REACTIVE ION ETCHING	40
2.3.4 FOCUSED ION BEAM MILLING	47
2.4 ETCHING TECHNIQUES	52
2.4.1 SILICON NITRIDE	52
2.4.2 SILICON DIOXIDE	58
2.4.3 POLYSILICON	63
2.4.4 METALS	65
3 CHARACTERIZATION METHODS	68
3.1 OPTICAL REFLECTIVITY	68
3.2 OPTICAL MICROSCOPY	77
3.3 SCANNING ELECTRON MICROSCOPY	79

4	SAMPLE DATA AND ANALYSIS	87
4.1	WET ETCH EXPERIMENTS	87
4.1.1	DESIGN	87
4.1.2	Si ₃ N ₄ DATA AND ANALYSIS	88
4.1.3	SiO ₂ DATA AND ANALYSIS	103
4.2	FAILURE ANALYSIS	109
4.2.1	DIE REMOVAL AND DEPASSIVATION	109
4.2.2	TOP DOWN DEPROCESSING	114
4.3	CROSS SECTIONING	121
4.3.1	MANUAL METHOD	121
4.3.2	FIB METHOD	124
4.4	SEM IMAGING	127
5	CONCLUSION	141
	APPENDIX A NANOMETRICS AFT 210 OPERATIONS	144
	APPENDIX B PROPOSED EXPERIMENTAL PROTOCOL	146
	APPENDIX C WET ETCH RECIPES FOR FAILURE ANALYSIS.....	149
	APPENDIX D CHEMICAL SAFETY	152
	BIBLIOGRAPHY	154
	VITA	156

LIST OF TABLES

Table 2.1 Some common thin films and associated dry etch chemistries.	38
Table 2.2 RIE Operating Parameters and Characteristics	45
Table 2.3 Wavelength emission of some common dry etch methods for endpoint detection.	46
Table 2.4 Summary of Preparation Techniques for Si ₃ N ₄ Films.....	53
Table 2.5 Etch rates of silicon nitride.....	54
Table 4.1 Data table for phosphoric etch A.	92
Table 4.2 Data table for phosphoric etch B.	93
Table 4.3 Data table for phosphoric etch C.	94
Table 4.4 Data table for phosphoric etch D.	95
Table 4.5 Data table for phosphoric etch E.	96
Table 4.6 Data table for phosphoric etch F.	97
Table 4.7 Nitride etch comparisons.....	101
Table 4.8 Data table for HF etch.	104
Table 4.9 Colors associated with oxide thickness.....	117

LIST OF FIGURES

Figure 1.1 Moore's Law representation.	3
Figure 1.2 Comparison of wet and dry etch isotropy.	7
Figure 2.1 NMOS Process Flow.	12
Figure 2.2 Typical isotropic etch process showing the etch bias.	19
Figure 2.3 A graphical representation of activation energies for a two step reaction: $H_2 + I_2 \rightarrow 2HI$	25
Figure 2.4 Potential energy diagrams showing the effect of a catalyst. The catalyst reduces the activation energy for the formation of the products. A catalyzed reaction typically occurs in several steps, each with its own barrier, but the over-all energy barrier is lower than the uncatalyzed reaction.....	26
Figure 2.5 Schematic of a DC glow discharge.....	34
Figure 2.6 Schematic view of microscopic processes occurring at the surface during etching.	35
Figure 2.7 Etch rate dependence on percent O_2 in the CF_4/O_2 mixture.....	39
Figure 2.8 Etch rates of silicon (solid line, round points), silicon dioxide (solid line, square points), and PMMA and AZ1350B resists (dashed lines) vs. percentage of H_2 in CF_4	40

Figure 2.9 Schematic representation of a parallel plate plasma etcher. .	41
Figure 2.10 An example of ARDE in silicon. Notice the wider trenches etch more rapidly.....	43
Figure 2.11 Silicon trench etch rate dependence on aspect ratio.	43
Figure 2.12 Cross section schematic of a Kaufman ion source.	47
Figure 2.13 Schematic diagram of a focused ion beam column.	50
Figure 2.14 Boiling point vs concentration.....	55
Figure 2.15 Etch rates of silicon, silicon dioxide, and silicon nitride in hot phosphoric acid.....	57
Figure 2.16 Etch rate of thermal oxide as a function of HF concentration.	61
Figure 2.17 Pictorials of edge profiles as a function of temperature and HF concentration.....	62
Figure 2.18 Contact/via fabrication.....	66
Figure 3.1 Ellipsometer	69
Figure 3.2 Reflection at an interface.	71
Figure 3.3 Reflection and transmission at two interfaces.	73
Figure 3.4 Optical path length difference given by line segment ABC. ...	74
Figure 3.5 The upper graphs show how R varies with film thickness,d. The bottom graph shows how R varies with index of refraction. In both cases $k=0$	75
Figure 3.6 General layout of an optical microscope operating in reflection mode.	78

Figure 3.7 Schematic of energy excitation volume profile.	84
Figure 3.8 Various energy transition events.....	84
Figure 4.1 The color changes associated with film thickness variations. Starting with the 2 minute etch in the upper left and moving right and top to bottom to the 10 minute etch in the lower right. The blue squares are spacers.	91
Figure 4.2 Die measurement locations.....	91
Figure 4.3 Run A including clean and etch details.	98
Figure 4.4 Run B including clean and etch details.	99
Figure 4.5 Run C including clean and etch details.	99
Figure 4.6 Run D including clean and etch details.....	100
Figure 4.7 Run E including clean and etch details.	100
Figure 4.8 Run F including clean and etch details.	101
Figure 4.9 HF etch run graph.	105
Figure 4.10 Optical view of HF etch artifacts at 50X. Color variations suggest unetched oxide.....	106
Figure 4.11 Magnification of artifacts at 10X.	107
Figure 4.12 (Top to bottom) Silicon, oxygen and carbon EDAX maps of the dome feature. Taken at 1500X, 5 keV, 67 degree tilt. Courtesy of Dr. Carlos Gutierrez and Mr. Mike Mathaeus.	108
Figure 4.13 Optical view of device after 700s depassivation at 10X.	111
Figure 4.14 Optical view of device after 1000s depassivation at 10X. ..	112

Figure 4.15 Optical image of an EOS induced failure at 100X. 113

Figure 4.16 Metal 1 lines (brown) run vertically on the right while
remnants of metal 2 barrier run horizontally on the left..
Optical image at 125X. 115

Figure 4.17 Color variation of oxide over metal 2 layer as front
proceeds from right to left. 125X..... 116

Figure 4.18 Polishing front removing metal 1 as it proceeds from left
to right. 125X. 116

Figure 4.19 SEM image of EOS damage to the silicon substrate at
contact area. 119

Figure 4.20 Sem image of ESD damage to substrate in the gate area. . 119

Figure 4.21 SEM image of physically floating contacts around poly
gate structures. 120

Figure 4.22 The darkly outlined areas are p-doped regions over which
the gates were. The areas surrounding the contact
imprints are p-doped. Optical image at 300X. 123

Figure 4.23 A FIB cross-section showing 4 metal layers. 124

Figure 4.24 FIB top view of the above cross-section. The etch profile
gets deeper from bottom to top. 125

Figure 4.25 The same part cross-sectioned deeper. Notice the
rounding of the metal 4 lines due to the continued milling
while imaging. 125

Figure 4.26 Top and side views of the milling box and profile. 126

Figure 4.27 FIB cross-section image of a particle contaminant. The particle was in place prior to deposition of the passivation layers (top layer). It has impinged on the metal 1 and metal 2 layers resulting in a short. 128

Figure 4.28 A further FIB cut into the contaminant. The particle appears to be a piece of metal, most likely tungsten based on the metal lines being aluminum and the contrast between the particle and the lines..... 129

Figure 4.29 SEM image of substrate damage in the drain regions near the contact locations of an NMOS device. The delineated area running horizontally in the center is p-doped silicon over which the polysilicon gate existed. The damage was caused by a phenomenon known as bipolar snap-back; a low voltage, high current condition generating high temperatures which melt the silicon. 130

Figure 4.30 SEM image of over-etching which occurred during staining of a cross-section. for constructional analysis. The part was etched for 5 seconds in buffered oxide etch and 30 seconds in a 10:1:14 (HNO₃:HF:CH₃COOH). Both the interlevel dielectric and the active silicon areas have been nearly all etched away. 131

Figure 4.31 SEM image of a defective contact protruding up into the metal 1 line. The Ti/TiN cap over the metal lines can be clearly seen. 132

Figure 4.32 SEM image of a construction analysis cross-section of a 3 layer planarized metal device. The bottom shows clearly delineated n-wells on top of a grainy looking p-tub. These areas stain differently and the graininess is due to the chrome coating used for SEM prep. Shallow trench isolation oxide appears as square pads setting on the substrate. 133

Figure 4.33 SEM image of the passivation layer over two metal 4 lines shows the conformal coverage of the CVD deposition. 134

Figure 4.34 SEM image of metal 2 to metal 3 vias. The Ti underliner on the metal lines has been etched by the stain. The contrast between the Al metal lines and the W plugs is easy to see. 135

Figure 4.35 SEM image showing vertical streaks in the substrate; an artifact of polishing as tungsten is smeared in the direction of the polishing wheel rotation. Contacts to both active areas and poly (the short plug) can be seen and the lower left side shows a piece of a p-tub. 136

Figure 4.36 SEM image showing two transistors sharing a common drain. The gates are clearly delineated as are the nitride caps above them. The channel region under the gate is visible and the lightly doped drain (LDD) features appear as a curling up of the drain region ends. A set of stacked vias to the drain is shown as well.....137

Figure 4.37 SEM image showing shallow trench isolation of a pair of transistors. Slight over-etching provides good depth perspective as the etchant is highly selective to the interlevel dielectric (ILD) used above the active areas. It is likely a doped oxide and different from the ILD above metal 1 as evidenced by the minimal etching of that layer. Near the very bottom is the epi-layer boundary between the p^+ and p^- substrate.138

Figure 4.38 SEM image of etched area showing polysilicon lines (enclosed dark areas) and the nitride caps. The nitride sidewall spacers used to mask the LDD areas during the deep drain implant are slightly visible. The poly structures are sitting on top of field oxide made using shallow trench isolation. Taken with the help of Chris Maldonado-Cirrus Logic.....139

Figure 4.39 High magnification SEM image of the poly structure in figure 4.37 showing the sidewall spacers. Taken with the help of Chris Maldonado-Cirrus Logic.....140

CHAPTER 1

INTRODUCTION

1.1 THE IMPORTANCE OF THE ETCHING PROCESS IN THE MICROELECTRONICS INDUSTRY

In 1958, future cofounder of Intel Robert N. Noyce and Jack Kilby of Texas Instruments invented the integrated circuit; a series of interconnected transistors in a single device. With the advent of this technology, and its ability to perform multiple functions the world entered into a period of technological advancement unparalleled since the industrial revolution. In fact it was such a significant achievement that Kilby was awarded the Nobel Prize in 2000 (unfortunately Noyce had died so did not receive one as well).

In the last four decades sales of electronic products in the U.S. alone has increased thirtyfold to an estimated \$500 billion per year including some \$65 billion in IC sales while worldwide figures are now near \$1200 billion and \$170 billion respectively.¹ Concurrently the marginal cost of these devices has dropped drastically as device miniaturization has progressed at a rapid rate. For example the cost of a

memory circuit has gone from approximately \$10 in the late 1950's to less than a hundred thousandth of a cent currently.

The impetus to reduce device sizes was threefold. First, as more transistors and other devices can be fit onto a chip of a given size the less expensive it is to manufacture i.e. significant economies of scale accrue to the manufacturer. Second, as feature lengths get smaller device speeds increase which allows increased throughput. And third, power consumption decreases with smaller feature lengths resulting in lower energy requirements for device switching therefore lower heat buildup in the device. The upshot has been the fabrication of devices with current minimum feature sizes of 0.13 micron.

A corollary to this diminishing device size trend was summed up in 1965 when then head of Fairchild Semiconductor, Gordon E. Moore predicted that the number of transistors on a chip would roughly double every year. His prediction was so close that it would become known as Moore's Law, a benchmark recognized by the industry for nearly forty years. Over this time we have seen the number of devices on a single chip go from 50 to $\sim 10^7$. We now occupy the area on this growth curve known as ultra large scale integration or ULSI. Figure 1 gives a graphic representation of Moore's Law.¹ It is predicted that within the next decade we will start to deviate from this "law" as challenges, particularly in the area of photolithography, exceed the limits of current technology.

In the meantime however current process technology still has its roots in an idea conceived even prior to the integrated circuit.

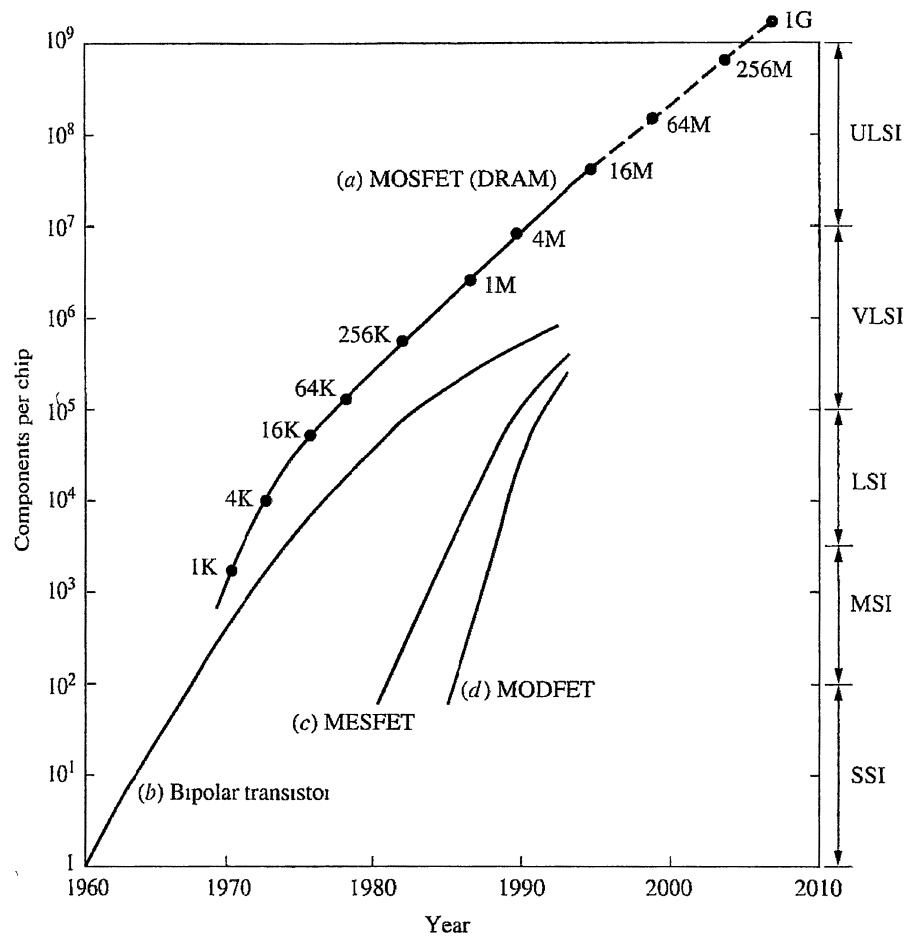


Figure 1.1 Moore's Law representation.¹

The pivotal development in the success of Noyce's integrated circuit was Jean Hoerni's development of a planar process of chipmaking in 1957.² This process provided a means of fabricating a multilayered structure on a silicon substrate. It consists of a number of different steps, which can be categorized into several areas as listed below.

- Chip design
- Patterning and photolithography
- Implant and diffusion
- Metal and dielectric film deposition
- Etching
- Interconnect

Following the chip design subsequent steps may be repeated many times over as a function of the number of layers in the design. Typically, patterning of the circuit one layer at a time begins with the photolithography process whereby a photosensitive polymer is spread over a piece of single crystal silicon with a thin layer of silicon dioxide on the surface. The polymer is exposed to UV light projected through a "mask" or reticle, which contains a specific layer or circuit pattern. Current technologies may have as many as 20 mask steps to produce a single integrated circuit. Cross-linking breaking in the exposed polymer areas results in hardening. Subsequent removal of the non-hardened areas then leaves a footprint of that layer on the substrate. Implants of dopants generate active areas in the unmasked substrate as the

hardened polymer acts as a barrier over the other areas. Following the creation of these active regions a series of thin film depositions serve to build up the layers on the device. Different layers include gate and field oxides, metallization lines, intermetal dielectrics, barrier metals and passivation layers.

As the fabrication process progresses, at times it becomes necessary to remove some of these deposited materials from certain areas. This is usually accomplished via a process known as etching (though a process known as chemical mechanical polishing is sometimes used). Etching is a process in which one or more chemical and/or physical interactions between atoms, ions or molecules and the surface occurs, resulting in the removal of material as required. It is also used extensively in deprocessing integrated circuits for failure or constructional analysis. Two common types of etching are used; wet etching and dry etching.

Wet etching involves contact between the die surface and liquid etchants. This can be accomplished by either spraying the surface of the die with the liquid or immersing the die into the liquid. Both have their advantages and disadvantages. Spraying has the advantages of 1) providing a continuous supply of fresh etchant to the die surface i.e., the etchant concentration is stable and 2) the spray carries reaction products away from the surface allowing maximum etching area to be maintained. Immersion has the benefit of being easier to conduct and

provides maximum contact between the surface and the etchant solution. The down sides are increased chemical usage and solution stagnation due to reaction product buildup. Wet etching has become a less favorable method in the ULSI era due to its isotropic character. This simply means that etch rates are nearly equal in all directions. This becomes problematic as aspect ratios of contacts get larger resulting in undercutting of features during wet etch processes. This will be explained in more detail in Chapter 2.

Dry etching relies on similar chemistries developed in wet methods however the reactive species are in the gas phase and these methods rely on the generation of a plasma in the form of a low level glow discharge. Several methods are employed the most common of which are plasma etching and reactive ion etching. Their primary benefit lies in the anisotropy of the etch.

Figure 1.2 shows the difference between wet and dry etch results.

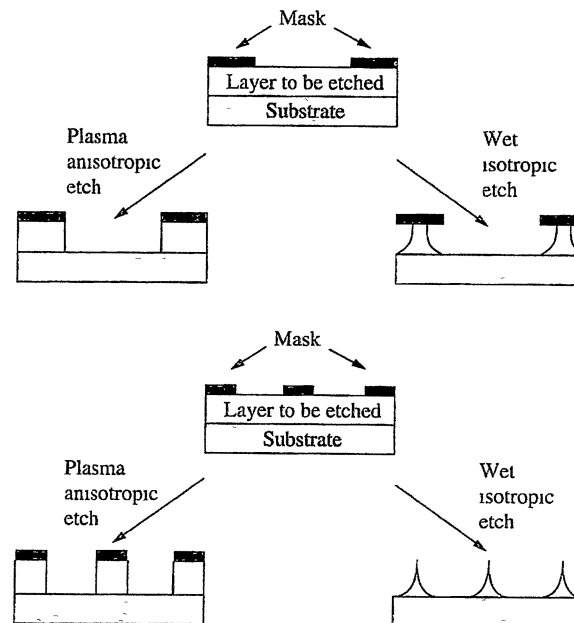


Figure 1.2 Comparison of wet and dry etch isotropy.³

1.2 OVERVIEW OF EXPERIMENTS AND PHYSICAL CHARACTERIZATION METHODS USED

Several wet etch protocols were carried out on both silicon dioxide (oxide) and silicon nitride (nitride) thin films in an effort to determine the effect on etch rates. Oxide films were etched using hydrofluoric acid at ambient temperatures and nitride films were etched using phosphoric acid at 153° C. Protocols varied based on differences in pre-clean protocols, bath agitation and etch time. In addition etch rates were explored and reported for other standard wet etch protocols. Additional

wet etching techniques were used in IC deprocessing to remove metals, dielectrics and polysilicon and in staining doped substrate areas. Dry etching using the reactive ion method was used in the removal of oxide, oxynitride and nitride passivation layers in integrated circuit deprocessing.

Physical characterization of a film or IC was carried out in several ways. Film thickness measurements in these experiments were done using optical reflectivity. This method relies on analysis of the interference pattern generated as a light wave reflects from both the surface and the film-substrate interface. It generally requires the films to be transparent so that some portion of the ray is transmitted to the interface. This works well for dielectric and non-metallic films. Knowing the corresponding indices of refraction of the film and substrate along with the interference data gathered allows for a reasonably accurate calculation of the film thickness. This will be discussed in more detail in Chapter 3.

In characterizing IC parts deprocessed for failure analysis, scanning electron microscopy (SEM), focused ion beam (FIB) techniques and optical imaging are frequently used. SEM imaging by secondary electrons was used for identifying various failure mechanisms resulting from physical defects as well as viewing the effects of electrical breakdowns such as electrostatic discharge (ESD) and electrical

overstress (EOS). FIB techniques were useful in cross sectioning of IC devices and imaging.

1.3 THESIS PROJECT GOALS

The goal of the thesis research is to investigate and physically characterize the results of certain wet and dry etch processes on various thin film materials used in integrated circuit fabrication and to test related protocols for deprocessing multilayered devices for failure analysis. Comparative tables were compiled where possible for different etch protocols for use as a source reference. Integrated circuit deprocessing methodologies are discussed in detail as they are not possible to perform without significant reliance on etching processes. In addition to the etch protocols required, layer by layer deprocessing will include focused ion beam cross-sectioning, SEM characterization and micrograph interpretation.

The experiments were carried out at the Southwest Texas State University Department of Physics and the Device Physics Lab at Cirrus Logic, Inc. (Austin, Texas). Thin film materials were provided by Motorola Inc. and Lucent Technologies and integrated circuit devices were provided by Cirrus Logic, Inc. Etching processes were carried out using cleanroom or trace metal grade chemicals and gases as listed in the text. Film thickness measurements were made on a Nanometrics AFT 210. Scanning electron micrographs were obtained with a JEOL

6350F with a Semicaps digital image capturing system. EDAX images were done by Mike Matheaus on SWT's Amray 1400 SEM. Focused ion beam work was done on an FEI Micrion 2100. Dry etching was done with a Trion Phantom reactive ion etcher. Optical images were obtained with a Zeiss Axiotron microscope equipped with a digital capture camera.

CHAPTER 2

ETCHING THEORY, TECHNIQUES AND APPLICATIONS

2.1 ETCHING APPLICATIONS

2.1.1 DEVICE FABRICATION OVERVIEW

Etching is a term used to describe the removal of a material from a surface by either physical or chemical means or both. This process is of widespread industrial importance, particularly in metallurgy and in the microelectronics industry. This thesis focuses on chemical etching in the microelectronics industry.

The etching process removes excess or unneeded materials as the layer by layer pattern transfer of an IC onto a die or wafer surface progresses. In order to get a clearer picture, consider a general overview of the fabrication process of an integrated circuit, particularly those steps which require some form of etching. Figure 2.1 will aid in following along.

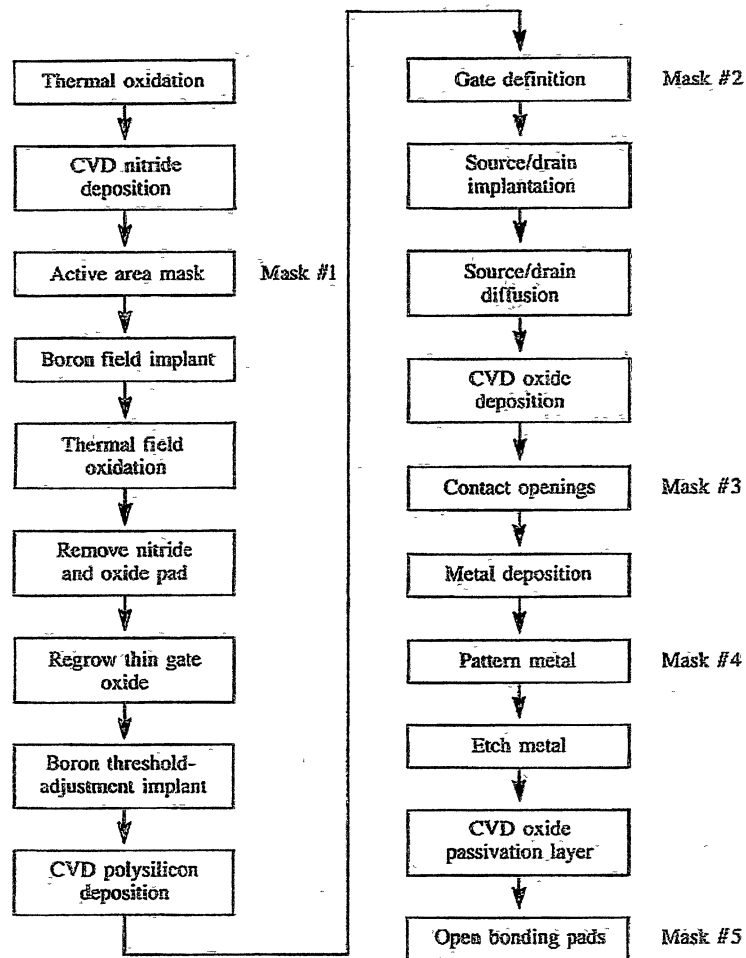


Figure 2.1. NMOS Process Flow.³

An IC is comprised of large numbers of transistors, capacitors and other components located on a silicon substrate die. The stacking technique mentioned previously makes it possible to fabricate these components on the die in a multi-layered configuration. For general MOS devices the process begins with a single crystal silicon wafer. The first step is the growth of a layer of thermally grown silicon dioxide

referred to as the field oxide. It will serve to isolate the electrically active regions of the individual components from each other. Since current design rules in ultra-large scale integration (ULSI) call for feature sizes in the deep sub-micron range (meaning that the length of the transistor channel or "gate" $\ll 1.0\mu\text{m}$) the component density on a die is quite high. Consequently the most widely used method of creating the field oxide is shallow trench isolation. Trenches are etched into the bare silicon followed by a CVD oxide deposition into the trenches and over the die surface. Chemical mechanical polishing, which is a form of etching, is then used to planarize the surface. Lower density technologies rely on the LOCOS or local oxidation of silicon method of fabricating field oxides which requires the use of a silicon nitride mask to create oxidation windows.

Following the oxidation the nitride mask is etched away leaving the non-planar isolation regions in the silicon. Next, ion implants into the unoxidized areas of silicon are accomplished by using photoresist, an organic polymer, to mask off around the implant areas and driving high dose dopant ions through the windows into the silicon. Etching again is used to remove the remaining photoresist masks. The gate oxide and polysilicon gate are now deposited across the entire wafer surface followed by another mask applied to the area where the transistor gate will be. The unneeded oxide and polysilicon are then etched away.

Another layer of oxide is deposited on the die, which at this stage is not flat. The gate structures are higher than the rest of the surface, which results in a bowing of the oxide deposited on the sidewall of the gate. This in fact is desirable and forms the sidewall “spacers” when the other oxide is etched using a dry etch process. Titanium is next deposited over the entire wafer forming titanium silicide (TiSi_2) over the exposed active regions. These form the pads for the electrical contacts. The remaining unreacted titanium is removed by a wet etch process. A thick interlayer dielectric (ILD) oxide is deposited over the die surface which will isolate the metal contacts from each other and then a dry etch is used to open the holes for the tungsten contacts down to the silicide pads. Following another titanium deposition to line the contact holes tungsten is deposited over the surface then polished back to form the contacts. A sandwiched layer of titanium, aluminum, titanium and titanium nitride is then deposited over the die, masked and etched to form the first metal layer.

For multilayer devices an ILD is required between each layer hence the etching and deposition processes are also repeated for the contact vias and upper layer metal lines. Finally, passivation layers are deposited on top of the completed circuit to insure electrical isolation and protection from environmental issues and contaminants. As can be seen from this discussion, etching is a necessary step at several points in the

fabrication process. It also plays a vital role in the deprocessing of electronic devices.

2.1.2 DEVICE DEPROCESSING

The deconstruction or deprocessing of a device is a routine function in the microelectronics industry. Often times following the failure of a device the manufacturer will conduct extensive electrical testing to isolate the location of a failure. It is then necessary to determine the cause of that failure. This usually requires the physical deprocessing of the part. Various etching methodologies are used in this process as well. Requirements for physical deprocessing can vary from job to job and may include any or all of the following steps.

- Decapsulation involves exposure of the die surface by removing part of the packaging material yet maintaining the electrical operation of the device. This requires insuring that the lead frame, bond pads and bond wires remain intact.
- Unpackaging involves complete removal of the die from the packaging material. The method used is dependent on the type of material used in packaging. These include plastics, ceramics and other polymers.
- Depassivation is the removal of the passivation layer(s) of the device. There are often two passivation layers, the topmost being silicon nitride or silicon oxynitride with the inner layer being some type of doped silicon dioxide.

- Mechanical polishing can be used to quickly remove several layers or to finely polish a surface for inspection in a high resolution scanning electron microscope.
- Wet etching techniques are used for gross removal of dielectric, metal and polysilicon films and for staining out doped epitaxial silicon. Etchants are also used to highlight or “decorate” different types of defects in silicon devices.
- Dry etching processes are used for highly anisotropic (and somewhat selective) etching to expose specific layers or features without removing the layers.
- Ion beam milling is used to cross-section a device leaving all stacked layers intact. This is a form of etching that relies on physical processes only rather than chemical or both to remove material. Consequently it will be included for further discussion.

Deprocessing is also conducted on competitor parts analyses where a chip designer/manufacturer, interested in protecting itself from patent infringement by a competitor, will cross section the competitor’s part, polish it and stain it and use SEM images to measure critical dimensions. This allows for direct comparison to their own design rules and ultimately a determination of whether infringement has in fact occurred.

In either case, the need for well-developed and consistently applied etching methodologies is of paramount importance. The remainder of this chapter will address several of these at length.

2.1.3 ETCH CHARACTERISTICS

There are several application and process dependent parameters to consider in developing and/or selecting an etch methodology. They are etch rate, uniformity, selectivity and anisotropy. These characteristics define how well the etchant and/or process is suited to removing a specific material. It must also be consistent with other requirements of the fabrication or failure analysis processes including process integrity issues, thermal budget considerations, time constraints, safety considerations and by-product disposal issues.

The idea of etch rate is conceptually straightforward. It is complicated by many factors so discussion of it will occur under specific processes throughout this paper. For now note that it is measured in $\text{\AA}/\text{min}$.

Throughout the fabrication process, any given etch step will most likely involve a substrate composed of several materials only one of which is to be removed. This introduces additional restrictions on the etch chemistries as now the etchant must be able to remove the material of interest at a reasonably fast and controllable rate, but leave the other materials intact. The ability of an etchant to accomplish this is called selectivity. It is defined as the ratio of the etch rates of the various

materials.⁴ A certain process may be quoted as having an etch selectivity of 15 to 1 for nitride over oxide, meaning the nitride etches 15 times faster than the oxide.

Another parameter is etch uniformity. It is used to describe and compare the etch rate at different points on a wafer as well as from wafer to wafer. It is measured as a percent variation from one to the other. This is a critical metric in the fabrication process. First in terms of ensuring that feature thicknesses are consistent across a single wafer to minimize inactive devices and second to ensure product consistency across wafers and wafer batches (yield issues).

The last parameter is etch anisotropy. Etching is said to be isotropic if the process etches equally in all directions. This means the lateral etch rate, R_L , is equal to the vertical etch rate, R_V . Etch anisotropy then describes the extent to which a process deviates from this and can be calculated as

$$A = 1 - R_L / R_V$$

In many etch steps throughout the fabrication process, it is desirable to have anisotropic etching. For instance, during the shallow trench isolation process, trenches are etched into the silicon substrate through windows in the photoresist mask. In order to create straight sidewalls on the trenches, the etchant must etch with a higher vertical etch rate than lateral etch rate, i.e. $R_V > R_L$. In fact, it would be most desirable for R_L to equal 0 guaranteeing a perfectly vertical sidewall.

While this is intuitively impossible, some etch processes can at least generate $R_V \gg R_L$ giving nearly vertical sidewall profiles. The above equation shows, as R_L goes to 0, A goes to 1 so a perfectly anisotropic etch gives $A = 1$ and a perfectly isotropic etch gives $A = 0$. Another way of viewing anisotropy is in terms of the etch bias. In Figure 2.2 below, the etch bias is the distance between the optimal sidewall location (directly below mask edge) and actual location. Etch bias is commonly known as “undercutting.”

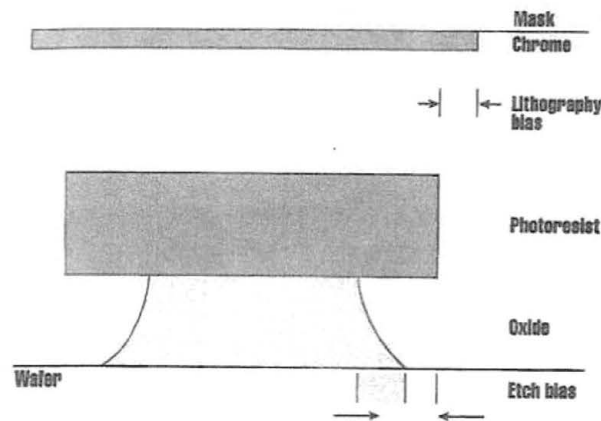


Figure 2.2 Typical isotropic etch process showing the etch bias.⁴

In general, wet etching methods result in highly selective isotropic etching while dry etching methods are somewhat less selective, but anisotropic. The reasons for this are discussed below.

2.2 CHEMICAL ETCHING THEORY

The first step in identifying an etch process is to understand the properties of the material to be removed and in particular its chemical

reactivity. Chemical reactivity is determined by the molecular or atomic structure of the material. Properties of elemental materials can be understood in the context of their electron configurations. The outermost valence shell of an atom will, in keeping with the “octet rule”, either give up or receive enough electrons to complete the shell. Any valence shell will hold up to eight electrons (with the exception of the *K* shell). Atoms with full valence shells are very unreactive due to high binding energies. These elements are the noble or inert gases and are located to the far right of the periodic table. Due to their non-reactivity, they are used in many etching and deposition processes where they are ionized and used to bombard target surfaces to remove materials. Argon is the most commonly used.

The most reactive elements are typically those needing to either gain or lose one electron to complete the valence shell. These include the Group I and Group VII elements respectively. Group VII elements are the halogens, three of which are used often in etch processes, fluorine, chlorine and bromine. They are highly reactive. The Group I elements are also highly reactive and include sodium and potassium both of which have recognizable properties in the semiconductor industry.

Characterizing chemical reactions draws on two bodies of knowledge, reaction thermodynamics and reaction kinetics. Both are necessary to assess the viability of a particular etching strategy.

2.2.1 REACTION THERMODYNAMICS

Reaction thermodynamics deal with energy/mass balances and equilibrium. It is important in the development of etch chemistries in that it determines two critical things. First, it will determine whether or not the reaction is spontaneous, i.e., will it proceed without adding energy to the system. This is particularly relevant in that minimizing the thermal budget at all stages of the fabrication process is quite important. Excessive heat in processes can cause unwanted diffusion of dopants in previously profiled active regions and migration of impurities that may cause killing defects on a wafer. Second, it will determine the extent of the reaction, i.e., assuming constant temperature and pressure (usually the case in both wet and dry etch processes), does the equilibrium point lie closer to the product or reactant side of the equation at a given point in the process.

Both of these concepts are related to the intrinsic thermodynamic properties of enthalpy (H) and Gibb's free energy (G). While an extensive treatment of these properties is beyond the scope of this thesis, some general background is required. Intrinsic energy states of a system can not be measured directly, however, measuring changes in these states is possible. These are referred to as ΔH and ΔG respectively. The change in enthalpy, ΔH , is basically the heat energy generated in various ways. It is a useful concept in determining whether a chemical reaction requires or generates heat as it proceeds.

It can be summarized as:

$$\Delta_r H = \Delta H_{\text{products}} - \Delta H_{\text{reactants}}$$

$$\Delta_r H < 0 \Rightarrow \text{reaction is exothermic}$$

$$\Delta_r H > 0 \Rightarrow \text{reaction is endothermic}$$

Here $\Delta_r H$ is the enthalpy of reaction and $\Delta H_{\text{products}}$ and $\Delta H_{\text{reactants}}$ are determined by summing the bond formation energies for the reactants and products.⁵ Again, this is important in thermal budget considerations and process design.

The Gibbs free energy of reaction, $\Delta_r G$ is a bit more complicated. It is defined thermodynamically as

$$\Delta_r G = \Delta_r H + T \Delta_r S$$

where an additional energy component, entropy (S) is included. Entropy is the measure of disorder in the system and cannot be ignored particularly at high temperatures where it dominates the free energy.⁵ Since a system, a reaction in our case, always tends toward lower energy (or higher entropy) a negative change in free energy will be thermodynamically favored. This translates to

$$\Delta_r G < 0 \Rightarrow \text{reaction is spontaneous}$$

$$\Delta_r G > 0 \Rightarrow \text{reaction is not spontaneous}$$

Furthermore, since the free energy of the system is dependent on the amount of reactant and product in the mixture, the extent of the reaction

can be determined. This is more germane to wet etching since products build up in the reaction mixture.

2.2.2 REACTION KINETICS

The second and arguably most important subject governing chemical reactions is reaction kinetics. The primary metric used in comparing etch methodologies is the etch rate. The etch rate is driven by the rate of reaction between the etchant and substrate. Reaction rates are a main focus of kinetic studies and can be quite complex. Quite often they are found to be proportional to the concentrations of the products, reactants or both and are defined by an empirically determined rate law. It expresses the rate as a function of the concentrations. As an example, consider some reaction



having the rate law

$$v = k [A] [B]$$

where the brackets around A and B imply their concentrations in moles per liter and k is the rate constant. [The rate constant is an important concept. It can only be determined empirically, is independent of concentrations and is temperature dependent.] This is a second order reaction, as determined by adding the exponents of [A] and [B], but is independent of the product concentration [C]. This is not always the case. The reaction order does not have to be an integral value and may depend on the product concentration if the reaction is reversible.

This is often the case for reactions carried out in the gas phase as typically occurs in dry etching processes. It is also important to note that most reaction rates increase as the temperature increases. This can be seen in empirical observations and is described mathematically by the Arrhenius equation

$$\ln k = \ln A - E_a/RT$$

$$\ln k = -\Delta G/RT$$

or

$$k = Ae^{-E_a/RT}$$

$$k = e^{-\Delta G/RT}$$

where k is the rate constant, A is the frequency factor, R is the gas constant, T is the absolute temperature, and E_a is the activation energy.

The second set of equations clearly shows the temperature dependence of the rate constant and hence, the reaction rate.

The concept of activation energy E_a is central to understanding how a reaction proceeds energetically. Kinetic transition theory attempts to explain this based on a potential energy barrier. It postulates that the free energy of a system must overcome some activation energy for the reaction to proceed. This can be seen graphically in Figure 2.3 for a multi-step reaction mechanism.

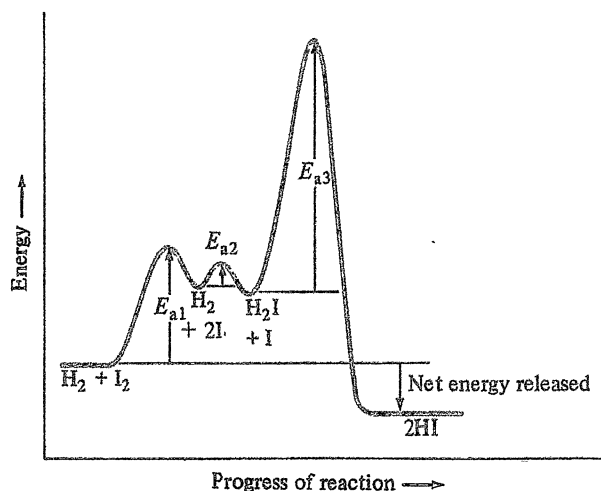


Figure 2.3 A graphical representation of activation energies for a two step reaction: $\text{H}_2 + \text{I}_2 \rightarrow 2\text{HI}$.⁶

The theory predicts the formation of a highly unstable activated complex in which the reactants are bound together and contain some amount of energy known as the threshold energy. Threshold energy is equal to the activation energy plus the internal energy of the reactants. This activated complex intermediate then decomposes by breaking and reforming new bonds to create the reaction products. Some reaction systems, however, do not have enough free energy to overcome this potential barrier. In these cases, energy in the form of heat must be added or a catalyst may be used to lower the activation energy (Figure 2.4). These are both possible strategies to explore in order to promote the desired reaction.

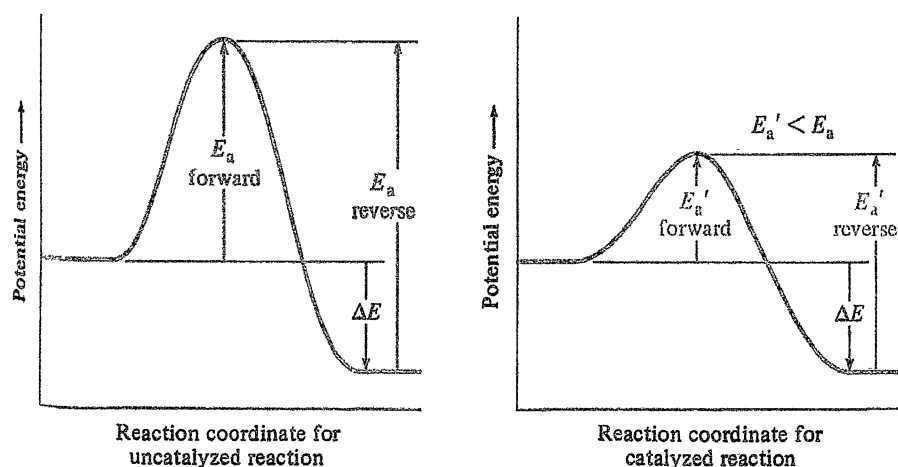
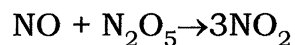
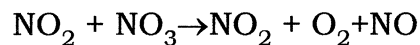


Figure 2.4 Potential energy diagrams showing the effect of a catalyst. The catalyst reduces the activation energy for the formation of the products. A catalyzed reaction typically occurs in several steps, each with its own barrier, but the over-all energy barrier is lower than the uncatalyzed reaction.⁶

Reaction kinetics are also used to determine any intermediate steps occurring over the course of a reaction. This is necessary to interpret the rate law data described above and to carry out thermodynamic calculations on heats of formation ($\Delta_f H$). A most critical concept here, however, is identifying the rate-determining step in a reaction. A typical chemical reaction is not usually fully characterized by its stoichiometric equation. In fact, it frequently occurs in multiple steps. For example, the decomposition of N_2O_5 proceeds through four steps.⁵ The stoichiometric equation is given by



The reaction mechanism proceeds in the following manner. Note that adding the equations results in the stoichiometric equation.



Now each intermediate step has a reaction rate associated with it, the slowest one of which will determine the overall reaction rate. This is a complicated empirical process and lies outside the scope, but it is easy to anticipate the complexity involved in developing etch processes involving numerous reaction intermediates since at each step the intermediates may have side reactions with other species.

2.2.3 WET ETCHING

Wet etching is a purely chemical process. The wafer or die surface is brought in contact with the etchant solution by either spraying or immersion. Three separate steps characterize the process. First, the etchant species must be moved to the die surface. Second, the chemical reaction must take place and third, the reaction products must be moved away from the die surface.⁴

For immersion methods these processes can be facilitated by agitation of the etch bath. This reduces the possibility of a stagnant layer containing high concentrations of reaction products shielding the

surface and thereby increases etch rates and improves uniformity. Note that an effective etch process requires the solubility of the reaction products in the etchant. Reaction products which are not soluble in the etching solution will redeposit on the die surface or build up in the solutions until the reaction reaches a state of dynamic equilibrium that inhibits further etching. Bath recirculation will help prevent this in immersion methods while spraying methods avoid this problem by providing a continuous supply of fresh etchant to the surface.

Another problem with immersion is the potential for particulate contamination at the air/solution interface. ULSI technologies demand tighter control of particulate contaminants to improve yields which is being addressed by improved filtration systems.⁴

Overall wet etching is not considered practical for $\leq 2 \mu\text{m}$ technologies. Etch rates often are reduced near feature edges as a result of uncontrollable bubbling of the reaction products. It is, however, used extensively in failure analysis for deprocessing where the most important requirements are etch rate and selectivity since destruction of die surfaces at other than the area of interest is usually inconsequential.

The wet etching of several materials is still industrially important. These include silicon nitride, silicon dioxide, polysilicon and some metals and are discussed further in section 2.4.

2.3 PHYSICAL ETCHING THEORY

In response to the inherent problems with wet etching alternative methods were sought which would support the move to larger scale integration. The response has been development of several dry etching technologies. These include ion beam etching, plasma etching, and reactive ion etching.¹ Ion beam etching relies solely on physical interactions between the beam and surface and relies on a plasma only to generate the ion beam. Plasma etching and reactive ion etching however both rely on plasmas for etching with the former being a purely chemical process and the latter hybrid of both processes.

The primary advantage of dry etch processes is the ability to control anisotropy. This does not mean that all plasma etching is anisotropic however. In fact, barrel etchers typically generate isotropic etch profiles since the reactive etchant ions are transported to the surface by diffusion. Consequently impingement occurs at angles other than near normal as is required to etch anisotropically. Other plasma-assisted methods such as reactive ion etching control incident angles to produce highly anisotropic profiles. In this way steep sidewall profiles in high aspect ratio features are consistently obtained without sacrificing much selectivity.

Anisotropy is attributable to physical processes taking place while selectivity is related to concurrent chemical processes. Since plasma based methods are most frequently used in fabrication environments, I

will consider them first followed by ion beam etching which is used frequently in failure analysis deprocessing.

2.3.1 PLASMAS AND GLOW DISCHARGES

As mentioned, generating a plasma is central to plasma and reactive ion etching. A plasma consists of a combination of charged and neutral atoms, molecules and electrons. Its overall charge is neutral, containing nearly equal amounts of positively charged ions and electrons. Some negatively charged ions may also exist in small amounts as discussed later. Plasmas most frequently used in ULSI applications are relatively weakly ionized (usually less than 10% of the particles are ionized) and are referred to as glow discharges.¹ The characteristics of a glow discharge are quite different however from a simple molecular or atomic gas that contains no charged species. It is subject to influence by electric and magnetic fields. While many of the processes occurring within a plasma-assisted etcher are not completely understood, the general properties of the glow discharge are well known.

A plasma is generated when voltage is applied across two electrodes, anode and cathode, between which is confined a low-pressure gas. The source may be either DC or AC (commonly referred to as RF since the frequency is 13.56MHz as designated by the FCC for scientific instrumentation). The gas is neutral overall but may contain some equally small numbers of positive ions and electrons generated by thermal energy, $k_B T$. In some cases a high voltage capacitor may be used

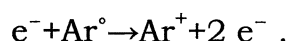
to strike an arc across the electrodes, exceeding the breakdown field of the gas and causing ionization.⁷ At sufficiently low pressures, the mean free paths of the particles are large enough to prevent significant recombination events within the confines of the gas. The positive ions will be accelerated toward the cathode and the free electrons will accelerate toward the anode. Upon striking the cathode, the ions will knock off electrons from the cathode material if their energy exceeds the binding energy of the electrons. These secondary electrons are then accelerated back toward the anode. As they traverse the area containing the gas and, providing the voltage is high enough, the electrons will undergo inelastic collisions with other neutral gas atoms resulting in impact ionization of the gas. These new ions then accelerate toward the cathode and the process repeats. At this point the plasma is self-sustaining and no longer requires the capacitive voltage arc.

This is a rather simplistic view of plasma generation. It implies the existence of some equilibrium between ion-electron pair production and recombination. And in fact these processes do take place in numerous ways as shown by the possible interactions between the charged species.

In The Materials Science of Thin Films (pages 108-109) Ohring⁷

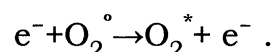
summarized these processes as follows:

- 1. Ionization.** The most important process in sustaining the discharge is electron impact ionization. A typical reaction is

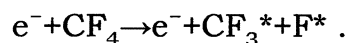


The two electrons can now ionize more Ar° , etc. By this multiplication mechanism the glow discharge is sustained. The reverse reaction, in which an electron combines with the positive ion to form a neutral, also occurs and is known as recombination.

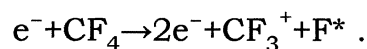
2. Excitation. In this case the energy of the electron excites quantitized transitions between vibrational, rotational, and electronic states, leaving the molecule in an excited state (denoted by an asterisk). An example is



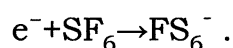
3. Dissociation. In dissociation the molecule is broken into small atomic or molecular fragments. The products (radicals) are generally much more chemically active than the parent gas molecule and serve to accelerate reactions. Dissociation of CF_4 for example, is relied on in plasma etching or film removal processes; i.e.,



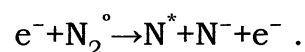
4. Dissociative Ionization. During dissociation one of the excited species may become ionized., e.g.,



5. Electron Attachment. Here neutral molecules become negative ions after capturing an electron. For example,



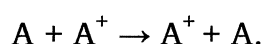
6. Dissociative Attachment.



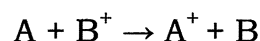
In addition to electron collisions, ion-neutral as well as excited or metastable-excited, and excited atom-neutral collisions occur.

Some generic examples of these reactions are as follows:

7. Symmetrical Charge Transfer.



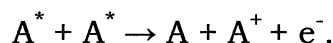
8. Asymmetric Charge Transfer.



9. Metastable-Neutral



10. Metastable-Metastable Ionization.



“Evidence for these uncommon gas-phase species and reactions has accumulated through real-time monitoring of discharges by mass as well as light emission spectroscopy. As a result, a remarkable picture of plasma chemistry has emerged. For example, a noble gas like Ar when ionized loses an electron and resembles Cl electronically as well as chemically. The fact that these species are not in equilibrium confounds the thermodynamic and kinetic descriptions of these reactions.”⁷

Before proceeding consider those steps above which result in the formation of an excited state species. Since it is not thermodynamically favorable for the atom to remain in this excited state, de-excitation or relaxation must occur. Recall that excitation results from one of more electrons absorbing energy and moving to a higher energy level. In the plasma, this occurs through momentum transfer associated with the inelastic collision between the atom and the free electron. Subsequent relaxation occurs spontaneously and results in light emission. This process is the source of the glow discharge that represented in Figure 2.5.

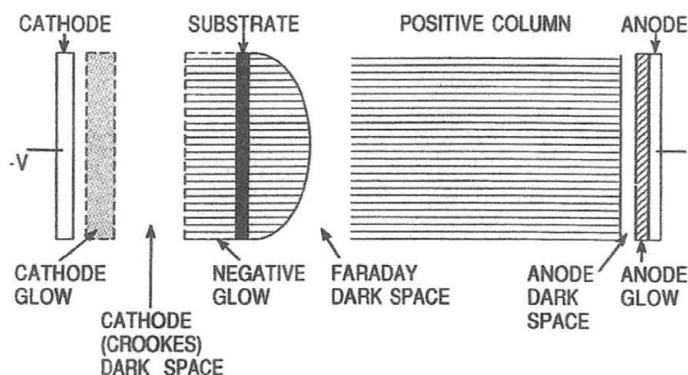


Figure 2.5 Schematic of a DC glow discharge.⁷

An RF discharge is slightly more complicated due to alternating charges on the electrodes. A complete description is not warranted here since the related etching characteristics are the same. The primary need for RF driven processes is in etching insulator materials such as oxides

and nitrides. When mounted on one electrode of a DC system, their high band gaps preclude generating the current needed to sustain the plasma.

It follows now that etching processes can be driven by plasmas when the material to be etched is placed on one of the electrodes and subjected to the physical and chemical processes specific to the etch chemistry. Figure 2.6 provides a schematic view of these processes at the die surface.

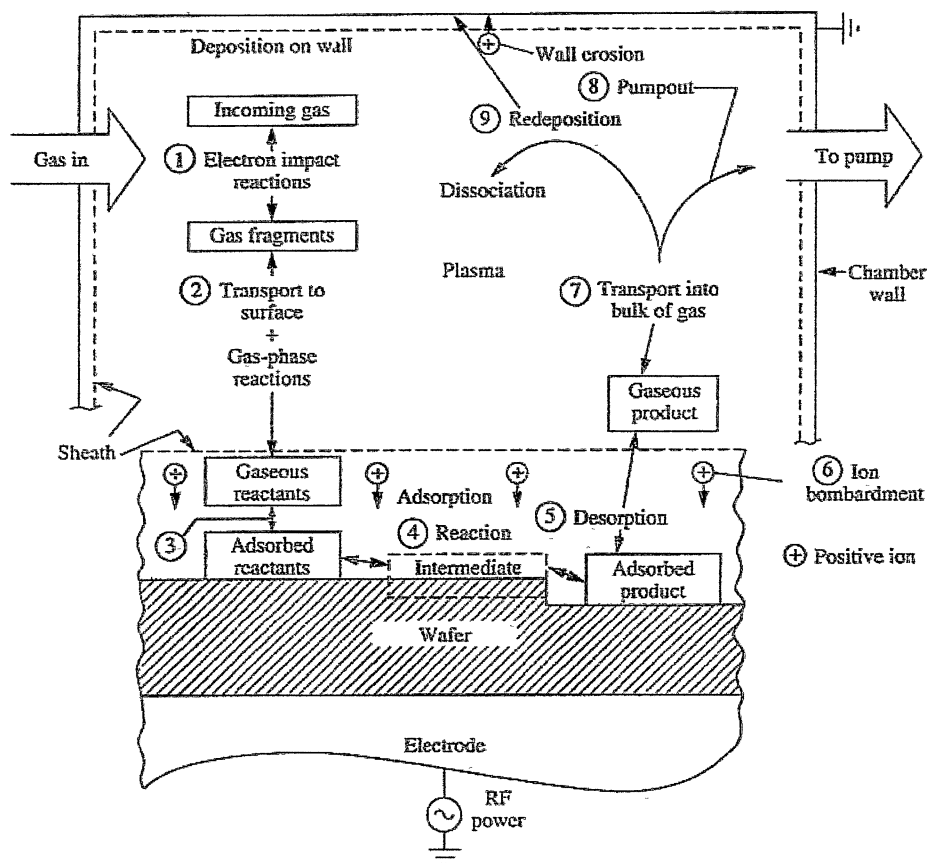


Figure 2.6 Schematic view of microscopic processes occurring at the surface during etching.¹

Physical etching occurs as a result of gas phase ion bombardment of the surface. The ions may be both reactive and non-reactive species which impinge on the surface with high enough energy to eject atoms of the matrix material from the surface. In order for the process to be highly anisotropic it is necessary that the angle of incidence be nearly normal. Lower angles of incidence can result in etching of the sidewalls.

It can be seen how physical etching exhibits poor selectivity. Since the ions are not chemically reacting with the surface etching is strictly a function of ion energy. If multiple materials are exposed, the only criteria differentiating the etch susceptibility is the binding energy of the matrix atoms. If the ion energy exceeds this binding energy, the atoms will be removed. This use of physical etching is seen in focused ion beam milling discussed later.

Chemical etching results when various reactive species in the plasma are transported to the surface and chemical reactions take place. These species can include charged ions as well as atomic and molecular radicals. As these gaseous reactants come into contact with the surface some will be adsorbed. Whether a specific particle is adsorbed or not is governed by statistical thermodynamics and reaction kinetics as discussed in sections 2.2.1 and 2.2.2 and is specific to the particular etch chemistry employed. Following adsorption, the species may react with surface (if it possesses sufficient energy to overcome the activation

energy) or it may desorb back into the gas mixture. (Recall that these species may also contribute to physical etching).

The reaction products generated must now desorb in order for chemical etching to continue. This requires that they have relatively high vapor pressures. If they do not desorb, the surface becomes shielded and continued etching ceases. Furthermore, the molecules must have high binding energies to insure they do not dissociate in the plasma but are pumped out of the reaction chambers.¹

Other interactions also occur, most notably those with the chamber walls including deposition, outgassing, and erosion which may have substantial consequences on the etch results. These are primarily design considerations that can be minimized by careful matching of equipment and chemistry. In combination with physical etch processes, these chemical processes form the basis for reactive ion etching.

2.3.2 HALOGEN CHEMISTRIES

While initial chemistries for dry etch processes were born out of traditional wet chemistries, the 1980's saw significant experimental research on the use of fluorine based chemistries.¹ The primary reason was the relatively high volatility and often non-toxic nature of the fluorine-silicon reaction products. Fluorine is the most reactive of the Group VII elements known as the halogens. This group also contains chlorine, bromine and iodine. Relative reactivities in the group are proportional to their electronegativity such that $F > Cl > Br > I$.⁶

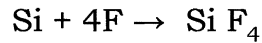
As can be seen in Table 2.1 fluorine, chlorine and, to a lesser extent, bromine are constituents of a variety of etch chemistries.

Table 2.1 Some common thin films and associated dry etch chemistries.⁴

Si	CF ₄ /O ₂ , CF ₂ Cl ₂ , CF ₃ Cl, SF ₆ /O ₂ /Cl ₂ , Cl ₂ /H ₂ /C ₂ F ₆ /CCl ₄ , C ₂ ClF ₄ /O ₂ , Br ₂ , SiF ₄ /O ₂ , NF ₃ , ClF ₃ , CCl ₄ , CCl ₃ F ₃ , C ₂ ClF ₅ /SF ₆ , C ₂ F ₆ /CF ₃ Cl, CF ₃ Cl/Br ₂
SiO ₂	CF ₄ /H ₂ , C ₂ F ₆ , C ₃ F ₈ , CHF ₃ /O ₂
Si ₃ N ₄	CF ₄ /O ₂ /H ₂ , C ₂ F ₆ , C ₃ F ₈ , CHF ₃
Organics	O ₂ , CF ₄ /O ₂ , SF ₆ /O ₂
Al	BCl ₃ , BCl ₃ /Cl ₂ , CCl ₄ /Cl ₂ /BCl ₃ , SiCl ₄ /Cl ₂
Silicides	CF ₄ /O ₂ , NF ₃ , SF ₆ /Cl ₂ , CF ₄ /Cl ₂
Refractories	CF ₄ /O ₂ , NF ₃ /H ₂ , SF ₆ /O ₂
GaAs	BCl ₃ /Ar, Cl ₂ /O ₂ /H ₂ , CCl ₄ /F ₂ /O ₂ /Ar/Hc, H ₂ , CH ₄ /H ₂ , CClH ₃ /H ₂
InP	CH ₄ /H ₂ , C ₂ H ₆ /H ₂ , Cl ₂ /Ar
Au	C ₂ Cl ₂ F ₄ , Cl ₂ , CClF ₃

Chlorine, while often used for etching conducting and semiconducting materials, is highly toxic and presents safety issues. Fluorocarbons on the other hand used in etching semiconducting and insulating materials such as Si, SiO₂ and Si₃N₄ contribute to ozone destruction in the upper atmosphere. Each therefore require care in process development.

Many of the fluorine based etches employ freon, CF₄ or a chloro-fluorocarbon derivative, CF_xCl_y (where x+y= 4). These compounds are highly stable but can easily be plasma-cracked into F atoms and CF_x molecules. The F radicals then act as the etchant. Both Si and SiO₂ react with F in this manner:



Both F and CF_x (where $x \leq 3$) are radicals, i.e., neutral species containing one or more unpaired electrons. They are highly reactive so when other gases such as H_2 or O_2 are introduced into the plasma mixture, various side reactions may occur which alter the etch characteristics. Figures 2.7 and 2.8 are examples of the results of such a strategy.

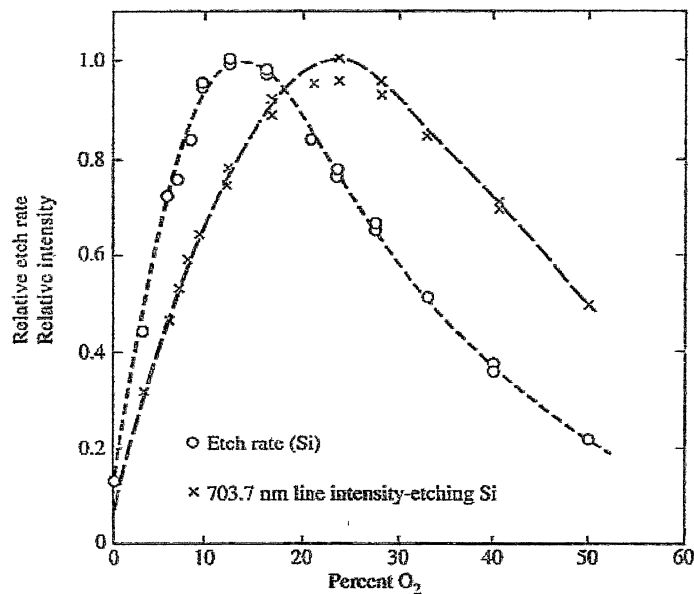


Figure 2.7 Etch rate dependence on percent O_2 in the CF_4/O_2 mixture.¹

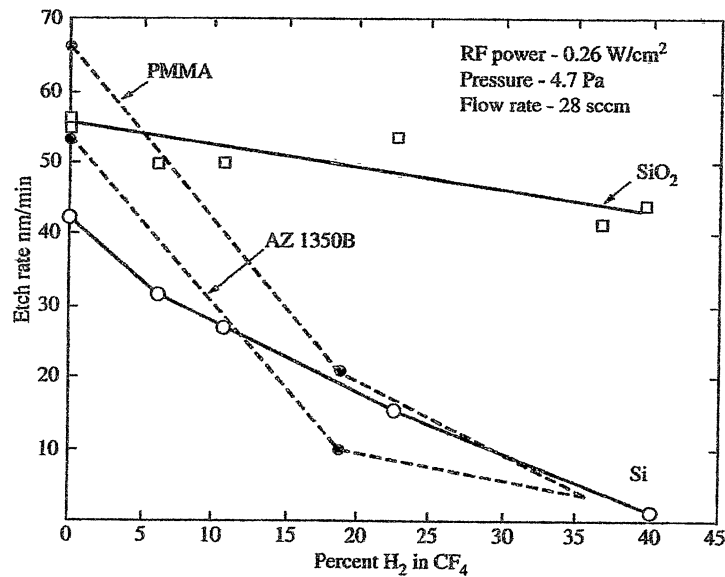


Figure 2.8 Etch rates of silicon (solid line, round points), silicon dioxide (solid line, square points), and PMMA and AZ1350B resists (dashed lines) vs. percentage of H₂ in CF₄.¹

In the case of O₂ it is used to scavenge the carbon by-products while the use of H₂ is to improve selectivity of oxide over silicon.

2.3.3 REACTIVE ION ETCHING (RIE)

RIE processes arose from the need to increase the selectivity of anisotropic ion milling methods. The idea incorporates both chemical and physical etching as discussed earlier though it should be noted that chemical processes dominate the etch characteristics. Ion assisted etching therefore is a more accurate descriptor. It is used extensively in both fabrication and deprocessing.

RIE designs include both planar and hexagonal geometries. The schematic of a planar reactor is shown in Figure 2.9.

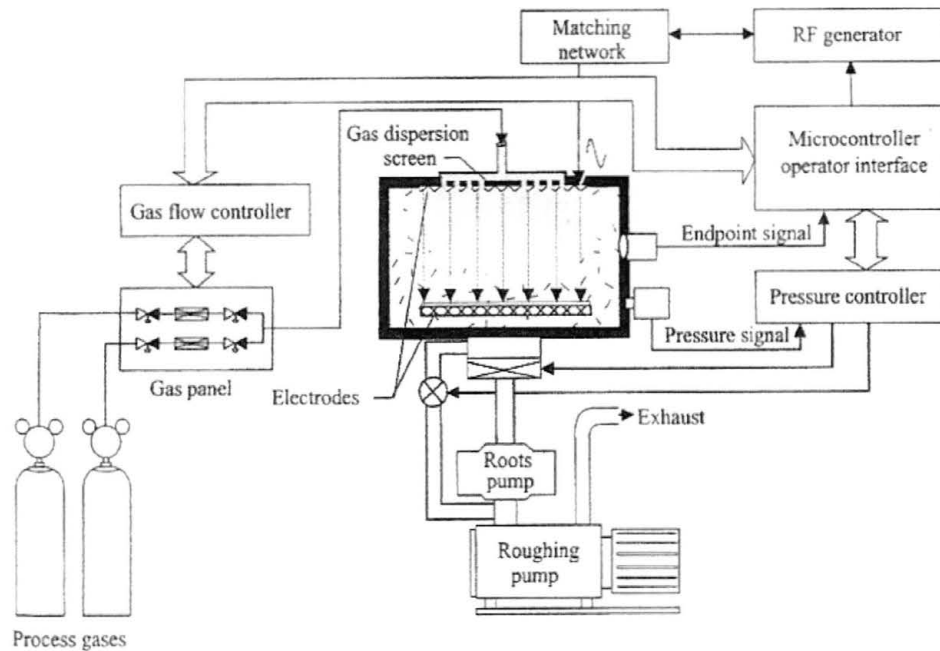


Figure 2.9 Schematic representation of a parallel plate plasma etcher.⁸

An RIE plasma reactor consists of a vacuum chamber, pumps, mass flow controllers, pressure sensors, a power supply generator, and endpoint detectors. In contrast to plasma etchers, RIE's operate in a low pressure regime of 10^{-3} to 10^{-1} torr. This results in mean free ion paths on the order of millimeters.⁸ Increased mean free paths occur as plasma density is decreased. The number of particles in the plasma drops thereby reducing the probability of ion-particle collisions. The number of ions reaching the surface at near normal incidence therefore increases. Consequently etching will be faster and more anisotropic.

In the planar design, the large upper electrode is grounded while a smaller electrode holding the wafers is powered by RF and is kept at a high negative bias. The RF power is supplied by a generator and impedance matching network designed to increase the power dissipation in the plasma and protect the power supply. The potential difference between the plasma and the powered electrode is several hundred volts resulting in the large electric fields needed for normal incidence ion bombardment. To realize this large potential drop, the powered electrode is attached to the chamber wall increasing its effective area while the low pressure allows the plasma to spread enough to contact the walls.⁴ The plasma is therefore held at ground potential. To maintain the low plasma density requires good regulation of the operating pressure. Pressures greater than 1 torr will cause the plasma to contract and further ion bombardment hence etch rate is impaired.

The anisotropy of dry etch processes was previously discussed and is applicable to RIE processes. In general the etch rate is quite good though it is subject to phenomena known as microloading and aspect ratio-dependent etching (ARDE).¹ Figure 2.10 provides a visual interpretation of ARDE in which the smaller trenches have etched at slower rates and Figure 2.11 graphically illustrates this relationship.

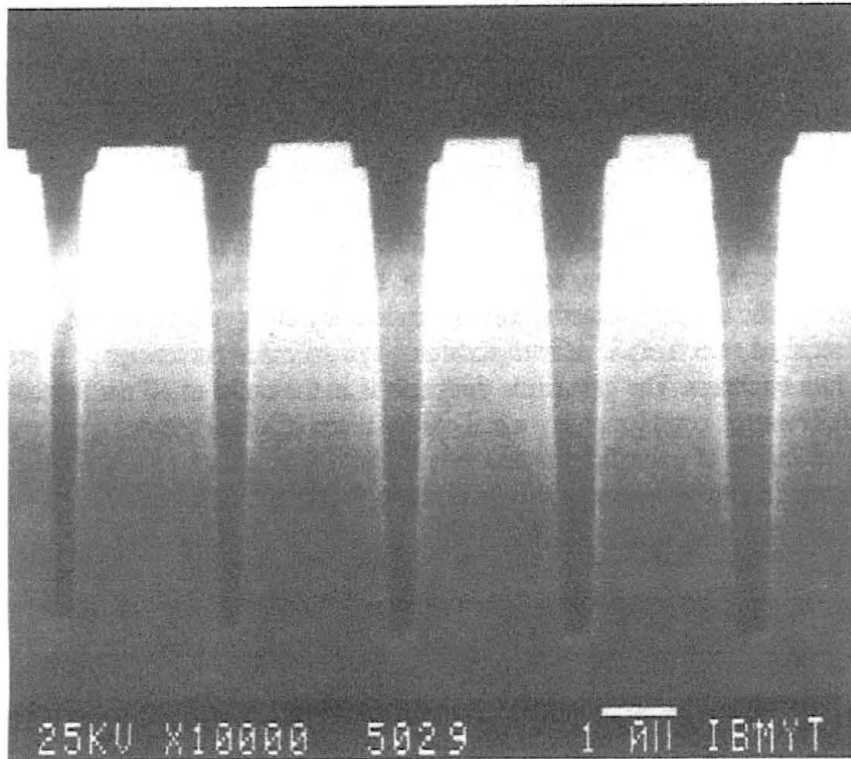


Figure 2.10 An example of ARDE in silicon. Notice the wider trenches etch more rapidly.¹

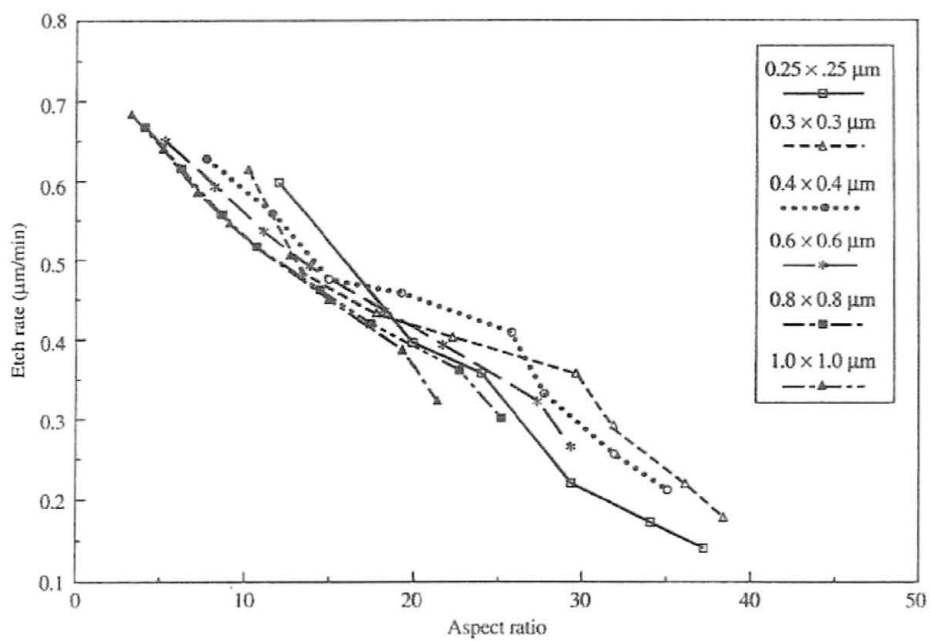


Figure 2.11 Silicon trench etch rate dependence on aspect ratio.¹

The mechanisms involve transport of etchant-ions and neutrals to the surface and associated shadowing due to collisions and geometry and ion scattering induced by charging of the surface. Microloading also results in reduced etch rates and is attributable to reactant depletion in a localized area where high densities of repeating features exist.

Use of RIE for failure analysis is based on etch anisotropy and selectivity. Deprocessing requirements may be such that sidewall profiling of given layers in three dimensions is necessary. This precludes cross-sectioning via focused ion beam (FIB) methods which result in a 2-dimensional view. It can also preclude wet etching methods if the device needs to remain electrically active. In the latter, the packaging material directly over the die can be removed permitting access to the surface while maintaining the lead frame, bond wires, and die attach intact. In cases where RIE is used on decapped parts, it is critical that the only area exposed to the plasma is the die surface itself. All surrounding package materials, bond wires, and lead frames must be masked with a photoresist to eliminate sputtering and redeposition of these materials on to the reactor walls and back on the die surface itself producing a phenomena known as RIE “grass” which will cover the surface features. Once this occurs further deprocessing can be time consuming as grass removal and chamber contamination require additional work. Table 2. 2 below summarizes the characteristics of RIE.

Table 2.2
RIE Operating Parameters and Characteristics

Pressure	$10^{-3} - 10^{-1}$ torr
Temperature	Ambient
Etch mechanisms	Chemical and physical
Anisotropy	High
Etch rate	Fast; subject to microloading and ARDE
Selectivity	Good with right chemistries and configuration
Uniformity	Good; subject to microloading and ARDE

Much of the RIE data available for failure analysis is determined empirically in the lab. Techniques to optimize results often rely on individual lab protocols based on previous experience. Processes are less controllable from lab to lab and repeatability can be problematic.

Endpoint detection in plasma reactors is a requirement for improving process repeatability. Two methods are available. The first relies on optical reflectivity and is effective only if 1) the films being etched are optically transparent, and 2) a relatively large area of the film is unpatterned, as will be discussed in more detail in Chapter 3, optical reflectivity.

Basically this technique involves measuring the interference of a light wave reflected from both the surface and the film/substrate interface. The sum of the two reflected amplitudes will oscillate with film thickness until the film is etched away. This can be carried out by laser interferometry in situ. Reflectivity measurements are typically difficult to

obtain for integrated circuit film stacks due to the component density on the film. An unpatterned area of film larger than the spot size of the laser is required. This is often impossible since spot sizes are usually $>10\mu\text{m}$ while current technology feature sizes are $\ll 1\mu\text{m}$.

A frequently used alternative involves monitoring the optical emission spectra of the plasma. Recall as relaxation of excited species occurs, light is emitted at characteristic wavelengths. As etching progresses, reaction product species build up in the plasma and so the intensity of their emission increases. Conversely the intensity of the reactant species decreases. One can choose to monitor any of these species and then project an endpoint intensity. When this is reached, the reactor shuts off. Table 2.3 provides examples of several common etch processes and associated optical emission data.

Table 2.3 Wavelength emission of some common dry etch methods for endpoint detection.⁴

Film	Etchant	Wavelength (Å)	Emitter
Al	CCl ₄	2614	AlCl
		3962	Al
Resist	O ₂	2977	CO
		3089	OH
		6563	H
		6156	O
		7037	Fl
Si	CF ₄ /O ₂	7770	SiF
		2882	Si
		3370	N ₂
Si ₃ N ₄	CF ₄ /O ₂	7037	F
		6740	N
		1840	CO
SiO ₂	CHF ₃		
W	CF ₄ /O ₂	7037	F

It is also possible to use mass spectrometry to analyze the reaction products as they are removed from the chamber. Many species etched from the surface are singly ionized. A mass spectrometer generates a spectra of the mass to charge ratio of these ions allowing them to be identified. Again, relative intensity can be used to monitor the endpoint and stop the process.

2.3.4 FOCUSED ION BEAM MILLING

Focused ion beam milling or sputter etching, in its simplest form is a purely physical etching process. In fact, the etch mechanisms are the same as those in a film sputtering process.

Some ion sources generate ions through plasma cracking of various non-reactive or weakly reactive elements including the noble gases such as argon, krypton and xenon. Kaufman sources are often used in ion beam sputtering systems. Figure 2.12 shows a schematic representation.

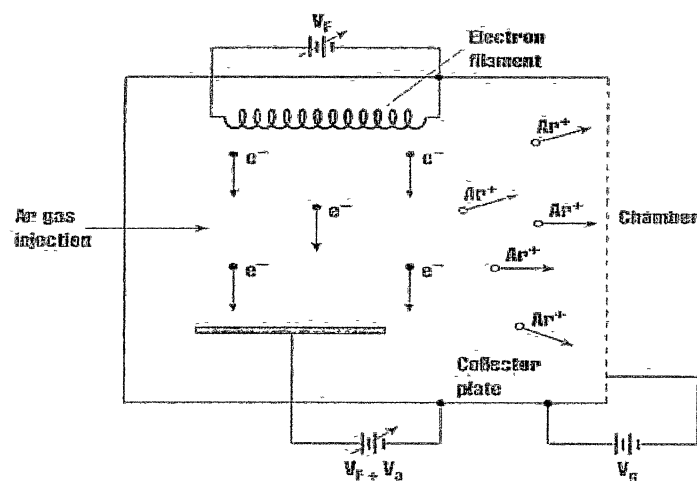


Figure 2.12 Cross section schematic of a Kaufman ion source.⁴

The process begins as electrons are thermionically boiled off of a filament kept at a high negative potential. The electrons are accelerated toward an anode at a lower potential. The gas to be ionized is introduced in between the electrodes and subsequent collisions with the electrons will cause ionization providing the electron energies are ~40eV. Higher energies are undesirable since highly energetic ions will strike and erode the chamber walls causing contamination in the system.⁹

The ion stream generated is referred to as the emission current and consists only of the collimated beam exiting the source chamber. An accelerating potential established between the source and the sample stage accelerates the ions to the surface where milling occurs. Accelerating potentials are usually 0.5-1.0kV which impart ion energies as described by

$$E_{\text{ion}} = q | V_p - V_g | = q | V_a + V_{pa} - V_g |$$

where V_p is the plasma voltage with respect to ground and V_{pa} is the plasma voltage with respect to the anode.⁴ The other variables are identifiable in the schematic.

In addition, Kaufman sources use a magnetic field to increase ion density in the plasma. Field strengths are $\sim 10^2$ Gauss and result in layer ion current densities.

The current density is limited however by the electric field the beam produces and is approximately

$$j_{\max} \approx K \sqrt{\frac{q}{m}} \cdot \frac{V_t^{3/2}}{I_g^2}$$

where K is a chamber dependent constant, q/m is the charge/mass ratio, I_g is the distance between the screen and acceleration grid and V_t is the voltage drop between them.⁴

Another ion source and the type used in focused ion beam applications uses a needle-like tip coated with gallium kept at a very large positive potential relative to ground. The high field causes the gallium to liquify and flow by capillary action toward the tip. In close proximity is an extractor electrode at low potential that is capable of stripping an electron from each gallium atom thereby positively ionizing them. These ions then form the emission current as they accelerate toward the target. Since various phenomena such as simple Brownian motion will cause the emission current to vary slightly over time, a suppressor located near the source is used as a stabilizer. Essentially what happens is that the extractor voltage is set higher than that needed to produce the required current. The suppressor is then used to retard the current back to the desired level. In this way, the final current is buffered from these small fluctuations.

After the ions have been generated, they will enter the beam column through an aperture and be focused by a series of electrostatic elements on the target. Figure 2.13 provides a schematic diagram of the beam column. At the surface then sputtering processes occur whereby substrate material is knocked off the surface. Due to the relatively large mass of the Ga^+ ions (atomic weight 70) and the beam energy, milling can proceed deep into the silicon substrate of the device.

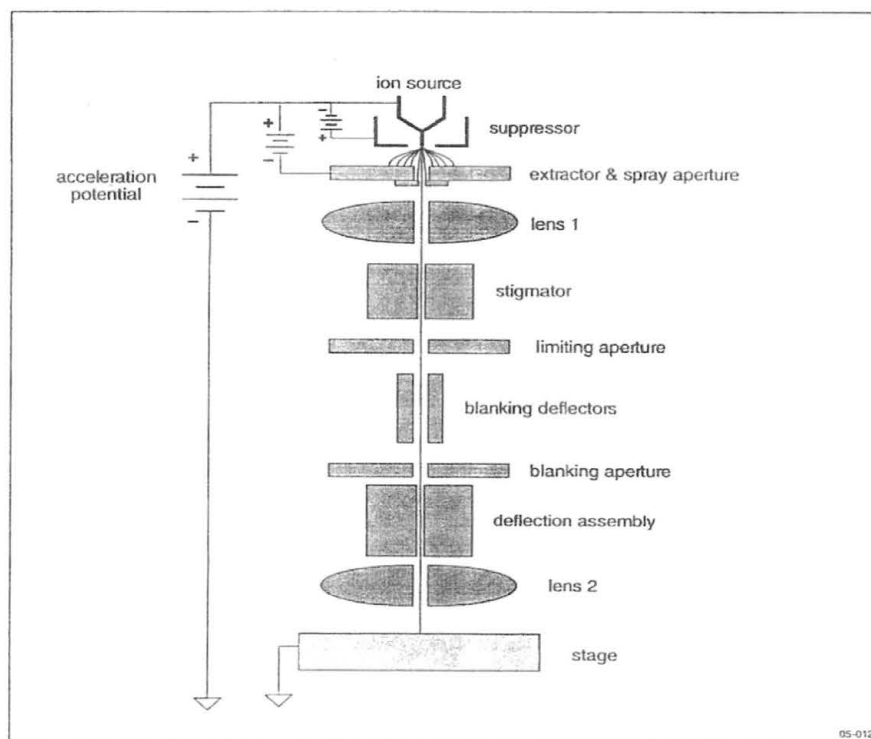


Figure 2.13 Schematic diagram of a focused ion beam column.⁹

FIB's are used extensively in FA labs. Cross sectional cuts of an IC can be made to look at the multi-layer structures at any point on the circuit. This is often done once electrical isolation of a defect indicates a possible particle containment, metal bridging or electromigration. Operating parameters including beam size, beam current and accelerating voltage can be adjusted to control cut depth and quality.

FIB based modifications are common in FA as well. Electrical testing of a failed IC may involve isolating, cutting and rerouting specific circuit elements to fix the location of the failure. This specifically requires being able to access different metal layers for cross-connects without rendering the device inactive. Specific FIB applications are designed to remove dielectric materials around the area of interest and then cut and redeposit tungsten metal lines for rerouting. Xenon difluoride (XeF_2) is used to remove dielectric materials, having a high selectivity to these materials over metal. Chlorine gas (Cl_2) is used to cut metal lines and hexacarbonyl tungsten, $(\text{CO})_6\text{W}$, is used to redeposit metal lines.

As the milling profile becomes deeper there is a tendency for the sputtered material to redeposit on the sidewalls. This can be minimized by bleeding in a gas which reacts with the sputtered material to produce volatile reaction products which can be evacuated from the chamber. The reactive gas is injected very close to the sample surface, referred to as a gas-assisted etching (GAE). In contrast to RIE in which the

dominant etch mechanism is chemical, FIB milling is completely physical. Interaction of the bleed gas with the sample surface is negligible.

2.4 ETCHING TECHNIQUES

2.4.1 SILICON NITRIDE

Silicon nitride films have several applications in microelectronics fabrication. They are used as diffusion barrier against oxygen and water, masking layers for LOCOS (local oxidation of silicon) processes, caps over polysilicon gates and sidewalls, and passivation layers for integrated circuits. Nitride films can be formed in many ways as shown in the table below.

Table 2.4 Summary of Preparation Techniques for Si₃N₄ Films.¹⁰

Preparation Technique	Chemical Reaction	Substrate Temp. (°C)
Nitridation of Si wafers	$3\text{Si} + 2\text{N}_2 \rightleftharpoons \text{Si}_2\text{N}_4$	1300
Nitridation of Si wafers	$3\text{Si} + 4\text{NH}_3 \rightleftharpoons \text{Si}_2\text{N}_4 + 6\text{H}_2$	1100-1300
Nitridation of Si wafers	$3\text{Si} + 2\text{N}_2\text{H}_4 \rightleftharpoons \text{Si}_2\text{N}_4 + 4\text{H}_2$	1100-1300
Nitridation of SiO ₂ films	$3\text{SiO}_2 + 4\text{NH}_3 \rightleftharpoons \text{Si}_2\text{N}_4 + 6\text{H}_2\text{O}$	1100-1300
Nitridation of native Si films	$3\text{Si} + 4\text{NH}_3 \rightleftharpoons \text{Si}_2\text{N}_4 + 6\text{H}_2$	800-1200
Nitridation of native Si films	$3\text{Si} + 2\text{N}_2\text{H}_4 \rightleftharpoons \text{Si}_2\text{N}_4 + 4\text{H}_2$	700
Chemical transport	$\text{Si}_2\text{N}_4 + 12\text{HCl} \rightleftharpoons 3\text{SiCl}_4 + 2\text{N}_2 + 6\text{H}_2$	500-800
Chemical transport	$\text{Si}_2\text{N}_4 + 12\text{HBr} \rightleftharpoons 3\text{SiBr}_4 + 2\text{N}_2 + 6\text{H}_2$	500-800
Normal pressure CVD	$3\text{SiCl}_4 + 4\text{NH}_3 \rightleftharpoons \text{Si}_2\text{N}_4 + 12\text{HCl}$	550-1100
Normal pressure CVD	$3\text{SiBr}_4 + 4\text{NH}_3 \rightleftharpoons \text{Si}_2\text{N}_4 + 12\text{HBr}$	550-800
Normal pressure CVD	$3\text{SiF}_4 + 4\text{NH}_3 \rightleftharpoons \text{Si}_2\text{N}_4 + 12\text{HF}$	700-1100
Normal pressure CVD	$3\text{SiH}_4 + 4\text{NH}_3 \rightleftharpoons \text{Si}_2\text{N}_4 + 12\text{H}_2$	700-1100
Normal pressure CVD	$3\text{SiCl}_4 + 2\text{N}_2\text{H}_4 + 2\text{H}_2 \rightleftharpoons \text{Si}_2\text{N}_4 + 12\text{HCl}$	700-1100
Normal pressure CVD	$3\text{SiH}_4 + 2\text{N}_2\text{H}_4 \rightleftharpoons \text{Si}_2\text{N}_4 + 10\text{H}_2$	550-1150
Normal pressure CVD	$3\text{SiH}_2\text{Cl}_2 + 4\text{NH}_3 \rightleftharpoons \text{Si}_2\text{N}_4 + 6\text{HCl} + 6\text{H}_2$	700-1100
UV-sensitized CVD	$3\text{SiH}_4 + 2\text{N}_2\text{H}_4 \rightleftharpoons \text{Si}_2\text{N}_4 + 10\text{H}_2$	200
Catalyzed CVD (Pt)	$3\text{SiH}_4 + 4\text{NH}_3 \rightleftharpoons \text{Si}_2\text{N}_4 + 12\text{H}_2$	600
Low pressure CVD	$3\text{SiH}_4 + 4\text{NH}_3 \rightleftharpoons \text{Si}_2\text{N}_4 + 12\text{H}_2$	750-850
Low pressure CVD	$3\text{SiH}_2\text{Cl}_2 + 4\text{NH}_3 \rightleftharpoons \text{Si}_2\text{N}_4 + 6\text{HCl} + 6\text{H}_2$	750-850
R.f glow discharge	$3\text{SiH}_4 + 2\text{N}_2 \rightleftharpoons \text{Si}_2\text{N}_4 + 6\text{H}_2$	25-500
R.f glow discharge	$3\text{SiH}_4 + 4\text{NH}_3 \rightleftharpoons \text{Si}_2\text{N}_4 + 12\text{H}_2$	25-400
D.c glow discharge	$3\text{SiCl}_4 + 2\text{N}_2 \rightleftharpoons \text{Si}_2\text{N}_4 + 6\text{Cl}_2$	300-800
Microwave excitation	$4\text{N} + 3\text{SiI}_4 \rightleftharpoons \text{Si}_2\text{N}_4 + 6\text{I}_2$	280-600
Reactive r.f. sputtering	$3\text{Si} + 2\text{N}_2 \rightleftharpoons \text{Si}_2\text{N}_4$	200-450
Direct r.f. sputtering	$\text{Si}_2\text{N}_4 \rightarrow \text{Si}_2\text{N}_4$	100
Electron beam evaporation	$\text{Si}_2\text{N}_4 \rightarrow \text{Si}_2\text{N}_4$	200-250
Ion implantation	$\text{Si} + \text{N}_2^+ (\text{N}^+) \rightarrow \text{Si}_2\text{N}_4$	500

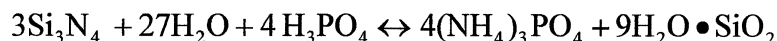
The etch rate for these films is dependent on several variables including substrate temperature during deposition, film stoichiometry and density. Typically, lower temperatures result in less dense films as larger amounts of hydrogen are incorporated into the films. CVD nitrides tend to be more dense. In efforts to improve film stress characteristics silicon oxynitride films of differing stoichiometries have been grown. They actually consist of oxide/nitride/oxide stacks where the compressive stress of the oxides offsets the tensile stress of the nitride.¹

Stoichiometrically these film compositions have the form $\text{Si}_x\text{O}_y\text{N}_z$ and will often etch at significantly higher rates as shown below.

Table 2.5 Etch rates of silicon nitride.¹⁰

Preparation method	Etch rate ($\text{\AA}/\text{min}$)		
	HF	1 10 HF . NH_4F	H_2PO_4
CVD, $\text{SiH}_4 + \text{NH}_2$	90	5	60
CVD, $\text{SiCl}_4 + \text{NH}_2$	-	11	100
CVD, $\text{SiH}_4 + \text{N}_2\text{H}_4$	300	-	-
CVD, $\text{SiH}_2\text{Cl}_2 + \text{NH}_2$	600	150	75
RFGD, $\text{SiH}_4 + \text{NH}_2$	-	50	-
RFGD, $\text{SiH}_4 + \text{N}_2$	-	100	-
LPCVD, $\text{SiH}_4 + \text{NH}_2$	150	-	-
LPCVD, $\text{SiH}_2\text{Cl}_2 + \text{NH}_2$	200	-	-
Direct rf sputtering	750	-	-
CVD, $\text{Si}_x\text{O}_y\text{N}_z$	>360	>600	>600

Nitride films can be wet etched by hydrofluoric acid (HF) and hot phosphoric acid (H_3PO_4). The etch rate in HF is sufficiently slow that it is not a viable alternative. The reaction equation for nitride in H_3PO_4 is as follows:



The reaction products are hydrated silica and ammonium phosphate. The reaction is reversible suggesting that a dynamic equilibrium will be reached in which the reaction products recombine to form reactants at the same rate that product is being formed. This is important in that one of the reaction products is hydrated silicon dioxide. If a nitride/oxide film stack were being etched (as might be done on a

passivation layer), when the nitride was completely etched there would be a large amount of oxide in the spent etchant solution that would inhibit any etching of the oxide layer. Thus H_3PO_4 is highly selective to nitride over oxide. In actuality some small amount of oxide would be etched but would decrease with time in keeping with LeChatlier's Principle of maintaining equilibrium.

As mentioned earlier, this reaction requires hot H_3PO_4 typically between $150^\circ - 180^\circ \text{C}$. This presents a non-trivial problem that is difficult to present. Phosphoric acid is commercially available at a maximum concentration of 85% by weight with a boiling point of 154°C . At higher temperatures the concentration increases as shown in the graph below.

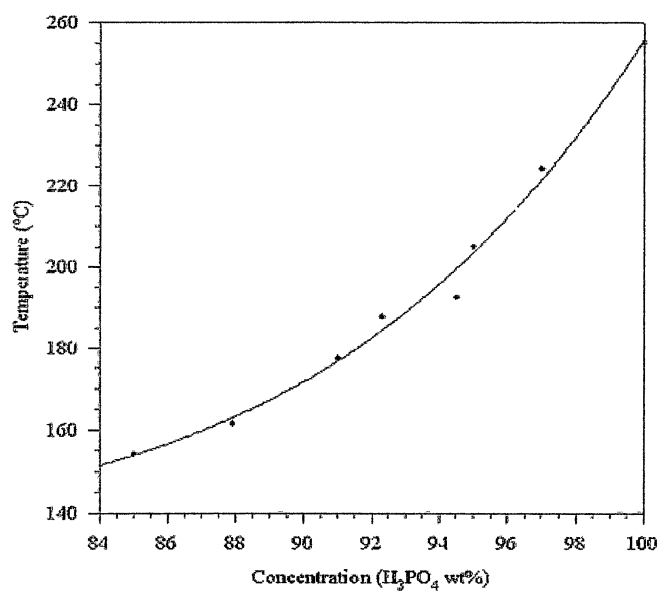


Figure 2.14 Boiling point vs concentration. 10

Since it is impossible to heat a solution beyond its boiling point (at a given pressure) it becomes necessary to remove some water from the acid thereby increasing the concentration and so the boiling point increases. Therefore, the acid concentration must be maintained in the order to maintain the temperature. What appears to be a conundrum is understood in terms of the Gibb's phase rule:

$$F = 2 - \pi + N$$

where F = number of degrees of freedom, N = number of chemical species in the system and π = number of phases in the system. For the acid-water system there are two chemical species each having a gas and a liquid phase. Therefore $F = 2$. When considering the pressure, temperature and concentration, selecting ambient pressure leaves only one more choice -- temperature or concentration. When one is chosen the other is then pre-determined i.e.; for any given temperature the concentration is fixed or for a given concentration the temperature is fixed.¹⁰

The upshot here is that in order to effectively control the etch rate, a reflux system is required which would capture the gases boiled off and condense them back into the system. While feasible in a research environment, it is not practical in a fab, therefore, the method of choice is to carefully monitor and replace the water boiled out of the system. It should be noted that temperature control via adjustable heat sources can lead to increased concentration of acid as water boils off but is not

evident by a temperature change as would be the case normally. This will result in etch rate variations. The graph below compares etch rates for silicon, silicon dioxide and silicon nitride in hot H_3PO_4 .

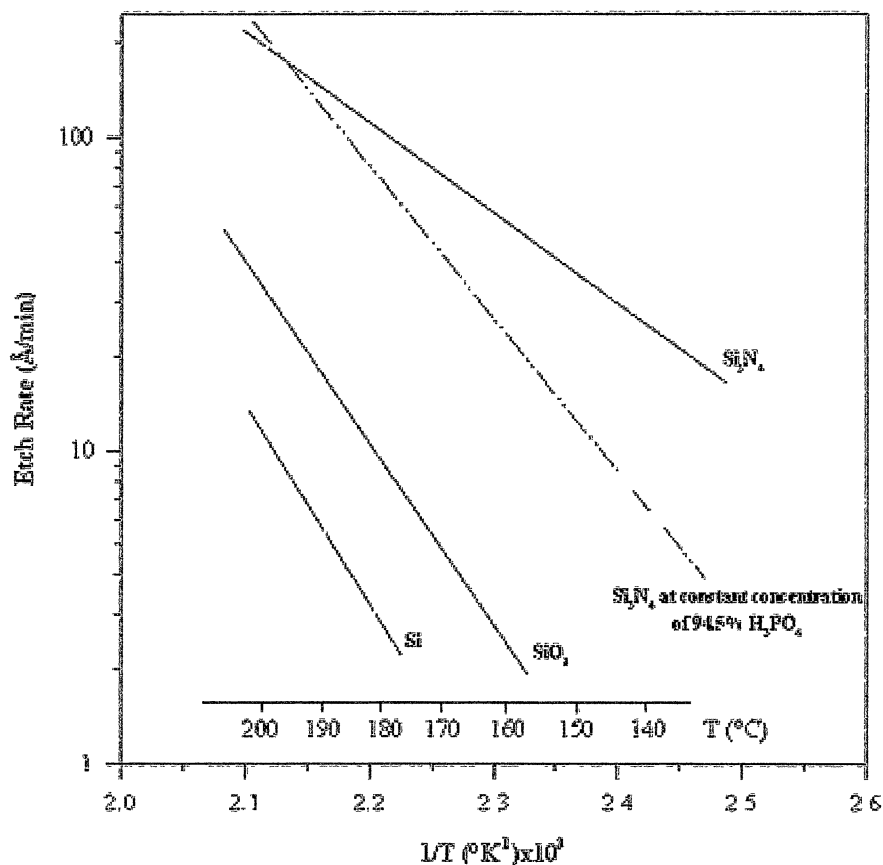


Figure 2.15 Etch rates of silicon, silicon dioxide, and silicon nitride in hot phosphoric acid.¹⁰

In general, while this is a highly complex mechanism, hot H_3PO_4 can be effectively used to selectively etch nitride films. Experimental etch run data is presented in Chapter 4.

2.4.2 SILICON DIOXIDE

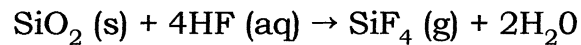
Silicon dioxide, SiO_2 , is one of the most important materials used in silicon semiconductor device fabrication. In one of its most basic forms it is known as sand and is one of the most abundant compounds on earth. It is amorphous, meaning it does not have a crystalline structure in its atomic arrangement which gives rise to its tendency to etch isotropically. (The other common form, quartz, which is crystalline would be preferred for thin films however its lattice parameter is poorly matched to silicon and therefore not used). This can be problematic in IC fabrication.

Oxide, as it is commonly referred to, is used for several things. It is used as a mask during ion implantation where it acts as an effective barrier to doping of other than desired areas. This begins with covering the silicon wafer with oxide uniformly over the surface. Windows are then etched through the oxide down to the silicon surface where source and drain regions will be formed. However the amorphous character and resulting etch isotropy makes it difficult to etch straight down. Instead, the sidewalls tend to etch laterally at the same rate as vertically resulting in undercutting. Therefore, wet etching is not a viable method here. Dry etch methods described later are much more effective in these cases.

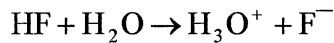
On the other hand, blanket films of oxide lend themselves well to wet etching which in some cases is desirable for its selectivity and

reduced incidence of interface damage. Furthermore, in deprocessing for failure analysis, wet etching of oxides is used often to remove the interlayer dielectric films quickly.

The preferred wet etch method for oxide removal is hydrofluoric acid (HF). The chemical reaction is as follows



HF in aqueous solution dissociates (albeit weakly) as

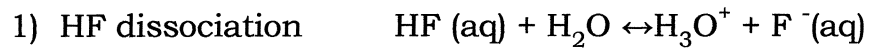


where H_3O^+ (a hydronium ion) is a source of protons (H^+ ions). Within this context Prigot et al. has described the reaction mechanism as follows.¹¹

- 1) Protons adsorb to oxygen on the surface.
- 2) The oxygen adsorbing the proton needs a valence electron that it gets from a neighboring silicon atom in the matrix.
- 3) As silicon gives up these valence electrons to oxygen, the electron density around silicon decreases causing the Si-O bond to weaken and eventually break.
- 4) The silicon then becomes positively charged.
- 5) HF_2^- then facilitates etching.

HF is available commercially in several ways. The highest concentration available is 49% by weight but is seldom used due to its high etch rate. Failure analysts may however use this strength to very rapidly remove layers to reach substrate. Typically very dilute solutions

are used which use ammonium fluoride, NH_4F , as both a diluent and a buffer and are available at 10:1 and 6:1 dilutions. They are commonly referred to as buffered oxide etch. The NH_4F buffering occurs through the following mechanism:



The fluorine ions generated in the first step quickly react with the oxide surface thereby depleting F^- concentration. As this occurs the NH_4F dissociation equilibrium is shifted to the products in order to replenish the F^- supply. In this manner the concentration of fluorine ions is maintained over long periods thereby maintaining consistent etch rates. Figure 2.16 shows the relationship between etch rate and HF concentration at different temperatures.

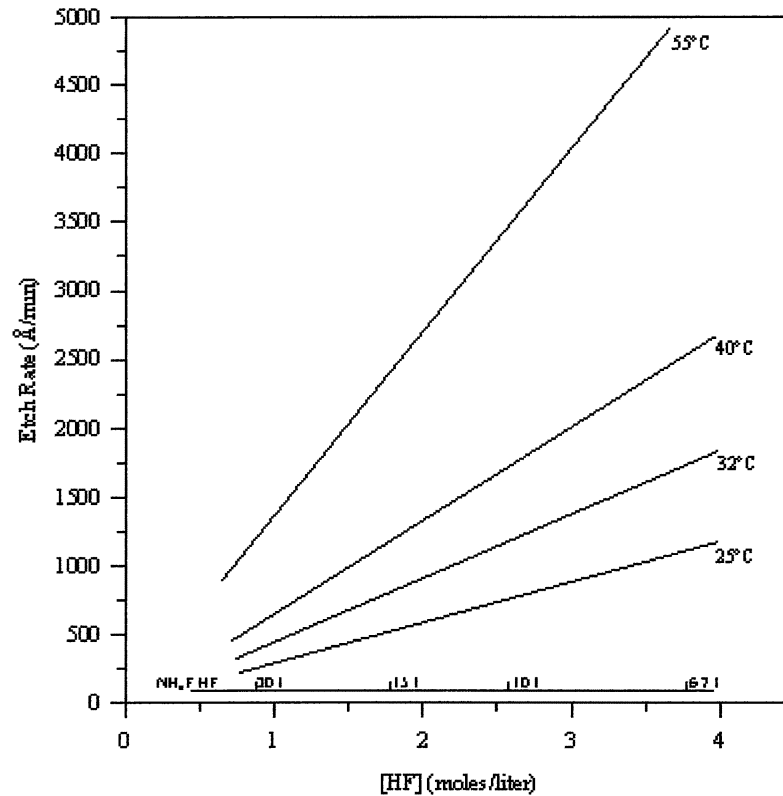


Figure 2.16 Etch rate of thermal oxide as a function of HF concentration.¹¹

As discussed, oxide/HF etching, like most wet etches, is highly temperature dependent. Parisi, et.al. empirically determined that the vertical etch rate could be modeled as

$$R_v = 4.5 \times 10^9 [\text{HF}] e^{-4980/T}$$

where [HF] is the molar concentration of HF and T is the absolute temperature. This is valid for $0.9\text{M} \leq [\text{HF}] \leq 3.8\text{M}$ and $25^\circ\text{C} \leq T \leq 55^\circ\text{C}$.¹¹

In addition, they determined that the slope of the sidewall was a function of both vertical and lateral etch rates and is given by

$$\sin \theta = \frac{R_V}{R_L}$$

where θ is the angle between the sidewall and the surface. Factors affecting the lateral etch rate include type of photoresist used, oxide/photoresist interface condition and whether a wetting agent was used. Consequently a precise correlation between R_L and HF concentration can not be made. However edge profiles tend to become steeper as [HF] increases. This is displayed pictorially in Figure 2.17.

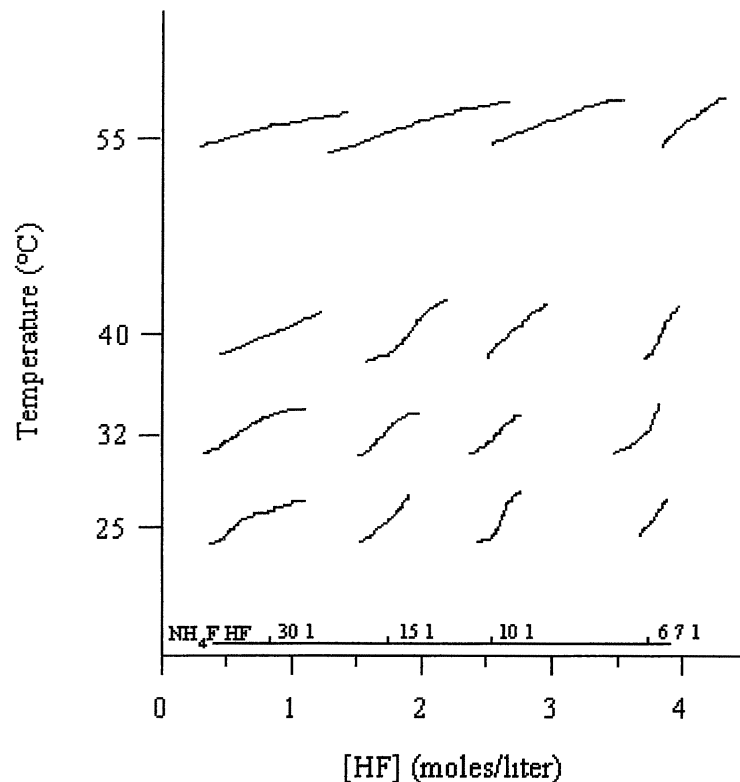


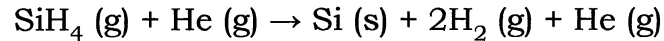
Figure 2.17 Pictorials of edge profiles as a function of temperature and HF concentration.¹¹

The use of various doped silicon dioxide films in current process technologies is commonplace. These “glasses” may be either n or p doped and are used for interlevel dielectrics and passivation layers. Stress and flow related properties account for their popularity. These films typically have etch rates significantly different from undoped oxides based on electron availability. N doped materials etch more quickly since the additional electrons weaken the Si-O bonds which are then broken more quickly. The converse is true for p-doped materials.

RIE etching of oxides is effectively accomplished with CHF_3 and O_2 gases as discussed in section 2.3.2. It is used frequently in failure analysis to depassivate die surfaces for further processing. Failure to remove all the passivation layers can inhibit subsequent wet deprocessing techniques. Interlevel dielectrics may also be removed in this manner when sidewall profiling of intact metal lines and vias is required. In very carefully controlled wet techniques, metal lines may actually be undercut leaving them “suspended” and still electrically active.

2.4.3 POLYSILICON

Doped polysilicon films are generally used as the gate material of transistors though it may also serve as a resistor in memory cells. It is a polycrystalline substance and is typically deposited by LPCVD methods in a pyrolytic reaction as follows:¹²



This reaction is carried out at 600°C with diborane (B_2H_6) often used as a catalyst to lower the activation energy. In fabrication environments, polysilicon etching is strictly a dry etch process. These gate structures determine the channel length in MOS devices and hence are significant drivers of device performance. The need to maintain strict etch tolerances is therefore critical. Dry etching provides the anisotropy needed to provide steep sidewall etches.

It is also essential to develop chemistries with very high selectivity. Current technology with 0.15 μm gate sizes have gate oxide thicknesses of 20 to 30Å. This is about 6 to 10 monolayers. Therefore any etch chemistry must limit oxide etching to no more than 5Å. This is now done in a multi-step process using both fluorine and chlorine as the reactive species. Chlorine provides both anisotropy and selectivity in the etch but is highly toxic and requires special handling and safety protocols.

Poly etching in failure analysis applications may be done with RIE or wet etching methods. In cases where it is not necessary to keep the gate oxide layer intact, a few seconds in 49% HF will remove all layers from a die surface if it has already been depassivated. However, this strategy is not good if the oxide must be preserved. In this case a “poly etch” made up of 99% glacial acetic acid:49% HF:90% HNO_3 (at 20:1:8) can be used.¹³ RIE recipes using pure chlorine or CF_4 and O_2 are also available. Pure chlorine provides the best selectivity for poly over oxide.

The following provides an etch rate of $\sim 8500\text{\AA}/\text{min}$.¹²

RF Power	200 W
Pressure	200 mtorr
Gas	Cl_2
Gas Flow	60 SCCM
Temp	40°

2.4.4 METALS

Metals are used throughout integrated circuit devices as interconnect wiring contacts and vias and various barriers and liners. Aluminum, copper, tungsten, and titanium/titanium nitride stacks are those most commonly used. Both wet and dry chemistries are used for various ones. Fabrication processes are predominantly dry methods while failure analysis may use both. Dry etch chemistries must have the following characteristics:⁸

- High etch rates, selectivity and uniformity
- No plasma induced damage
- Low residue contamination
- No corrosion

Pure chlorine (Cl_2) gas with CHF_3 is used to passivate the sidewalls to prevent etching laterally. An alternative is boron trichloride (BCl_3). It is heavier so will enhance the physical etching and hence increase anisotropy. Some N_2 may be introduced for sidewall passivation in this

case. Fluorine-based chemistries are not viable since the etch products are not volatile.

Tungsten, used to make contacts and vias, is also etched with chlorine or chlorine containing gases due to its good selectivity and anisotropy. The tungsten contact/via fabrication process is shown in Figure 2.18.

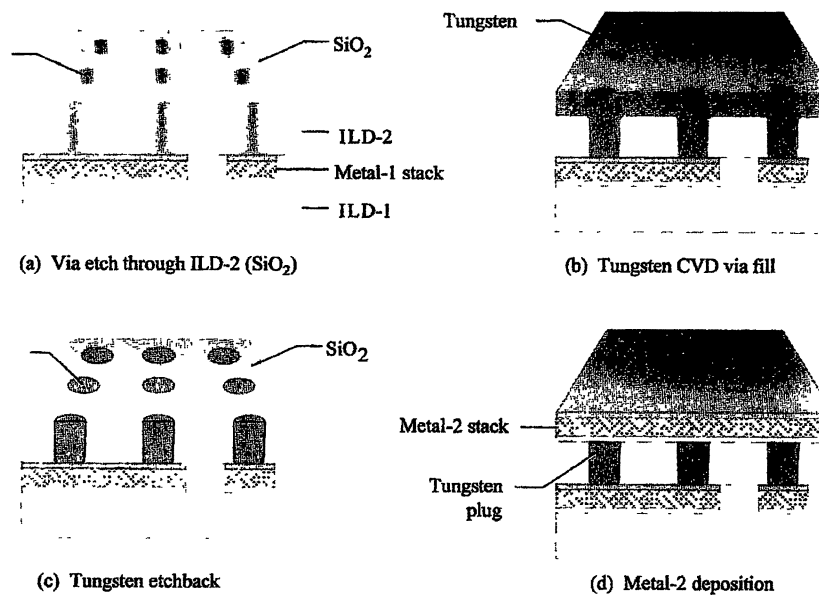


Figure 2.18 Contact/via fabrication.⁴

Titanium and titanium nitride are used as barrier metals and liners to improve contacts between metals and other films and to prevent diffusion of metal ions into substrate regions. The TiN layer provides an anti-reflective coating. These metals are also etched using chlorine chemistries. Multiple steps are used as they are typically components of a multi-layer film stack with aluminum. The reaction products are

highly corrosive and must be handled appropriately to minimize damage to the stack, process equipment, and waste handling systems.

The following RIE recipes have proven effective in FA applications:¹²

	<u>Aluminum</u>	<u>Ti-W Barrier</u>
RF Power (W)	150	250
Pressure (mtorr)	140	400
Gases	BCl ₃ , Cl ₂	BCl ₃ , Cl ₂
Gas Flows (SCCM)	25 , 5	60 , 25
Temperature	40°C	40°C
Etch Rate	12500 Å/MIN	~500 Å/MIN

Wet etching recipes commonly used in FA applications include¹²

- 1) Aluminum (2 recipes)
 - a) 65% H₃PO₄ @ 50° C with an etch rate of 2000 Å/min
 - b) 1 part by volume (PBV) 65% HNO₃
 5 PBV 98% glacial acetic acid
 25 PBV 85% H₃PO₄
 Etch rate @70 C° 2000 Å/min
 @20 C° 2000 Å/hour
- 2) Tungsten (2 recipes)
 - a) 30% H₂O₂
 - b) 34g KH₂PO₄
 13.4g K₃Fe(CN)₆
 mix to make 1 liter of solution
 Etch rate @ 23° 1600 Å/min
- 3) Titanium (2 recipes)
 - a) H₂SO₄ @ 80°C
 - b) H₂O₂ @ 50-60°C

Other wet etch recipes are available in Appendix D. Use depends upon specific needs and conditions.

CHAPTER 3

CHARACTERIZATION METHODS

Four methods have been employed to provide characterizations of thin films and/or patterned IC devices including optical reflectivity, optical microscopy, scanning electron microscopy (SEM) and focused ion beam (FIB). The first three will be discussed in this chapter. FIB theory and application were discussed in the previous chapter. It can be used in characterization due to its capability of providing in situ monitoring and inspection.

3.1 OPTICAL REFLECTIVITY

Film thickness measurements are often taken following deposition processes to determine uniformity, step coverage and evaluate process controls. It is also useful in post-etch determination of etch rates and etch uniformity. Tight control of thickness is required to insure that the desired electrical properties are achieved for device operation.

Two optically based methods for film measurement are common. Ellipsometry is based on non-normal incidence of light onto a surface and measures the polarization and phase properties of the reflected waves. It is the primary method used in fab environments. Fig. 3.1 shows a schematic diagram of an ellipsometer.

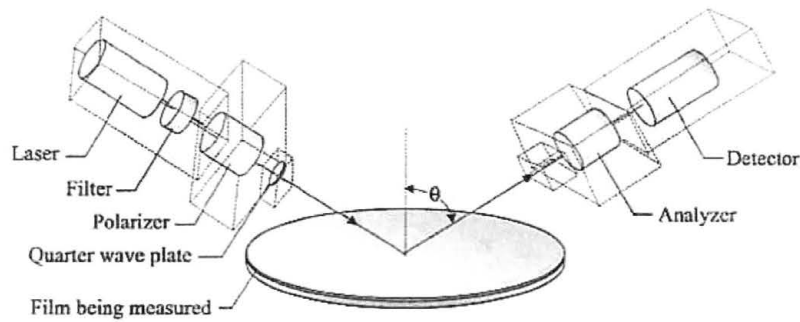


Figure 3.1 Ellipsometer⁸

Linearly polarized light is reflected off the film surface at an angle θ from the normal. The reflected beam will be elliptically polarized i.e., the wave will oscillate in an elliptically changing plane and will be analyzed by a polarizing element. The incident and reflected intensities are correlated with the change in polarization angle to determine the refractive index and film thicknesses. ULSI technologies require measurements at various angles of incidence to accurately determine these parameters. This technique is referred to as VASE for variable angle spectroscopic ellipsometry.

The second technique, known as optical reflectometry, relies on interference phenomena of light waves reflected from the top and bottom interfaces of the film and is not sensitive to polarization changes. Measuring the interference effect across a range of wavelengths will provide thickness estimates down to a level of a few hundred angstroms depending on the wavelength range selected for analysis. The advantages of reflectometry are its speed and lesser complexity but as a result it is less powerful than ellipsometry.

An understanding of how it works requires an understanding of how light behaves as it travels through a material. Consider a plane wave propagating in a material and described by the equation:¹⁴

$$E = E_o \cos\left(\frac{2n\pi x}{\lambda}\right) e^{-2\pi kx / \lambda}$$

where

n = index of refraction
 λ = wavelength
 x = distance traveled
 k = extinction coefficient

n and k are optical constants representing the real and imaginary components of the complex index of refraction, η , as defined by

$$\eta = n + ik$$

Note that for dielectric materials no light is absorbed so $k = 0$. For convenience, assume the wave is travelling in air. When the wave impinges on a surface, some portion will be reflected at the interface between the air and the surface and some portion will be transmitted into the material. See Fig. 3.2.

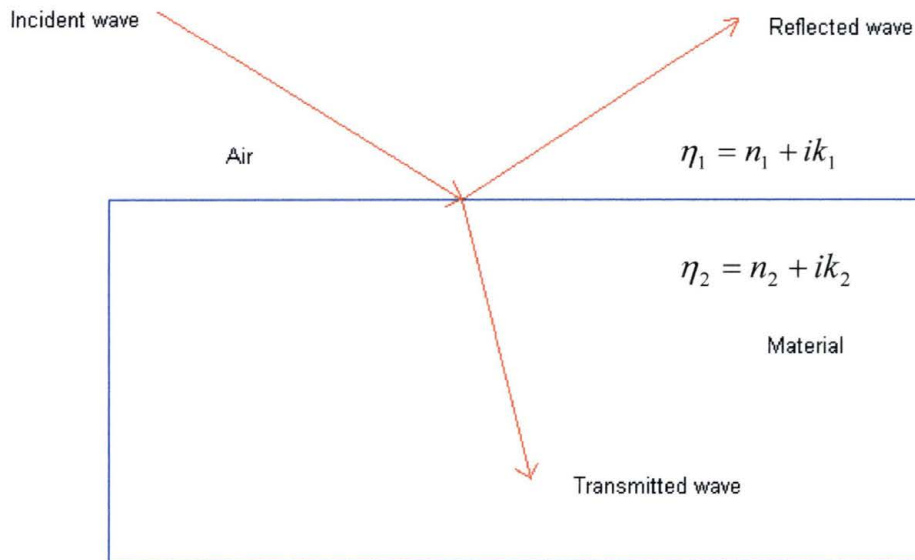


Figure 3.2 Reflection at an interface

The total of reflected and transmitted light must be 100%. Letting R represent the reflection coefficient and T the transmission coefficient we have

$$R + T = 1$$

Now R can be expressed in terms of n and k of the two materials such that

$$R = \frac{(n_2 - 1)^2 + k_2^2}{(n_2 + 1)^2 + k_2^2}$$

This can be simplified further for the case of dielectric materials with large bandgaps. Since light in the visible range ($\sim 3700 - 7000 \text{ \AA}$) typically has insufficient energy to affect lattice vibrational modes or

electronically excite ground state atoms, virtually none of the light is absorbed. Therefore $k_2 = 0$ leaving

$$R = \frac{(n_2 - 1)^2}{(n_2 + 1)^2} = \left| \frac{n_2 - 1}{n_2 + 1} \right|^2$$

The index of refraction for the material can therefore be determined.

After passing through the material the transmitted wave (t_1) strikes and reflects from the lower interface whereby second reflected and transmitted waves (r_2 and t_2) are generated. The reflected wave (r_2) will propagate up to the surface where it strikes the top interface causing its transmitted portion (t_3) to pass back into the air where it can now either constructively or destructively interfere with the first reflected wave (r_1). This process is shown in Fig. 3.3.

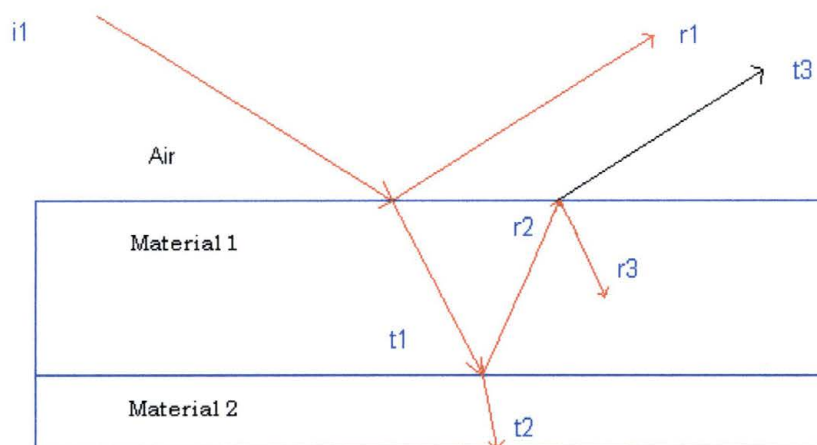


Figure 3.3 Reflection and transmission at two interfaces

This interference is the basis for thicknesses determination and is based on optical path length differences between r_1 and t_3 as shown in Figure 3.4. It should be noted that this is for illustrative purposes only. The actual incident wave will be at near normal incidence.

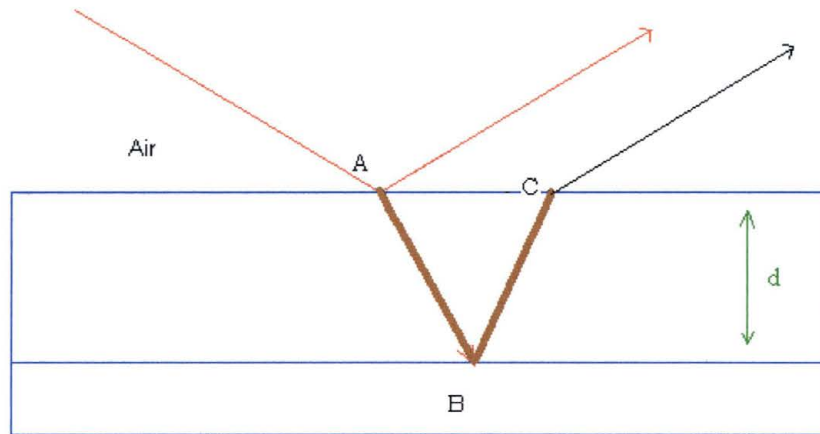


Figure 3.4 Optical path length difference given by line segment ABC

Since most reflectometry measurements are taken at normal incidence, the path length is then $2d$. Therefore the two waves are in phase when the path length equals integral multiples of the wavelength as

$$2d = m \lambda \text{ (for air)}$$

or

$$2nd = m \lambda \text{ (for any material)}$$

where m is an integer. It should be noted that this relationship depends on $n_3 > n_2 > n_1$. In this case a π phase change is introduced at each interface effectively canceling each other. In other cases where only one π phase change is introduced the equation below is required. In any event, this relationship implies a maximum value of R for a given wavelength. Minimum reflections will occur when the two waves are

exactly 180° out of phase, i.e., the path length differences are integral multiples of $\lambda/2$ or

$$2nd = (m + 1/2) \lambda \quad (\text{for any material})$$

The periodicity of these relationships can then be invoked to describe reflectance, R , as

$$R = A + B \cos (2\pi nd/\lambda)$$

where we see that R will vary periodically with wavelength. The thicker the film, the more oscillations will occur across a range of wavelengths since the path length will encompass more integral multiples. Fig. 3.5 illustrates this relationship.

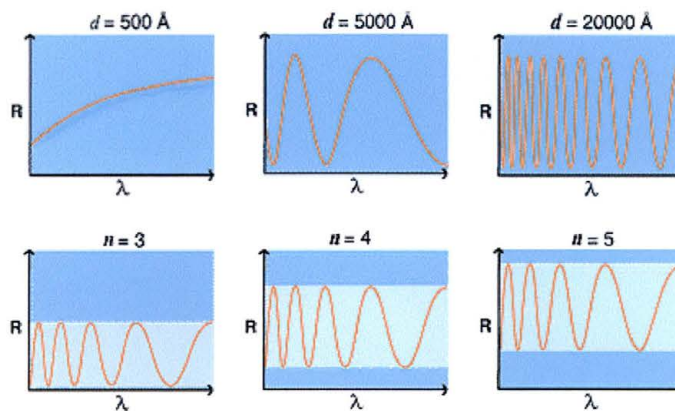


Figure 3.5 The upper graphs show how R varies with film thickness, d . The bottom graph shows how R varies with index of refraction. In both cases $k=0$.¹⁴

The figure also shows the dependence of reflectance magnitude on the index of refraction. As n increases, the magnitude of the R maxima and minima increase proportionally. These graphs are called interferograms.

Optical reflectometers measure these changes in R from the interferograms.¹⁵ The equipment used for this research is a Nanometrics AFT 210 reflectometer. It relies on a precision engineered diffraction grating to resolve white light into its component wavelengths over a range of 3700 - 8000Å. The wavelength is continuously changed over the range by rotating the grating such that they are scanned from smallest to largest. The light is directed normal to the surface of the wafer. The resulting patterns of high and low reflectances are then analyzed by proprietary curve fitting algorithms which take into account specific characteristics of the light source, diffraction grating, detector and film. Data on films is stored in files and contains information on n and k at different wavelengths. With the first three fixed, and given certain properties of the film, the thickness can be determined. This works well for films where the dependence of n and k on wavelength is known. For other materials complementary ellipsometry measurements to determine this would be required.

Various film types can be measured with the exception of metals and other highly reflective films due to the relatively low transmission coefficient. Thickness range capabilities are 100-500,000Å though models outfitted with UV capabilities have detection limits as low as 10Å. Spot sizes range from 5-50 μm depending on the objective lens used. Measurements in this research were done with a 50 μm spot size so were limited to blanket thin films. Integrated circuits rarely have unpatterned

areas smaller than even the minimum spot sizes of these instruments so critical measurements must be done with other methods.

3.2 OPTICAL MICROSCOPY

The use of light microscopes has been widely accepted for wafer inspections for many years. In a fab environment, they are used to inspect for surface damage such as scratches and particle contaminants. For older technologies with larger geometries, standard microscopes were adequate. However as device sizes shrink and the sizes of potential killing defects decrease, improvements in the equipment have followed. Optical lenses have gotten better as polishing techniques and production methods have improved and as new materials with lower dispersion have been developed. In addition new light sources with smaller wavelengths have been incorporated. Recall that the minimum size that can be seen is limited by the wavelength of the light. Smaller wavelengths therefore permit viewing smaller features. Fig. 3.6 shows an optical system schematic.

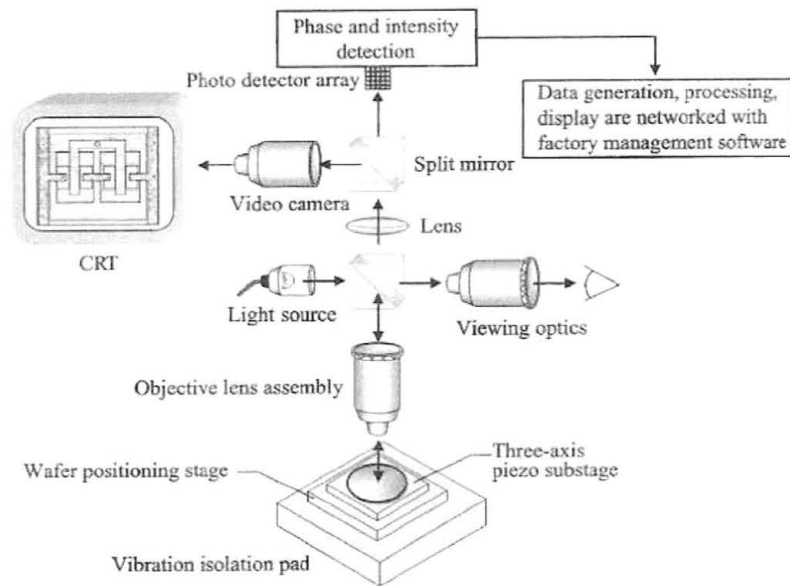


Figure 3.6 General layout of an optical microscope operating in reflection mode.⁸

The sample is located on a three axis stage where light from the source strikes the surface at normal incidence. Reflected light passes back up through the objective lens where a beam splitter will send part of the beam to the viewing optics and the remainder to a video capture system and/or detector interfaced to an integrated production software system. The degree of sophistication involved is application dependent. FA labs will often require minimal automation and magnifications on the order of 150-300X while fab environments may use magnifications as high as 1000X and be fully automated.

The most important operating capability of an optical microscope is the ability to distinguish between features on a sample. This is referred to as resolving ability (as described by the Rayleigh criteria) and is

critical in the detection of subtle features such as delineating n and p doped areas on a substrate. Many techniques such as staining have been developed to improve optical detection capabilities. A related technique, confocal microscopy, is also used to improve contrast by using either a laser or visible light source to scan the sample point by point to enhance contrast.

Optical microscopy is used often in FA labs for monitoring progress of manual polishing and inspection for gross defects. The highest magnification available was attained with a 150X objective and a doubler providing 300X. In addition the objective relied on water immersion to improve resolution.

3.3 SCANNING ELECTRON MICROSCOPY

The advantages and uses of SEM are innumerable in both production and failure analysis work. The amount of related research and data is voluminous. Consequently I will provide only a cursory review of SEM operation and refer readers to the thesis work done by Mr. Michael Matheaus in the fall of 2000.

Scanning electron microscopy is a versatile tool for characterizing many things in the microelectronics industry. First and foremost, it is useful in generating visual images at magnifications many times that available with standard optical microscopes. It also has the advantage of generating three-dimensional images based on changes in the operating

parameters. Furthermore with the appropriate detectors, it is capable of providing elemental analysis of selected areas of interest on a sample.

SEMs are used extensively in both production and FA environments. In the fab, they are used to monitor critical dimensions on deep sub-micron technologies, hence the term CD-SEM, and are capable of high throughput levels (up to 70 wafers/hour).⁸ They are also used for defect review and analysis functions associated with yield management. In the FA lab, they are primarily used to image and identify defects within a patterned IC. In either case, they are usually equipped with digital image capture technologies for archiving findings.

SEM operation relies on the generating of an electron beam that is then directed at the sample surface. Upon striking the surface, several interactions occur, each of which may be monitored independently to provide information on the sample. Different types of detectors are available for collecting and processing signals from secondary electrons, back-scattered electrons, Auger electrons, and x-rays. The detector(s) used is dependent on the type of information desired.

Electrons can be generated by using a tungsten “hairpin” filament, lanthanum hexaboride (LaB_6) crystal or by field emission.

Characteristics of each of these sources is shown below:

	Tungsten Filament	LaB ₆	Field Emission
Operating pressure	~10 ⁻⁶ torr	~10 ⁻⁶ torr	~10 ⁻⁹ torr
Average Life	~60 hrs	~3000 hrs	Virtually unlimited
Resolution	Good	Good	Very good

Tungsten filaments “boil” electrons off of a tip in the middle of a filament as a current is passed through it. This is called thermionic emission. It requires high vacuum to insure long mean free paths of the electrons as well as to prevent the filament from burning up. The LaB₆ crystal operates similarly though it requires less current for emission to occur and consequently has a longer useful life. Field effect emission is produced by applying a potential across a very sharp tip thereby providing the energy necessary for electrons to tunnel across the barrier to a free state. The process produces little energy dispersion, i.e., all of the electrons generated have nearly the same energy. Consequently a FE-SEM is capable of very high resolution.

Following emission the electrons are collimated and then accelerated toward the sample by applying a potential at the anode. The electron beam may be accelerated between 100eV and 100 keV and passes through a series of magnetic and electrostatic lenses which condense and focus it on the sample. The beam is rastered across the sample generating scanning images which are viewed in real time and/or

as an averaged signal. Digital image capture features are common and software driven programs can provide on board dimensional measurements of features.

Spot sizes range from 20-50Å or about 10,000 times smaller than optical equipment. In addition the short wavelengths of electrons allow for atomic scale viewing (recall atoms are on the order of a few Å and electron wavelengths range from .04 Å to 1.2Å for energies of 100 eV to 100 keV). While this can be theoretically determined by the DeBroglie

equation

$$\lambda = \frac{h}{p} = \frac{h}{\sqrt{2mE}}$$

it should be noted that lens limitations preclude sub-atomic scale imaging. Magnification capabilities may reach 100,000 – 300,000 X though imaging may be poor at the extreme limit. In combination these features provide SEM's with the theoretical capability of near-atomic scale imaging.

As the beam impinges on the sample surface several interactions take place. They may take place only near the surface or deeper into the sample depending on beam energy. The higher the energy, the more deeply the beam penetrates. Right below the surface an area known as the excitation volume is generated. The size and shape is dependent on beam energy and as the size of the sample atoms and the angle of incidence. The extent of the elastic and inelastic collisions the electrons have with matrix nuclei and electrons define this volume. Elastic

collisions occur when an electron strikes the core electron cloud of an atom. Since the nucleus is so massive this cloud is bound quite tightly resulting in the incident electron bouncing off with virtually no loss of energy. Elastic collisions also occur when the electron strikes another electron and transfers virtually all of its kinetic energy. Near-elastic collisions are more prevalent in the generation of back-scattered electrons. Back-scattered electrons have higher energies (several hundred eV) compared to secondary electrons (20eV) while the incident beam has energies ranging from 5keV to 35keV.

Inelastic collisions occur as electrons strike other electrons and transfer some portion of their kinetic energy. The amount of energy transferred may eject the atomic electron from its orbit where it can then collide with other electrons and nuclei causing a cascade event (which is responsible for the spreading of the excitation volume). The dislodged electron may also leave the sample as a secondary electron. They are characterized by having significantly less energy than incident electrons and are generated only within the top few Å of the excitation volume.

Other consequences of inelastic collisions include the generation of x-rays as outer shell (higher energy) electrons fall to a lower state to fill the vacancy created by the collision. Auger electrons are also generated when following the filling of the vacancy as described above, the energy loss of the transition is absorbed by another outer shell electron causing it to be ejected. Auger production occurs within only 10-50Å of the

surface while x-rays are produced well down to the bottom of the excitation volume. Figs. 3.7 and 3.8 provide more information on the above discussion.

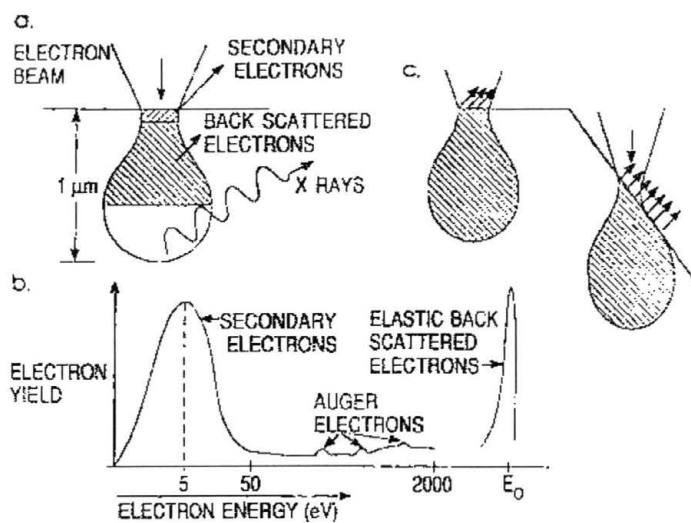


Figure 3.7. Schematic of energy excitation volume profile.⁷

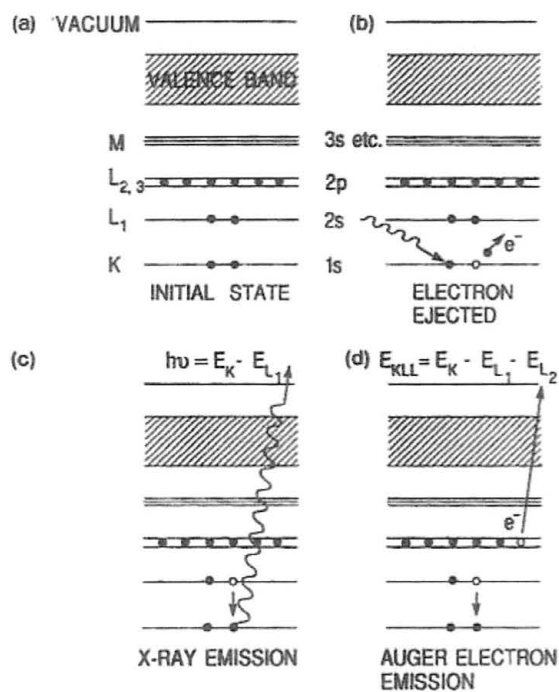


Figure 3.8. Various energy transition events.⁷

SEM's are designed with various detection capabilities depending on the need. Detectors are available for x-rays and Auger electrons as add ons while secondary and back-scattered detectors are usually standard.

In light of the previous discussion note that secondary and Auger electrons are highly surface sensitive and therefore provide good surface imaging. Back-scattered electrons, are dependent on atomic mass in an inverse root relationship therefore are not sensitive enough to draw useful elemental data. It can provide good contrast between areas of differing composition however as the relative Z (atomic number) dependence is exploited. X-ray detection can be done with either energy dispersive or wavelength dispersive spectroscopy (EDS or WDS respectively). Since the x-rays generated in electronic transitions are highly specific to the element in which the transition occurred these methods provide excellent elemental analysis. WDS offer better line-width resolution but is significantly slower as the detector requires rotation of a crystal diffraction grating.

Imaging techniques involve varying such operating parameters as working distance, accelerating voltage, probe current and sample orientations. Reducing the working distance provides higher magnification capabilities and improved resolution. Low accelerating voltages improve surface sensitivity while higher voltages offer deeper imaging and better contrast capabilities. Probe current can be adjusted

to reduce charging effects on non-conducting samples (although grounding techniques are needed also) and sample tilting can provide three-dimensional imaging. Note that sample tilting has inherent problem in that the focal plane is no longer on the surface so moving to a different location on the die may require refocusing.

The SEM work done for this thesis involves imaging for failure analysis and will be discussed in chapter 4.

CHAPTER 4

SAMPLE DATA AND ANALYSIS

4.1 WET ETCH EXPERIMENTS ON BLANKET FILMS

4.1.1 DESIGN

Motorola provided two sample films for wet etching to verify etch rates. Films were grown on boron doped ($N_A = 1 \times 10^{15} \text{ cm}^{-3}$) $\langle 100 \rangle$ silicon wafers 8 inches in diameter. SiO_2 and Si_3N_4 films were grown by chemical vapor deposition techniques however the exact process parameters were not available. Standard etch recipes were to be used including hot H_3PO_4 for Si_3N_4 etching and HF for SiO_2 etching.

The first step was to establish an experimental clean and etch protocol for each film which is detailed in Appendix B. The actual cleaning steps were modified for each etch run based on the results of previous runs.

Concurrently with the experimental design phase, it was necessary to establish an in-house safety protocol for handling HF. HF burns are particularly bad in that 1) someone may not realize he/she has had skin contact until several hours later, and 2) exposure on greater than two square inches of skin surface may be lethal. Consequently proper

handling, safety equipment, and waste management issues were addressed prior to the SiO_2 /HF etch runs. Appendix D provides additional information on HF safety as well as other chemical safety issues.

Film thickness analysis was performed on the Nanometrics Nanospec AFT 210 optical reflectometer. Nominal thicknesses were provided by Motorola and measured thicknesses were averaged over five points on each wafer surface and are compared below.

<u>Film</u>	<u>Nominal Thickness</u>	<u>Measured Thickness</u>
SiO_2	1500 Å	1493 Å±4 Å
Si_3N_4	2001 Å	1993 Å±1 Å

4.1.2 Si_3N_4 DATA AND ANALYSIS

In total, seven etch runs were carried out on the nitride films. Following the first etch run results, it was decided that we would also evaluate the effects of different pre-clean processes on the etch rate. This was in response to a hazy residue seen on the films after rinsing and drying. Changes in the pre-etch cleaning steps are summarized in the matrix below. All cleaning steps were done at ambient temperature 21° C – 23° C.

Clean Step \ Etch Run	Etch Run					
	A	B	C	D	E	F
5 min Micro sonic	X					
18 MΩ DI Rinse	X					
IPA rinse	X					
5 min ACT sonic	X	X	X	X	X	
5 min IPA sonic					X	
IPA rinse	X				X	
18 MΩ DI Rinse						
UP N ₂ dry	X	X	X	X	X	X

Micro → Micro -90™ detergent/surfactant
 DI → deionized water
 IPA → isopropyl alcohol
 ACT → acetone
 UP → ultra pure

Following run A, the samples had a visible haze that we thought could be the Micro cleaning agent. After following up with Motorola, it was decided the detergent would not be used. Etch runs B, C, and D retained the same protocol then as the effects of H₃PO₄ concentration in the etch bath were evaluated.

Each etch run required etching five die; one each for 2, 4, 6, 8 and 10 minutes. Each required heating the acid in an oil bath on a hot plate to 153°C ±1°. The oil bath, consisting of a crystallizing dish filled with Dow Corning DC 704 silicon based oil, provided for uniform heating of the acid. Silicon based oil was used to minimize heterogeneous particulate contamination of the die from condensed oil vapors.

Pursuant to the discussion in section 2.4.1 on nitride etching, we wanted

to determine the effects of the H_3PO_4 bath composition on the etch rate. Refluxing equipment was not available. To see these effects, several combinations of volume and solution refresh were used. These are shown below:

Etchant Vol. (ml)	A	B	C	D	E	F
	150	150	325	150	150	150
Die 1	0	0	0	X	X	X
2	0	0	0	X	X	X
3	0	0	0	X	X	X
4	X	X	0	X	X	X
5	X	X	0	X	X	X

The lower part of the matrix indicates whether a given die was etched in a fresh solution (X) or in the same solution used to etch other die (0). All etch runs subsequent to run C used fresh acid baths for each die. All runs were quenched in 18 M Ω DI, rinsed in IPA and dried with UP N₂ following etching.

Visual comparison of the surfaces showed color variation from one die to the next but was more pronounced in the last three. This is in keeping with the interference effects discussed in section 3.1 relative to the color patterns exhibited as film thickness changes.

Figure 4.1 shows the die color after each successive etch.

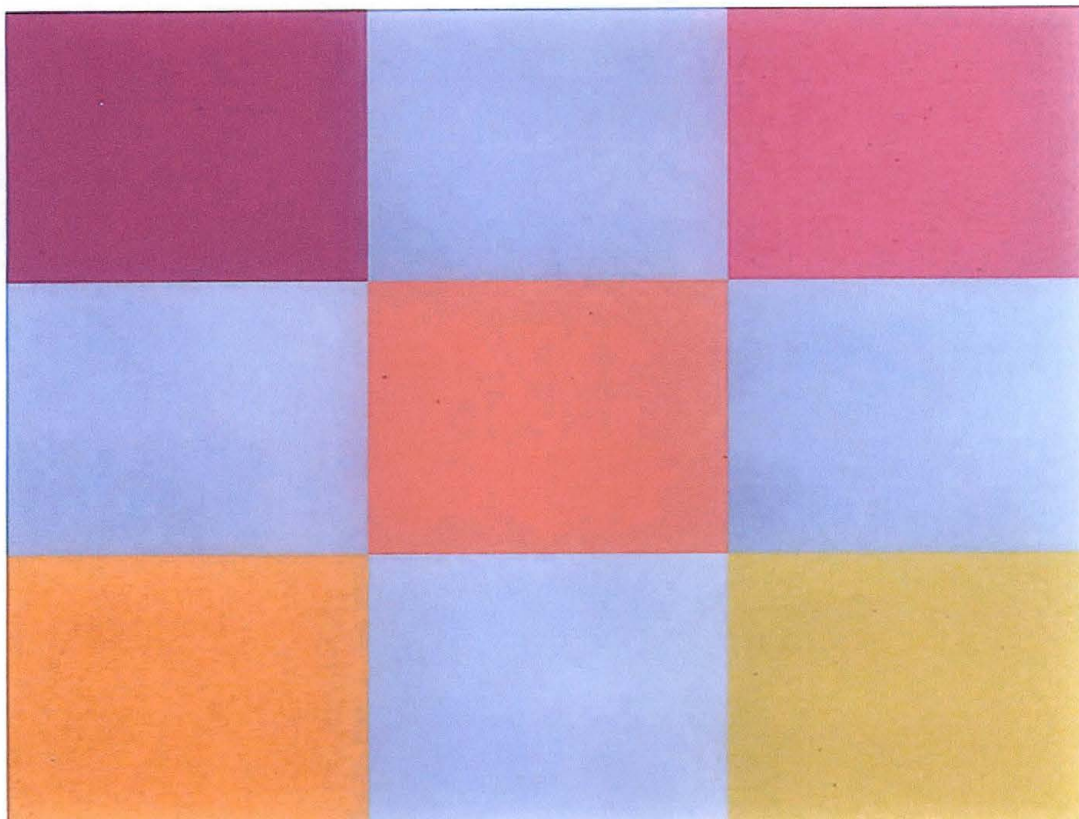


Figure 4.1 The color changes associated with film thickness variations. Starting with the 2 minute etch in the upper left and moving right and top to bottom to the 10 minute etch in the lower right. The blue squares are spacers.

Nanospec measurements were taken at five points on each die surface as shown in Figure 4.2.

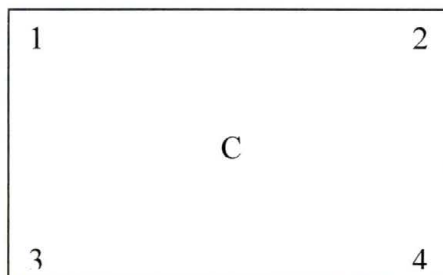


Figure 4.2 Die measurement locations.

Arithmetic means and standard deviations were automatically calculated by the equipment software. The data are included in Tables 4.1-4.6.

Table 4.1

Etch Run A					
Sample #	Position	Etch Time	Thickness (Å)	Mean (Å)	Std. Deviation (Å)
A1	1	2 minutes	1964	1959	5
	2		1955		
	3		1953		
	4		1961		
	C		1962		
A2	1	4 minutes	1948	1945	3
	2		1947		
	3		1942		
	4		1943		
	C		1947		
A3	1	6 minutes	1839	1844	4
	2		1840		
	3		1846		
	4		1849		
	C		1847		
A4	1	8 minutes	1872	1865	6
	2		1858		
	3		1862		
	4		1871		
	C		1863		
A5	1	10 minutes	1753	1752	2
	2		1752		
	3		1753		
	4		1749		
	C		1752		

Table 4.2

Etch Run B					
Sample #	Position	Etch Time	Thickness (Å)	Mean (Å)	Std. Deviation (Å)
B1	1	2 minutes	2013	2004	7
	2		1999		
	3		2010		
	4		2000		
	C		1997		
B2	1	4 minutes	1905	1905	7
	2		1895		
	3		1912		
	4		1911		
	C		1904		
B3	1	6 minutes	1814	1814	4
	2		1813		
	3		1813		
	4		1819		
	C		1809		
B4	1	8 minutes	1833	1828	3
	2		1830		
	3		1825		
	4		1828		
	C		1826		
B5	1	10 minutes	1743	1743	5
	2		1740		
	3		1738		
	4		1751		
	C		1741		

Table 4.3

Etch Run C					
Sample #	Position	Etch Time	Thickness (Å)	Mean (Å)	Std. Deviation (Å)
C1	1	2 minutes	1963	1960	3
	2		1963		
	3		1956		
	4		1959		
	C		1960		
C2	1	4 minutes	1966	1964	4
	2		1971		
	3		1963		
	4		1960		
	C		1961		
C3	1	6 minutes	1865	1875	6
	2		1877		
	3		1878		
	4		1881		
	C		1873		
C4	1	8 minutes	1864	1865	10
	2		1880		
	3		1867		
	4		1853		
	C		1860		
C5	1	10 minutes	1728	1727	12
	2		1707		
	3		1730		
	4		1741		
	C		1731		

Table 4.4

Etch Run D					
Sample #	Position	Etch Time	Thickness (Å)	Mean (Å)	Std. Deviation (Å)
D1	1	2 minutes	1963	1960	2
	2		1962		
	3		1961		
	4		1957		
	C		1959		
D2	1	4 minutes	1910	1910	3
	2		1913		
	3		1912		
	4		1906		
	C		1907		
D3	1	6 minutes	1841	1851	6
	2		1853		
	3		1856		
	4		1856		
	C		1848		
D4	1	8 minutes	1780	1771	6
	2		1770		
	3		1764		
	4		1773		
	C		1770		
D5	1	10 minutes	1763	1754	13
	2		1745		
	3		1736		
	4		1768		
	C		1756		

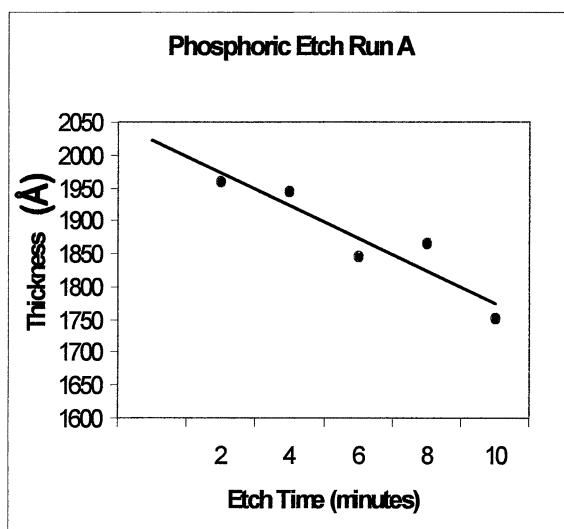
Table 4.5

Etch Run E					
Sample #	Position	Etch Time	Thickness (Å)	Mean (Å)	Std. Deviation (Å)
E1	1	2 minutes	1984	1984	2
	2		1981		
	3		1983		
	4		1986		
	C		1985		
E2	1	4 minutes	1893	1887	7
	2		1881		
	3		1880		
	4		1895		
	C		1885		
E3	1	6 minutes	1843	1843	4
	2		1844		
	3		1850		
	4		1839		
	C		1840		
E4	1	8 minutes	1747	1748	2
	2		1750		
	3		1751		
	4		1747		
	C		1745		
E5	1	10 minutes	1656	1650	17
	2		1673		
	3		1648		
	4		1627		
	C		1648		

Table 4.6

Etch Run F					
Sample #	Position	Etch Time	Thickness (Å)	Mean (Å)	Std. Deviation (Å)
F1	1	2 minutes	1929	1929	3
	2		1926		
	3		1928		
	4		1933		
	C		1930		
F2	1	4 minutes	1876	1874	2
	2		1872		
	3		1873		
	4		1874		
	C		1873		
F3	1	6 minutes	1786	1786	3
	2		1790		
	3		1782		
	4		1785		
	C		1789		
F4	1	8 minutes	1747	1754	6
	2		1753		
	3		1760		
	4		1760		
	C		1749		
F5	1	10 minutes	1633	1631	3
	2		1633		
	3		1625		
	4		1632		
	C		1631		

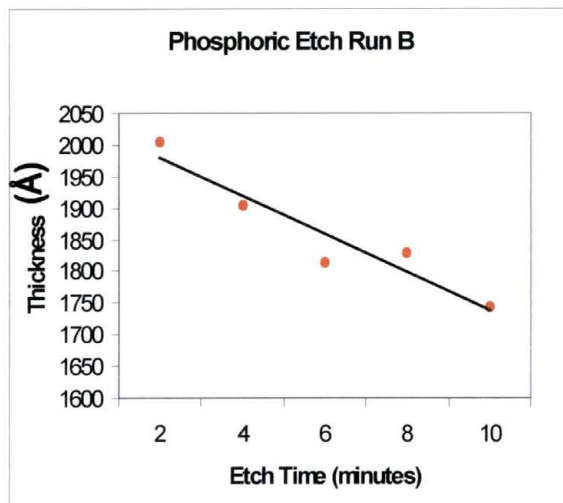
Thickness measurements were then plotted against etch times and linear regression analysis performed which provided a statistical etch rate from the slope and a regression parameter in the form of a correlation coefficient. The graphs are included in Figures 4.3-4.8.



- Micro sonic (5 minute)
@ 23° C
 - 18Meg H₂O (DI) rinse
 - Isopropyl alcohol (IPA)
rinse
 - Acetone (ACT) sonic (5
min) @ 23° C
 - Isopropyl alcohol (IPA)
rinse
 - filtered N₂ dry

 - The 2, 4 and 6 min etches
carried out in the same
acid solution (150 ml).
 - The 8 and 10 minute etch
solutions were fresh.
 - Baths at 153°C ± 1°.
- ⇒ Etched samples
“hazy”

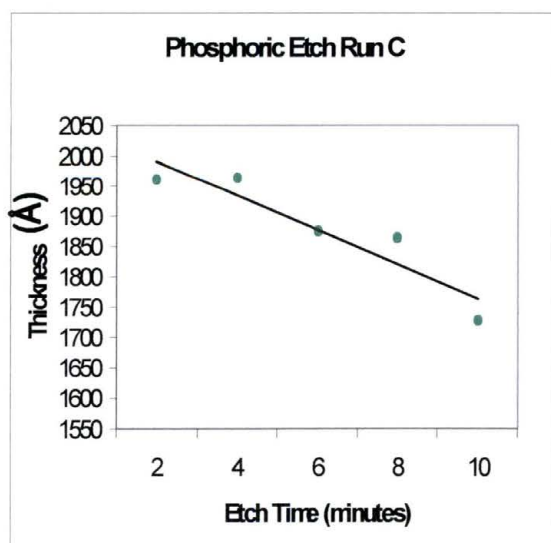
Figure 4.3 Run A including clean and etch details.



- Acetone (ACT) sonic (5 min) @ 23° C
- Isopropyl alcohol (IPA) rinse
- filtered N₂ dry
- The 2, 4 and 6 minute etches were carried out in the same acid soln (150 ml).
- The 8 and 10 minute etch baths were fresh solutions.
- Baths at 153°C ± 1°.

⇒ Etched samples “hazy”

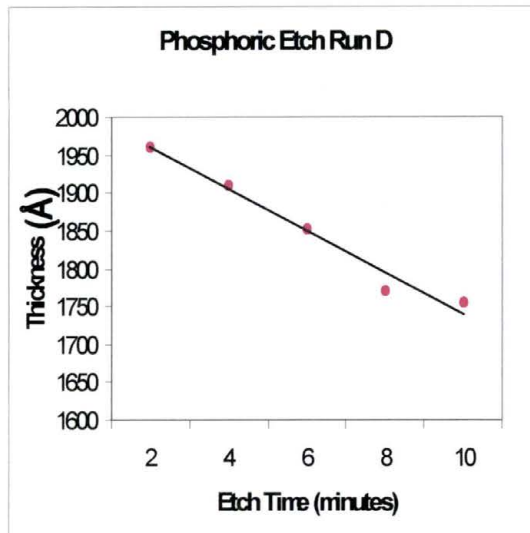
Figure 4.4 Run B including clean and etch details.



- Acetone (ACT) sonic (5 min) @ 23° C
- Isopropyl alcohol (IPA) rinse
- filtered N₂ dry
- ALL etches (2, 4, 6, 8 and 10 minutes) were carried out in the same acid solution (changed to 325 ml vol).
- Baths at 153°C ± 1°.

⇒ Etched samples “hazy”

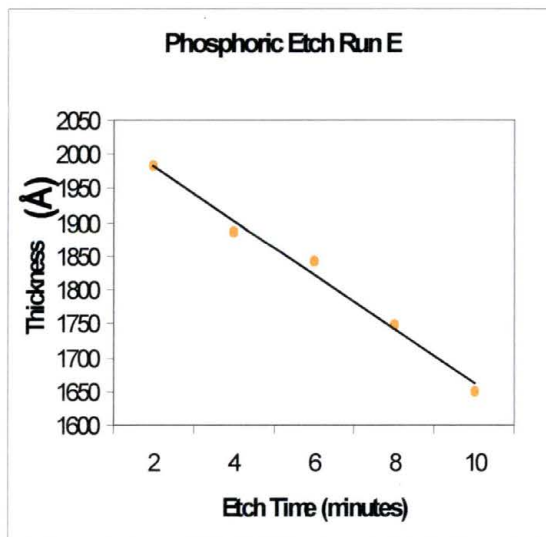
Figure 4.5 Run C including clean and etch details.



- Acetone (ACT) sonic (5 min) @ 23° C
- Isopropyl alcohol (IPA) rinse
- filtered N₂ dry
- ALL etches (2, 4, 6, 8 and 10 minutes) were carried out in INDIVIDUAL fresh acid solutions (150 ml).
- Baths at 153°C ± 1°.

⇒ Etched samples “hazy”

Figure 4.6 Run D including clean and etch details.



- Acetone (ACT) sonic (5 min) @ 23° C
- Isopropyl alcohol (IPA) sonic rinse @ 23° C
- IPA rinse
- DI H₂O rinse
- filtered N₂ dry

- ALL etches (2, 4, 6, 8 and 10 minutes) were carried out in INDIVIDUAL fresh acid baths (150 ml).
- Baths at 153°C ± 1°.

⇒ Less “hazy” samples

Figure 4.7 Run E including clean and etch details.

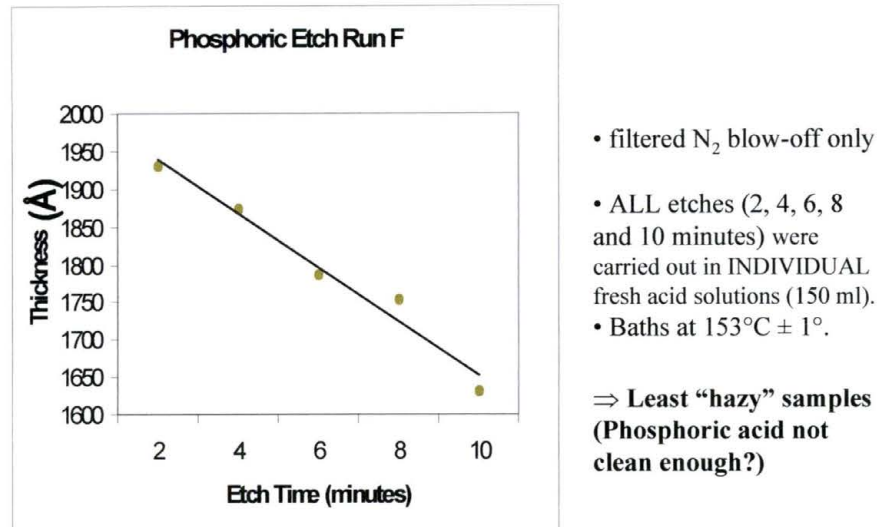


Figure 4.8 Run F including clean and etch details.

A summary of the results is provided below.

Table 4.7 Nitride etch comparisons.

Summary Nitride Etch Results

Series	Etch Rate (Å/min)	* Y-Intercept Film Thickness (Å)	Regression Parameter
Etch A	22.7	2006	0.948
Etch B	26.7	2015	0.956
Etch C	24.3	2019	0.929
Etch D	26	2003	0.989
Etch E	33.7	2013	0.986
Etch F	34.6	2001	0.990

* The nominal specified silicon nitride layer thickness provided by Motorola was 2,001 Å, N₂-blown sample measured 1,993 ± 1 Å with SWT Nanospec 210 optical reflectivity system.

All etched die exhibited a hazy residue. The degree of “haziness” appeared to decrease first after the detergent clean was discontinued, then again when the ACT sonic was followed by an IPA sonic and again when all pre-clean protocol was eliminated except an N₂ blow off. It is suspected that the detergent sonic was leaving some residue behind though it was not explored after the decision to discontinue use. We also suspect that the ACT residue after sonication was not being removed effectively by the IPA rinse. We did see some reduction however when the ACT sonic was followed by an IPA sonic. The ACT penetrating deep into the micro-structure through sonication seems to indicate the need for IPA sonications to then flush the micro-structure effectively.

Interestingly, the haze was minimized by N₂ cleaning only. This in and of itself is insufficient to eliminate the entire cleaning protocol since the haze was not visible to the eye until etching was completed. It is well known that ACT is suspected of not being as clean as once thought, i.e., residues can be significant problems as they can act as an etch mask.

Another potential cause of the hazing is the phosphoric acid. Though a cleanroom grade of H₃PO₄ was used (Ashland 85%), by comparison to other cleanroom grade chemicals it contains higher levels of impurities which could be responsible.

It is seen by the first three etch runs that changing the bath to maintain relative concentrations may be necessary. The low correlation coefficients and data point comparisons of runs with multiple die etched

in the same solutions suggests this as previously discussed in section 2.4.1. The last three runs showed significantly better correlation coefficients. The last two also yielded good etch rate results in keeping with rates reported by Stanford University (32-35Å/min) for hot H₃PO₄ etching of CVD silicon nitride. Generally speaking however precise comparisons are difficult since reported rates are dependent on maintaining bath concentration by refluxing which was unavailable.

4.1.3 SiO₂ DATA AND ANALYSIS

Only one SiO₂/HF etching run was conducted. The standard etch regime involved using an etch bath of 10:1 buffered HF at ambient temperature. The HF is buffered with NH₃F to maintain the F⁻ ion concentration over time. Five die were etched for 1, 2, 3, 4 and 5 minutes respectively. The pre-clean using the UP N₂ blow off was adopted based on the best nitride etch results. The buffered HF etch bath (J. T. Baker – low Na CMOS grade) required the use of teflon or polypropylene beakers instead of glass. Glass is primarily composed of SiO₂ which is easily and quickly etched by the HF.

When etching was complete, the die were rinsed in DI water to quench the reaction, rinsed with IPA and dried with N₂. Nanospec thickness measurements were conducted in the same manner as for the etched nitride films.

Data plotting and regression analysis were conducted identically as well. The data are shown in Table 4.8 and Figure 4.9.

Table 4.8

Etch Run HF					
Sample #	Position	Etch Time	Thickness (Å)	Mean (Å)	Std. Deviation (Å)
HF1	1	1 minute	906	932	4
	2		947		
	3		911		
	4		950		
	C		945		
HF2	1	2 minutes	367	370	21
	2		369		
	3		377		
	4		372		
	C		365		
HF3	1	3 minutes	209	205	5
	2		221		
	3		192		
	4		202		
	C		199		
HF4	1	4 minutes	206	184	11
	2		170		
	3		170		
	4		184		
	C		189		
HF5	1	5 minutes	<20	n/a	n/a
	2		<20		
	3		<20		
	4		<20		
	C		<20		

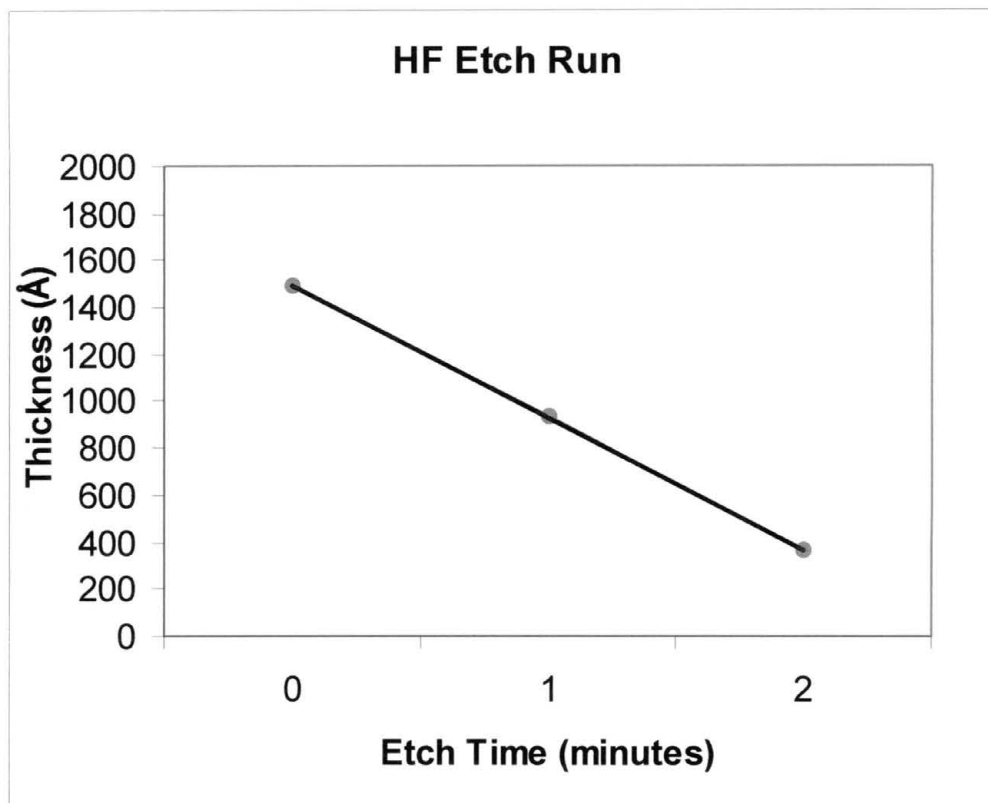


Figure 4.9 HF etch run graph.

Film thicknesses after one and two minutes were reliable when rechecked for repeatability. Thicknesses after 3, 4 and 5 minutes were deemed unreliable. Measurements were near or below the detection limit of the equipment ($\sim 200\text{\AA}$).¹⁵ as characterized by the inability to accurately repeat the measurements. Consequently, the linear regime of the regression produced an etch rate of $562\text{\AA}/\text{min}$. While there is insufficient data from one experiment to proffer statistically valid results it appears that this etch rate compares favorably with published etch rates of oxides ($100\text{-}1000\text{\AA}/\text{min}$).³ Oxide etch rates vary considerably

between 100-1000 Å/min depending on doping levels and processes used. Process parameter details were not available from the supplier for our films. Etch rates this large however do support our results of the last two two-minute etches. With a starting thickness of only ~1500 Å the film would be completely removed somewhere between 2½ and 3 minutes thereby giving readings consistent with approaching the detection limits.

Another interesting result in the experiment was the dome-shaped features on the surface observed upon optical examination (Figures 4.10 and 4.11).

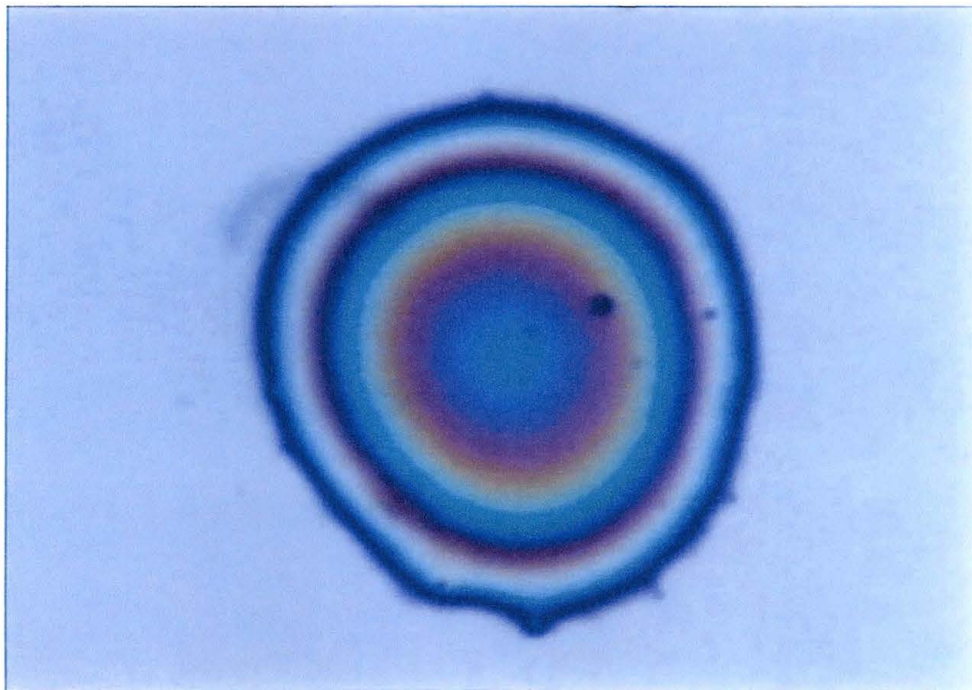


Figure 4.10 Optical view of HF etch artifacts at 50X. Color variations suggest unetched oxide.

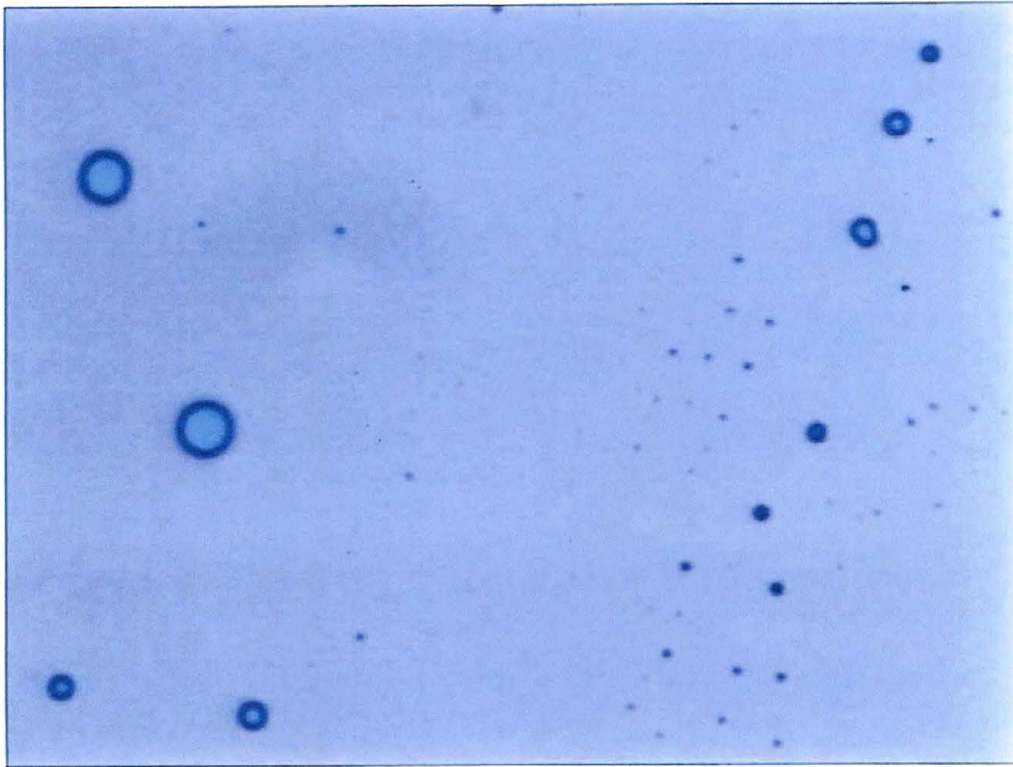


Figure 4.11 Magnification of artifacts at 10X.

A thickness measurement indicated a feature height of 300-500 Å and a slight rainbow color variation near the outer edges seems to suggest the presence of unetched oxide. This is consistent with interference effects of the reflected light waves one would expect as discussed in the section on optical reflectivity. Additional EDS scans (Figure 4.12) indicate the presence of carbon and oxygen suggesting possible hydrocarbon contamination as well.

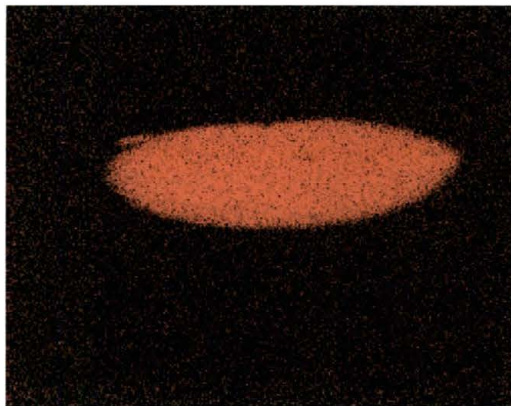
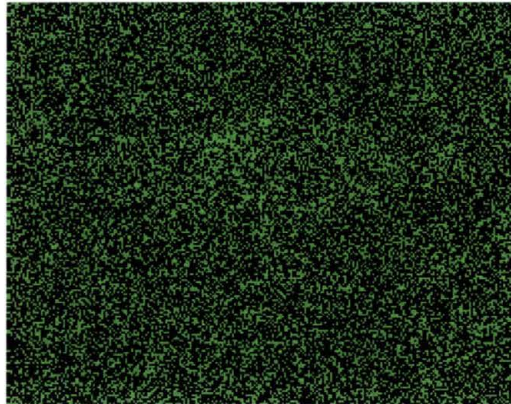
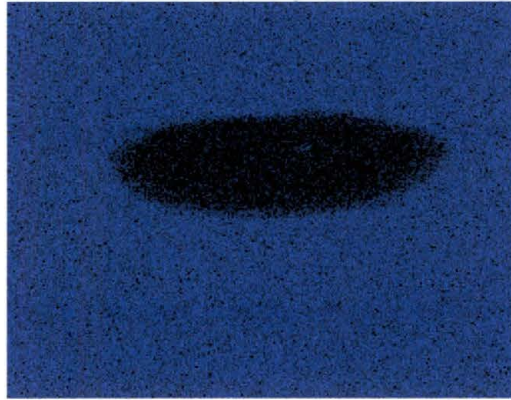


Figure 4.12 (Top to bottom) Silicon, oxygen and carbon EDAX maps of the dome feature. Taken at 1500X, 5 keV, 67 degree tilt. Courtesy of Dr. Carlos Gutierrez and Mr. Mike Mathaeus.

The oxygen map is evidence of a re-oxidation of the surface due to air exposure. The density of these features may be high enough to permit FTIR (fourier transform infrared) spectroscopy for possible organic contamination. This technique is capable detecting specific bonding arrangements in organic compounds based on absorption of IR wavelengths.

If the features are unetched oxide, it may be caused by a stagnant layer containing high concentrations of etch products near the die surface. Such a layer would negatively impact etch uniformity over the die surface. Its also possible that the carbon contaminant acted as an etch mask resulting in the presence of the unetched oxide domes. Additional experiments testing etch bath agitation and recirculation may bear this out.

4.2 FAILURE ANALYSIS

4.2.1 DIE REMOVAL AND DEPASSIVATION

The failure analysis work reported in this thesis required the die to be removed from the package. The process used for this is dependent on the packaging materials. Most die are encapsulated in a plastic polymer composed of amino- hardened novolac epoxides. This material can be removed by immersion in 90% yellow fuming nitric acid (HNO_3) heated in a glass beaker to $\sim 125^\circ\text{C}$. Depending on the package size, the time required may be from 2-10 minutes. This must be carried out in an acid

hood due to the dangerous vapors given off by this acid even at ambient temperature.

After removing the die it can be rinsed with 100% acetone under the hood (under no circumstances should isopropanol be used since it is explosive if mixed with fuming nitric acid) at this point the bond wires will still be attached but can be easily removed by hand. It should then be sonicated and is ready for depassivation if required.

Other package types including ball grid and pin grid arrays (BGA and PGA) are made of different material which can be removed by immersion in a sulfuric acid (H_2SO_4) bath at $\sim 215^\circ C$.

Removal times can easily be 20-30 minutes after which rinsing with isopropanol (IPA) and sonicating in acetone leaves the die ready for depassivation. Ceramic package designs are also occasionally used which require heating on an aluminum stub on a hotplate to $\sim 400^\circ C$. The bonding material will liquefy on the chip and then can be lifted easily from the package.

Depassivation was carried out in the Trion Phantom RIE using the following recipe:

RF Power	150 Watts
Pressure	125 mtorr
Gases	30 SCCM CHF_3 10 SCCM O_2

The time required for the deprocessing is dependent on the particular device being etched and can range from 600-1600 seconds. Determining if the device has been completely depassivated is often difficult. Figure 4.13 and 4.14 show a device after 700 seconds and 1000 seconds respectively.

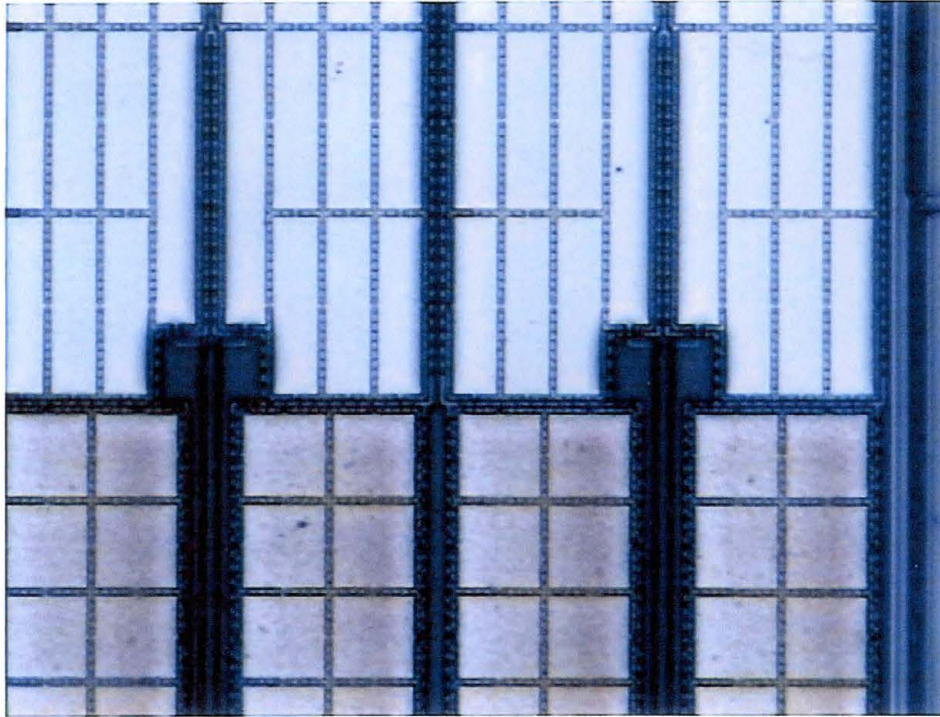


Figure 4.13 Optical view of device after 700s depassivation at 10X.

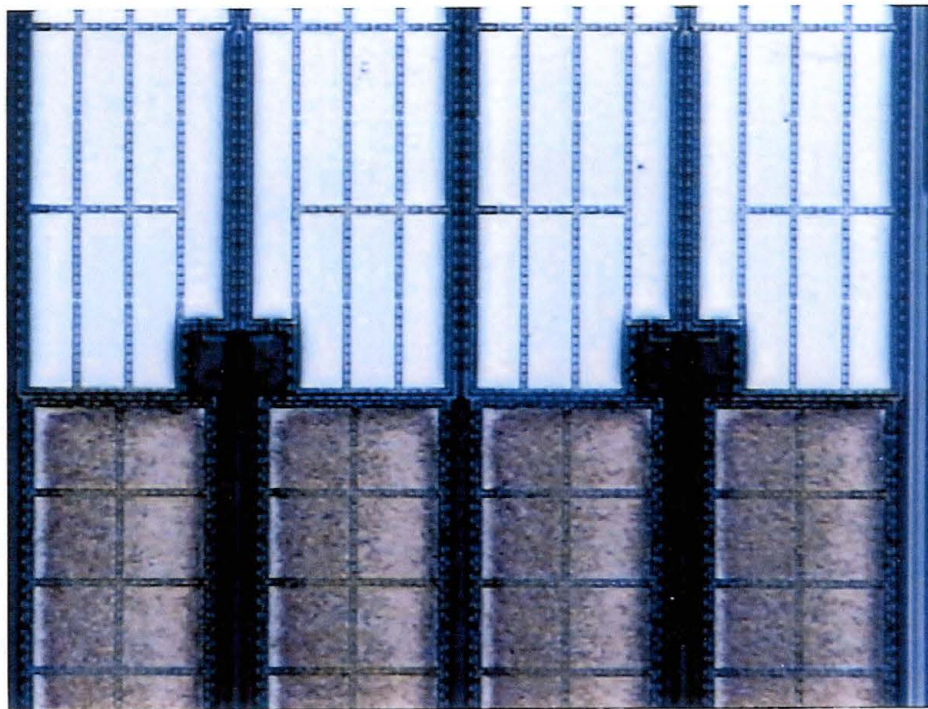


Figure 4.14 Optical view of device after 1000s depassivation at 10X.

Both exhibit signs of overetching as seen by the brown color over the lower sections of each. The upper white areas are exposed metal directly beneath the passivation layers and typically will indicate that passivation has been removed. Device layout however can make it difficult to compare side by side features viewed top down. There are other subtle methods involving visual inspection of certain features around the bond pads that will offer clues but I have not as yet done this. It is important to note here that the first 200 seconds of the reactive ion etch removed little material suggesting a non linear etch rate profile or some etch initialization requirement.. Therefore subsequent depassivation runs on

the same part are not additive. I will be conducting further analysis on this at a later date.

Occasionally following depassivation, optical scope inspection will provide physical evidence near the suspected failure site as seen in Figure 4.15. In this image an EOS (electrical overstress) event deep in the device blew a hole through the top passivation layer. If the defect can be viewed from this vantage point further processing into the device from the top

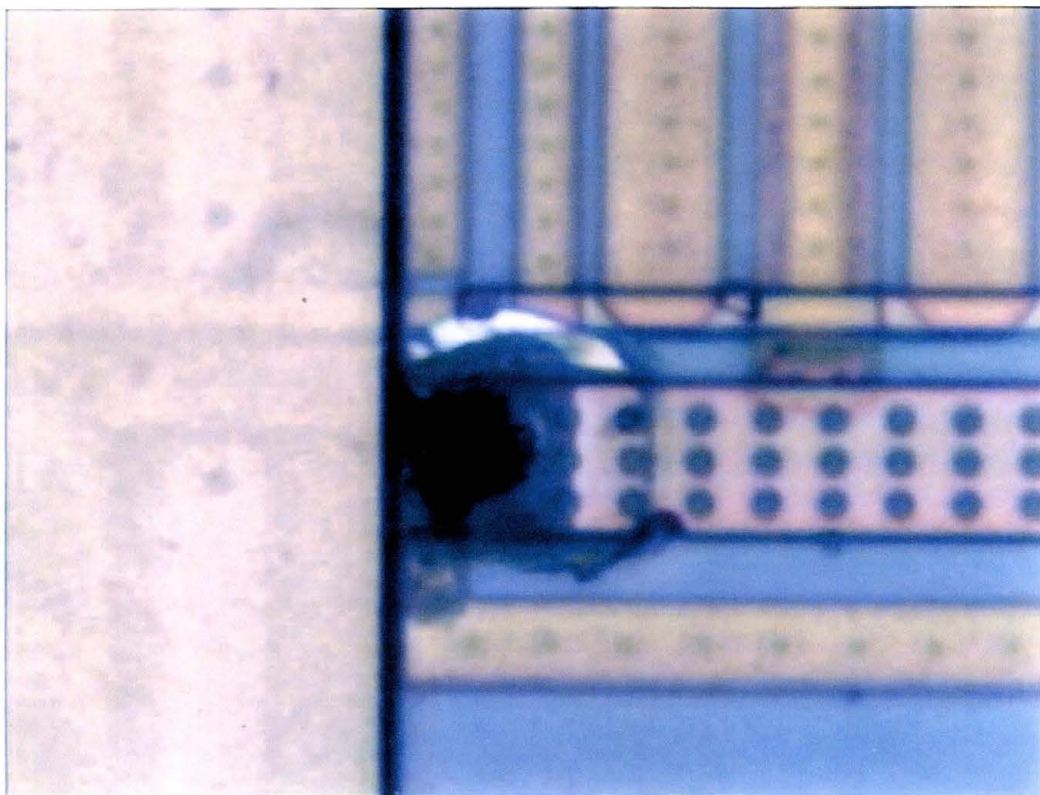


Figure 4.15 Optical image of an EOS induced failure at 100X.

4.2.2 TOP DOWN DEPROCESSING

Top Down Polishing

For defect areas lying deep within the device, polishing may be the quickest and most controllable way to reach it. Polishing is a mechanical process using a rotating wheel holding an abrasive pad on which the die surface rides. Material is removed at different rates depending on the force applied and the rotational speed. Polishing equipment may be fully automated whereby the sample is mounted or may be a manual system requiring the analyst to manipulate the sample on the polishing wheel. This failure analysis work was done manually.

The first step is to mount the die on an aluminum stub using melted wax and making sure the die is flat. A Chemomet[®] I polishing mat is placed on the wheel and a 1.0 μ m silica slurry is put onto the rotary wheel. Different size slurries and rotational speeds may be used and should be determined by how close to the area of interest you are. The closer you are, the slower the removal rate you need so you do not polish away the defect. As you get closer to the defect area, it is wise to optically view the sample often and capture images of anomalous structures.

It is also important to maintain an even and wide polishing front across the surface. This insures an even removal of material across the

die providing easier endpoint detection. Viewing of the polishing front will tell the trained eye what layer of the device is exposed.

Multilayered devices typically have metal layers overlaid perpendicular to each other so if you know which way the top layer runs relative to your view, you can identify them as you polish deeper. Metal lines will appear dark to light brown optically (see Figure 4.16). The dark brown is attributable to the very thin oxide layer remaining above as you begin to see the metal.

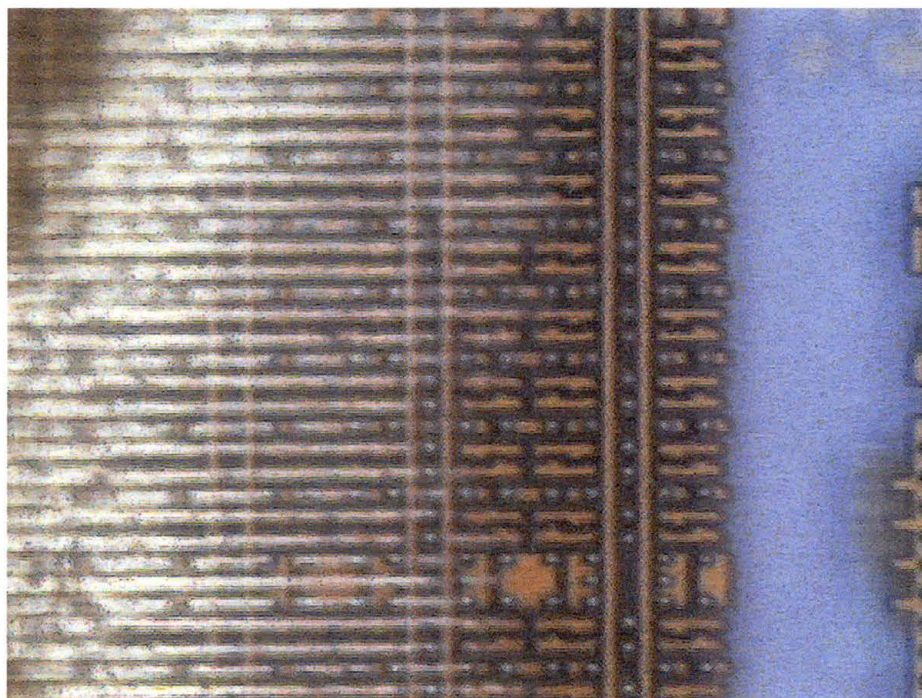


Figure 4.16 Metal 1 lines (brown) run vertically on the right while remnants of metal 2 barrier run horizontally on the left.. Optical image at 125X.

Below the metal lies the Ti barrier metal that appears white and below that, the oxide layer, which is quite thick ($\sim 7,500-10,000\text{\AA}$). The

polishing front across the ILD will exhibit a rainbow effect due to the interference patterns of the reflected light as discussed in section 3.1.

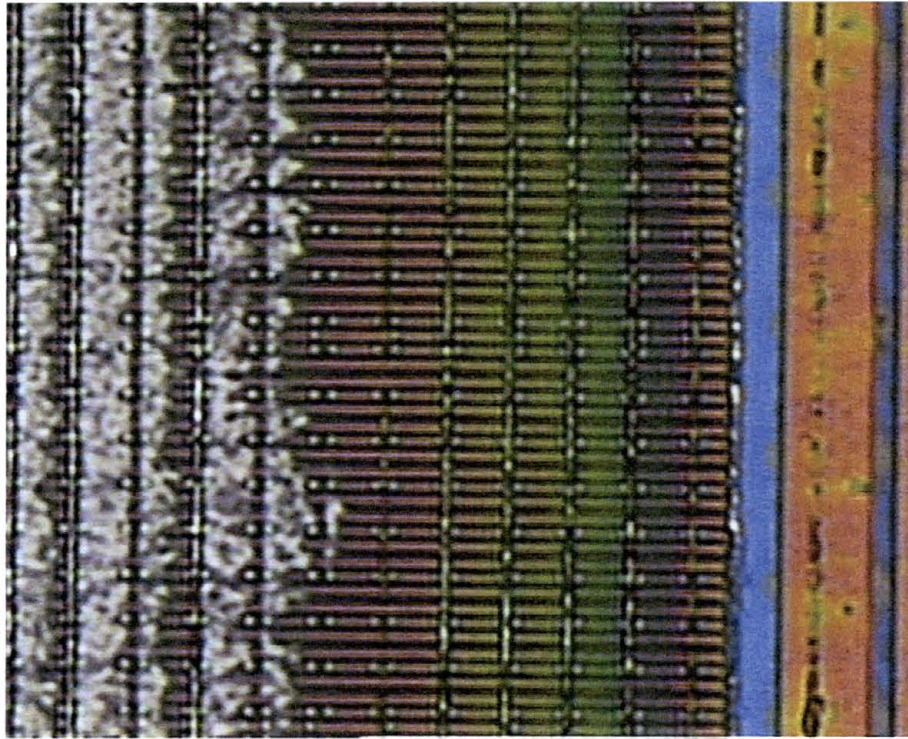


Figure 4.17 Color variation of oxide over metal 2 layer as front proceeds from right to left. 125X



Figure 4.18 Polishing front removing metal 1 as it

The oxide thickness remaining can be estimated by matching the color to the chart in Table 4.9.

Table 4.9 Colors associated with oxide thickness.³

Film Thickness (μm)	Color and Comments	Film Thickness (μm)	Color and Comments
0.05	Tan	0.54	Yellow green
0.07	Brown	0.56	Green yellow
0.10	Dark violet to red violet	0.57	Yellow to "yellowish" (not yellow but is in the position where yellow is to be expected; at times appears to be light creamy gray or metallic)
0.12	Royal blue	0.58	Light orange or yellow to pink borderline
0.15	Light blue to metallic blue	0.60	Carnation pink
0.17	Metallic to very light yellow green	0.63	Violet red
0.20	Light gold or yellow; slightly metallic	0.68	"Bluish" (not blue but borderline between violet and blue green; appears more like a mixture between violet red and blue green and looks grayish)
0.22	Gold with slight yellow orange	0.72	Blue green to green (quite broad)
0.25	Orange to melon	0.77	"Yellowish"
0.27	Red violet	0.80	Orange (rather broad for orange)
0.30	Blue to violet blue	0.82	Salmon
0.31	Blue	0.85	Dull, light red violet
0.32	Blue to blue green	0.86	Violet
0.34	Light green	0.87	Blue violet
0.35	Green to yellow green	0.89	Blue
0.36	Yellow green	0.92	Blue green
0.37	Green yellow	0.95	Dull yellow green
0.39	Yellow	0.97	Yellow to "yellowish"
0.41	Light orange	0.99	Orange
0.42	Carnation pink	1.00	Carnation pink
0.44	Violet red		
0.46	Red violet		
0.47	Violet		
0.48	Blue violet		
0.49	Blue		
0.50	Blue green		
0.52	Green (broad)		

This requires you know the starting thickness and, since the colors repeat for thick films you must know which color front is exposed (first blue, second blue or what).

Once the defect area is reached, the defects may be visible optically or may require SEM imaging or both. The decision is driven by whether it can be characterized by optical images.

Top Down Etching

The deprocessing of the die by wet or dry etching may be used if more specific information is known about the location of the defect area and/or the type of defect. In these cases certain wet or dry chemistries can be used to quickly remove layers above the defect. A most extreme example involves removing all patterned features from the die right down to the silicon substrate. This can be accomplished by immersing the die in 49% HF for ~30 seconds. It is very important that the device is completely depassivated before doing this. If not, the passivation remaining will act as an etch stop and inhibit etching of those areas. HF to substrate etching is often done when ESD (electrostatic discharge) or EOS (electrical overstress) is suspected. Both occur at the transistor level of the device and will often melt the substrate around the event location. Figures 4.19 and 4.20 show SEM images of EOS and ESD damage exposed with this technique.

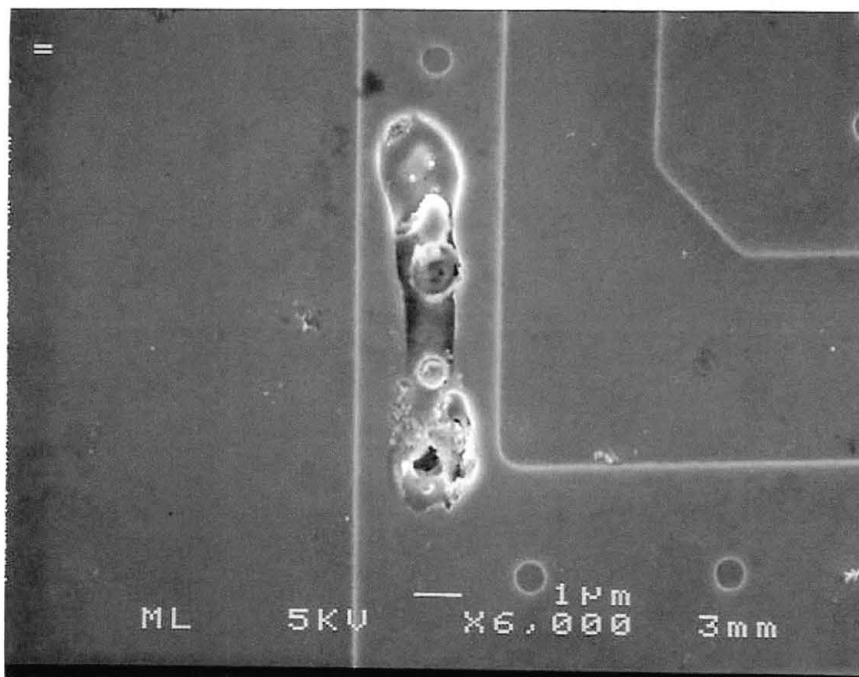


Figure 4.19. SEM image of EOS damage to the silicon substrate at contact area.



Figure 4.20 Sem image of ESD damage to substrate in the gate area.

Other common wet etches used are described in Appendix C. The most commonly used are Pad Etch and Standard Oxide Etch (SOE- developed by Dr. Lecia Khor of Cirrus Logic). SOE is used to etch oxide while leaving aluminum and tungsten plugs intact. It is useful if the analyst needs to keep the metal vias or contacts in place during etching. As an example a patterning defect in the titanium pad where the tungsten plugs contact the source and drain caused the plugs to fall out when the surrounding oxide was etched away (see Figure. 4.21).

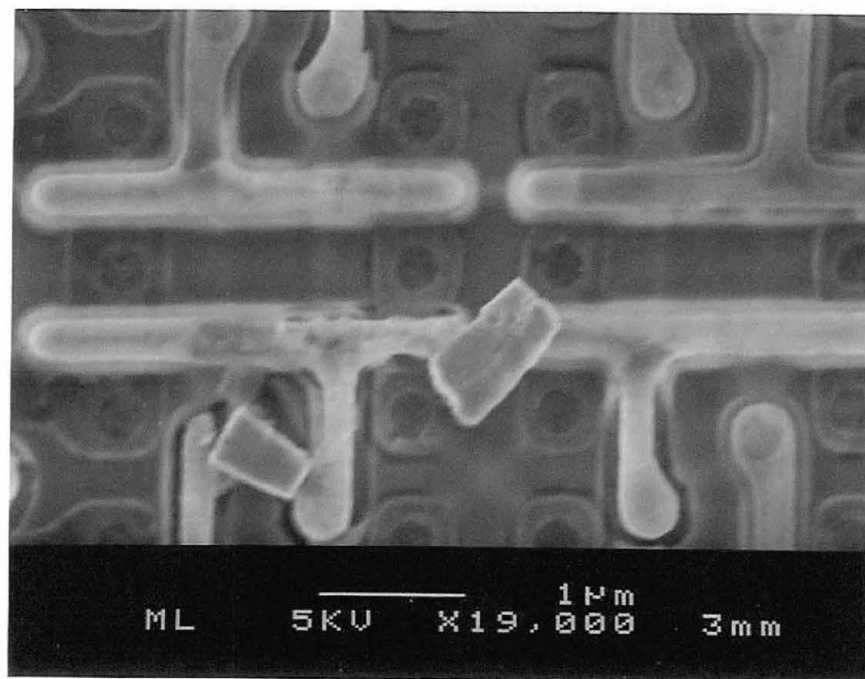


Figure 4.21 SEM image of physically floating contacts around poly gate structures.

Pad etch is used to etch around aluminum lines and tungsten plugs for SEM analysis in the metal 1 and metal 2 areas.

Dry etching is also used for top down deprocessing. In many areas it is the preferred method because of its anisotropic nature. In the FA environment this is particularly useful in deprocessing planarized technologies since they exhibit great variations in film thicknesses of the ILD layers. For this work however, dry etching was only used for depassivation as discussed in section 4.2.1.

4.3 CROSS-SECTIONING

Cross-sections of a device may be done when particle contaminants or metal bridging causing shorts between metal lines are suspected. These cross-sections are done using FIB techniques. By contrast, constructional analysis cross-sections for purposes of design rule compliance are done manually. The FIB techniques may or may not require follow up SEM imaging whereas constructional analysis cross-sections rely on subsequent SEM imaging to complete the task. We will discuss this one first.

4.3.1 MANUAL METHOD

For constructional and competitor parts analysis, the goal is to take measurements of the feature dimensions for comparison to design rules. Features to be measured include

<u>Feature</u>	<u>Width</u>	<u>Thickness</u>	<u>Pitch</u>	<u>Depth</u>
Metal stacks	X	X	X	
ILD's		X		
Contacts/vias	X	X		
Passivation		X		
Poly gates	X	X	X	
Sidewall spacers	X			
Doped areas				X

To get this information requires cutting and highly polishing the die and imaging it in the SEM.

The die is cut at a location that will yield the most information. This can be determined from the CAD layout of the device if available. Polishing begins by mounting the die to a heavy polishing block with wax. The block adjusts to insure that the polish remains parallel to the cut i.e. it cuts "in" the same distance from the edge across the die. The process requires polishing on the wheel for 2-4 minutes for each of several decreasing grit size diamond lapping films. These include:

600	grit silicon carbide paper
2400	grit silicon carbide paper
9	μm polishing film
6	μm polishing film
3	μm polishing film
1	μm polishing film
.5	μm polishing film
.1	μm polishing film

Water flow is continuous across the wheel for each run and rotating speeds may vary from 50-100 rpm depending on the quality of the polish desired, the slower the better. A final run on a polishing cloth for 5-10 minutes with water and a $.05\mu\text{m}$ non-crystallizing colloidal silica slurry completes the polishing process. The exposed face may then be viewed optically to check for major flaws.

The next step is a staining technique to delineate n-doped and p-doped areas in the substrate. It is actually an etching process which preferentially etches n-doped regions over p-doped regions. It is a two

step etch involving a first dip for 5-8 seconds in a 6:1 NH_4F : 49%HF followed by a second dip for 2 seconds in a 10:1:7 70% HNO_3 :49% HF: 99% glacial acetic acid. This cross-section is then complete and ready for SEM imaging. Figure 4.22 shows a sample of alternating n and p regions after staining.

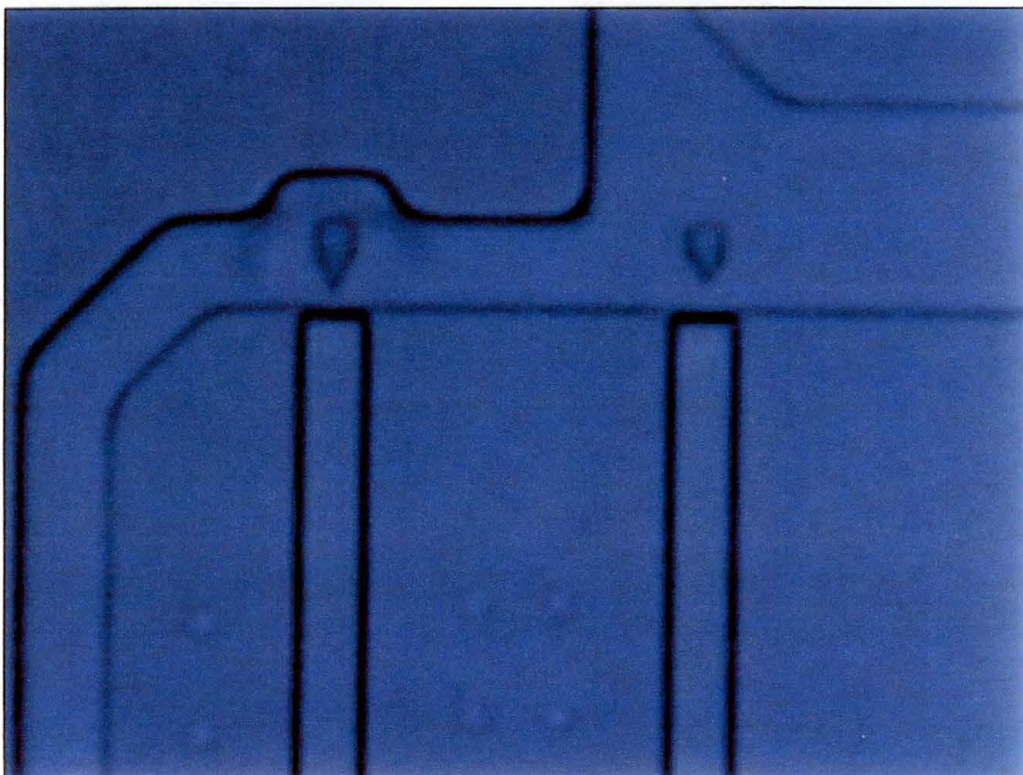


Figure 4.22 The darkly outlined areas are p-doped regions over which the gates were. The areas surrounding the contact imprints are p-doped. Optical image at 300X.

4.3.2 FIB METHOD

The use of the focused ion beam for cross-sectioning requires the analyst to know the precise area of the defect as well as having a CAD layout of the device for navigation purposes. The FIB has real-time imaging capabilities to permit high magnification of, and navigation to, the area of interest.

Sample preparation requires the die be removed from all packaging materials and be clean of particulate contaminants. Mounting involves adhering the die to the sample holder with silver paint to reduce charging effects from the GA^+ ion beam. Figures 4.23-4.25 show examples of FIB cross-sections.

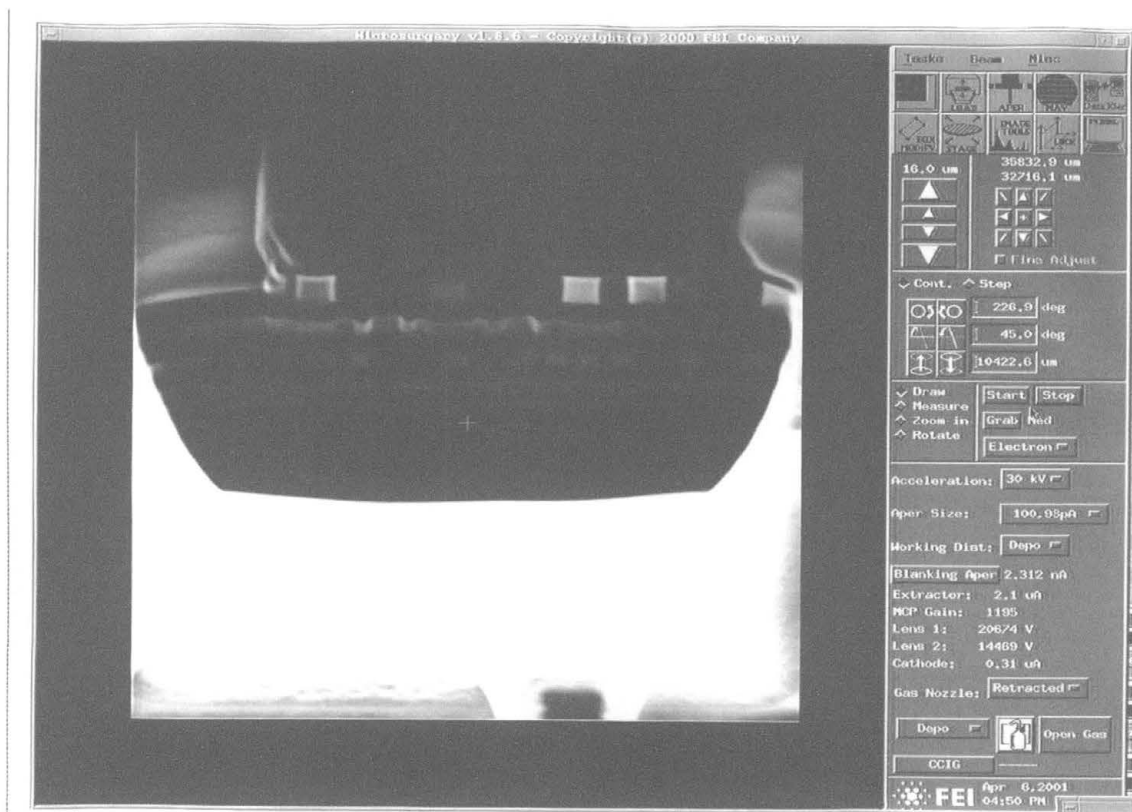


Figure 4.23 A FIB cross-section showing 4 metal layers.

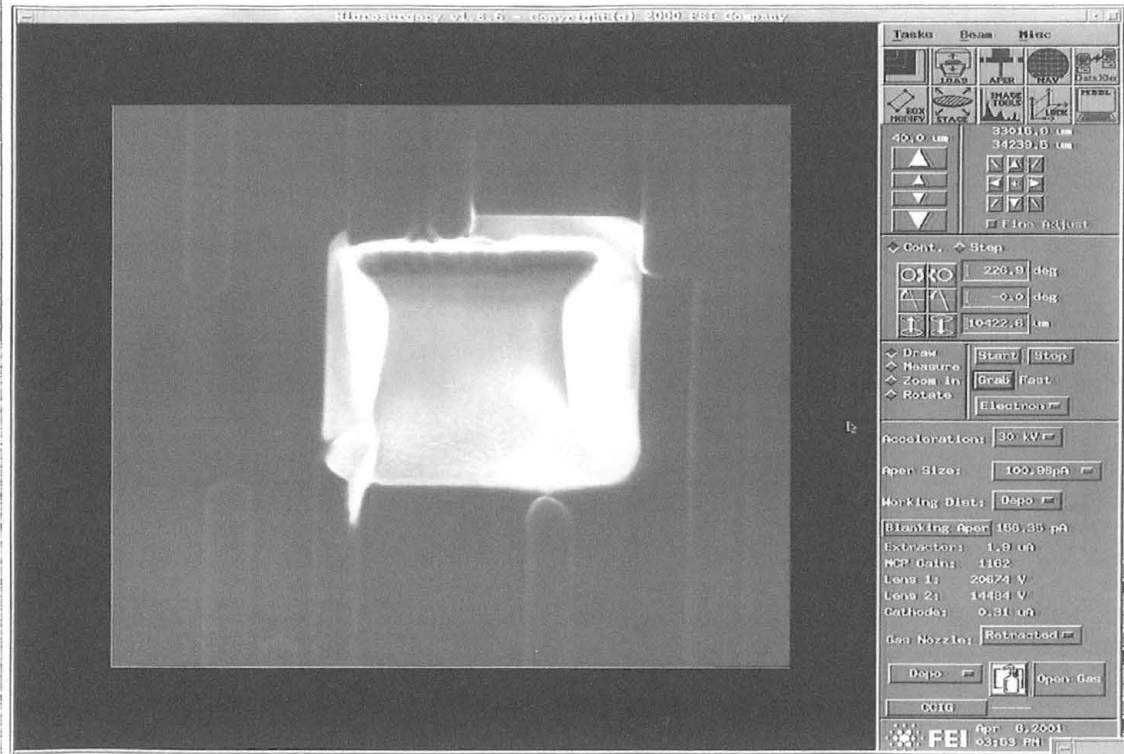


Figure 4.24 FIB top view of the above cross-section. The etch profile gets deeper from bottom to top.

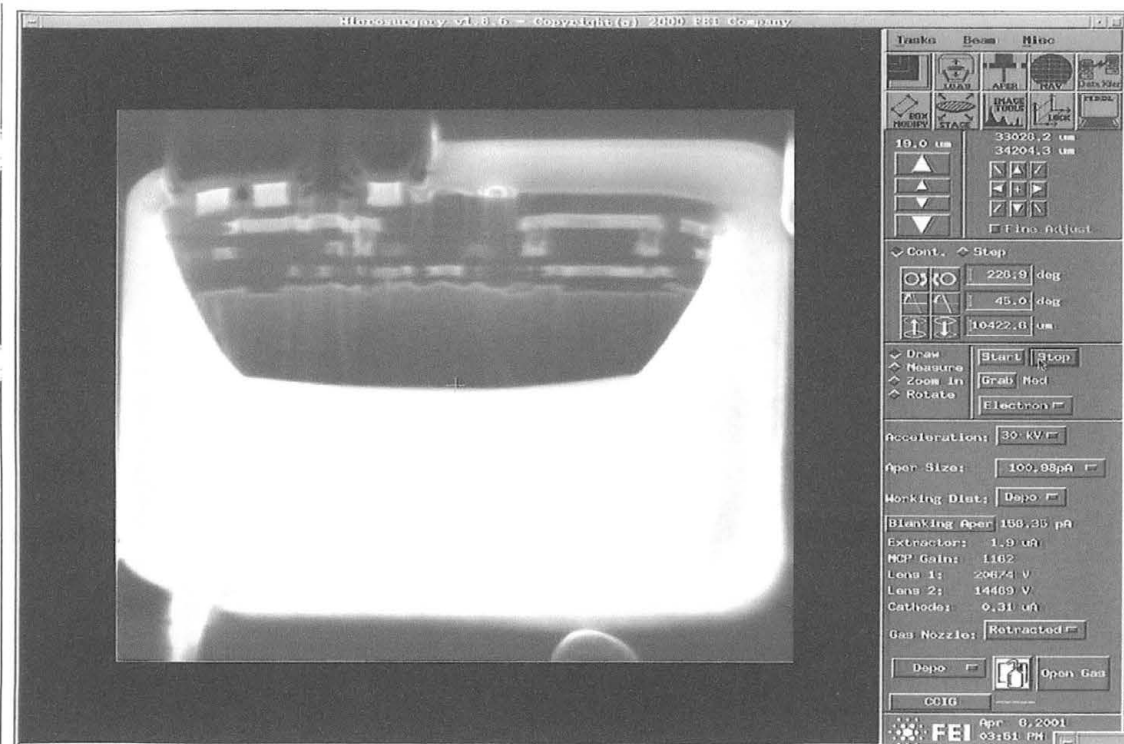


Figure 4.25 The same part cross-sectioned deeper. Notice the rounding of the metal 4 lines due to the continued milling while imaging.

Once the sample is loaded, imaging can begin. For single beam FIB's milling is actually taking place while generating the image hence caution is required to minimize milling on the area of interest while navigating and focusing. Imaging results as secondary electrons generated by ion bombardment of the surface are detected and converted to a signal. Therefore to generate an image, requires concurrent milling. Dual beam FIB's are freed of this nuisance by having a secondary electron beam to help with imaging tasks. Once focused on the area, a box is drawn on the screen to designate the area to be milled. The image is top down view. Initial cuts are $\sim 10\mu\text{m} \times 10\mu\text{m}$ with one edge of the box lined up close to the area of interest. A top and side on rendering of the milling profile is shown in Figure 4.26.

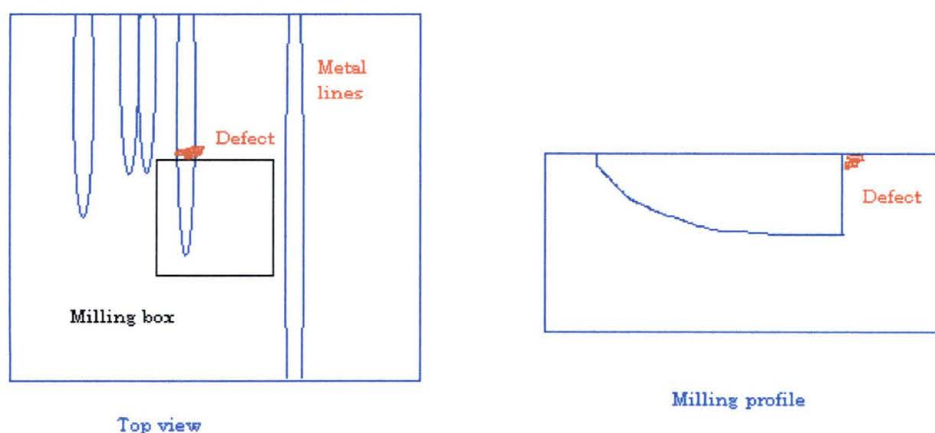


Figure 4.26 Top and side views of the milling box and profile

Following this cut the beam current is lowered for a finer cut and a new smaller milling box is drawn to mill in a little closer to the designated area. This sequence is repeated until the area is reached and/or the defect becomes visible. After each cut, however, it is necessary to tilt the sample to 45° to view the milled face. Focusing at this angle is problematic due to the depth of field issues just as with a SEM.

4.3 SEM IMAGING

Proficiency in using a SEM comes only with much practice and knowledge of the particular machine you are using. Numerous variables can be adjusted based on requirements of the shot. These include but are not limited to: accelerating voltage, probe current, magnification, imaging speed, and sample orientation (rotation and tilt).

Sample preparation is dependent on the type of material in the sample and what you need to see. Dielectrics or insulating materials are non-conducting therefore require grounding to prevent charging. This can be accomplished by either mounting the sample on a metal stub with silver paint or by coating the sample with a thin layer of a conducting material. The first method is used most often when doing top down imaging on an IC.

The second, coating the sample, is done often when SEM imaging FIB cross-sections. Samples are coated with gold, platinum or chrome to conduct electrons away from the imaging area. This work has relied on

the use of chrome exclusively due to its smaller grain size and cost effectiveness.

Included below are numerous SEM, FIB and optical images (Figures 4.27 to 4.38) I've taken. The SEM photos were all low kV applications (5kV) with various magnifications. The extractor current was fixed at 8.0 μ A and all shots were taken at a working distance of 3mm.



Figure 4.27 FIB cross-section image of a particle contaminant. The particle was in place prior to deposition of the passivation layers (top layer). It has impinged on the metal 1 and metal 2 layers resulting in a short.

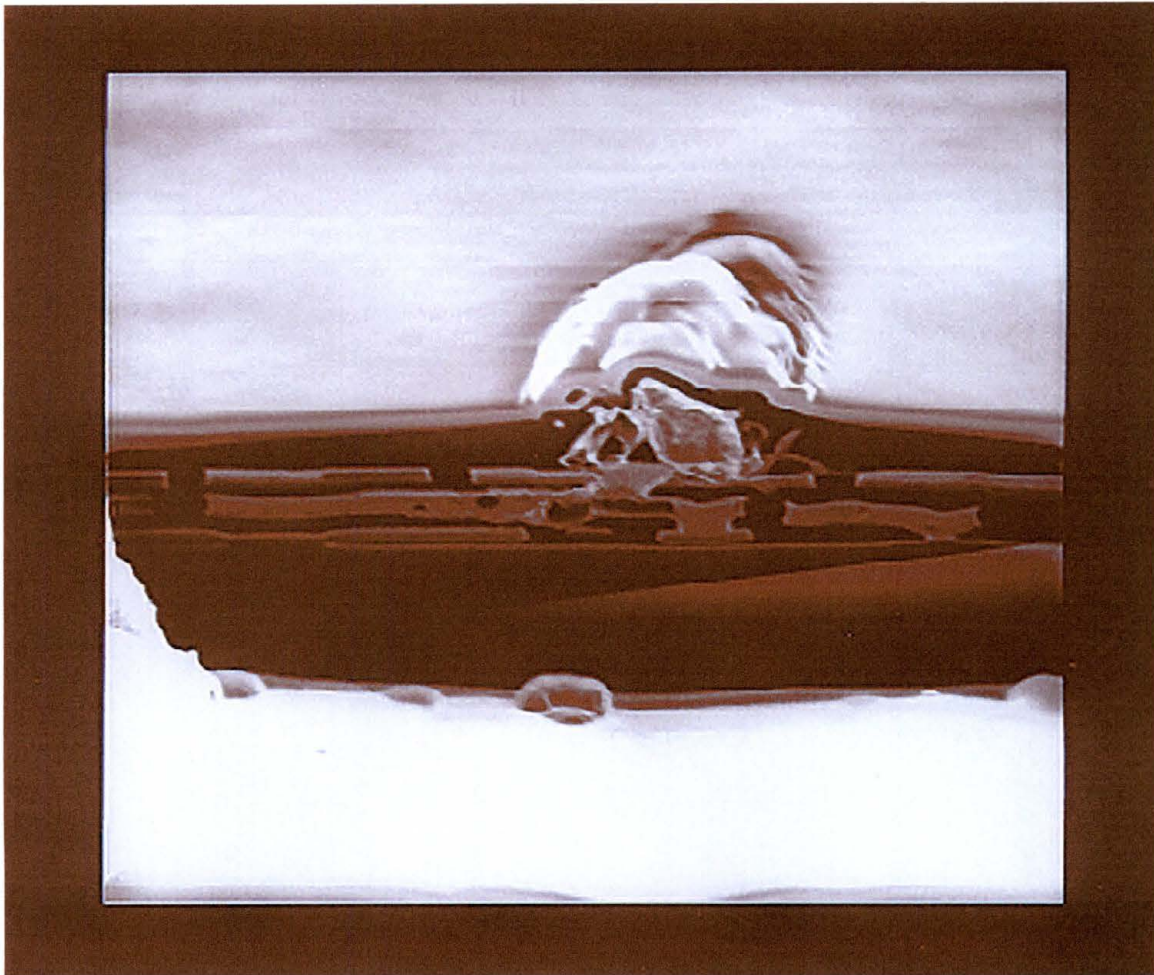


Figure 4.28 A further FIB cut into the contaminant. The particle appears to be a piece of metal, most likely tungsten based on the metal lines being aluminum and the contrast between the particle and the lines.

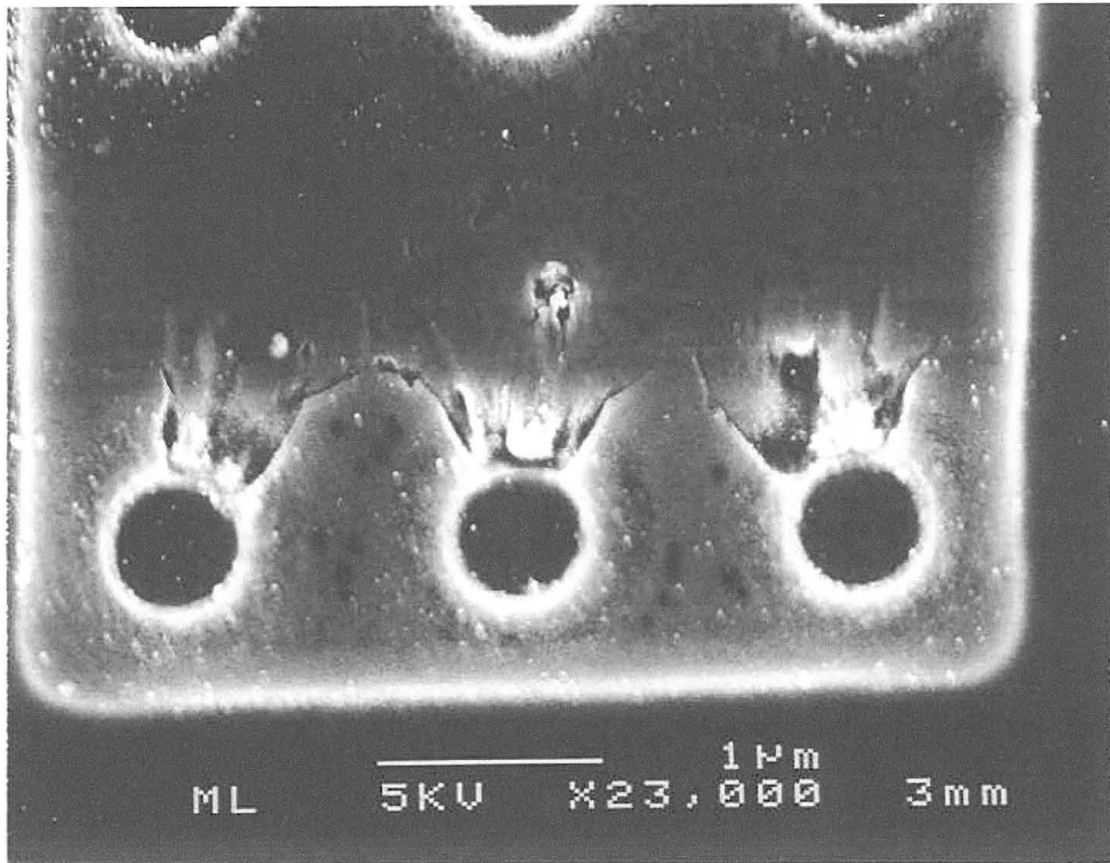


Figure 4.29 SEM image of substrate damage in the drain regions near the contact locations of an NMOS device. The delineated area running horizontally in the center is p-doped silicon over which the polysilicon gate existed. The damage was caused by a phenomenon known as bipolar snap-back; a low voltage, high current condition generating high temperatures which melt the silicon.

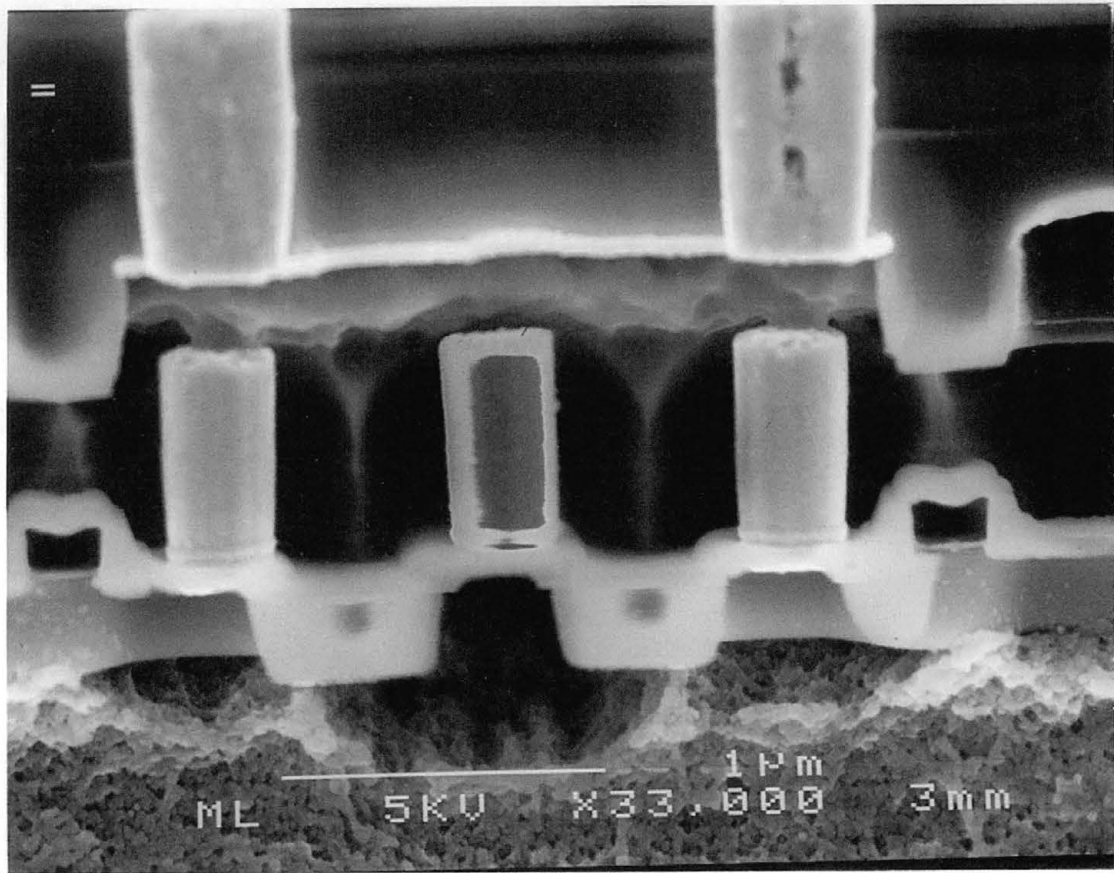


Figure 4.30 SEM image of over-etching which occurred during staining of a cross-section. for constructional analysis. The part was etched for 5 seconds in buffered oxide etch and 30 seconds in a 10:1:14 (HNO_3 :HF: CH_3COOH). Both the interlevel dielectric and the active silicon areas have been nearly all etched away.

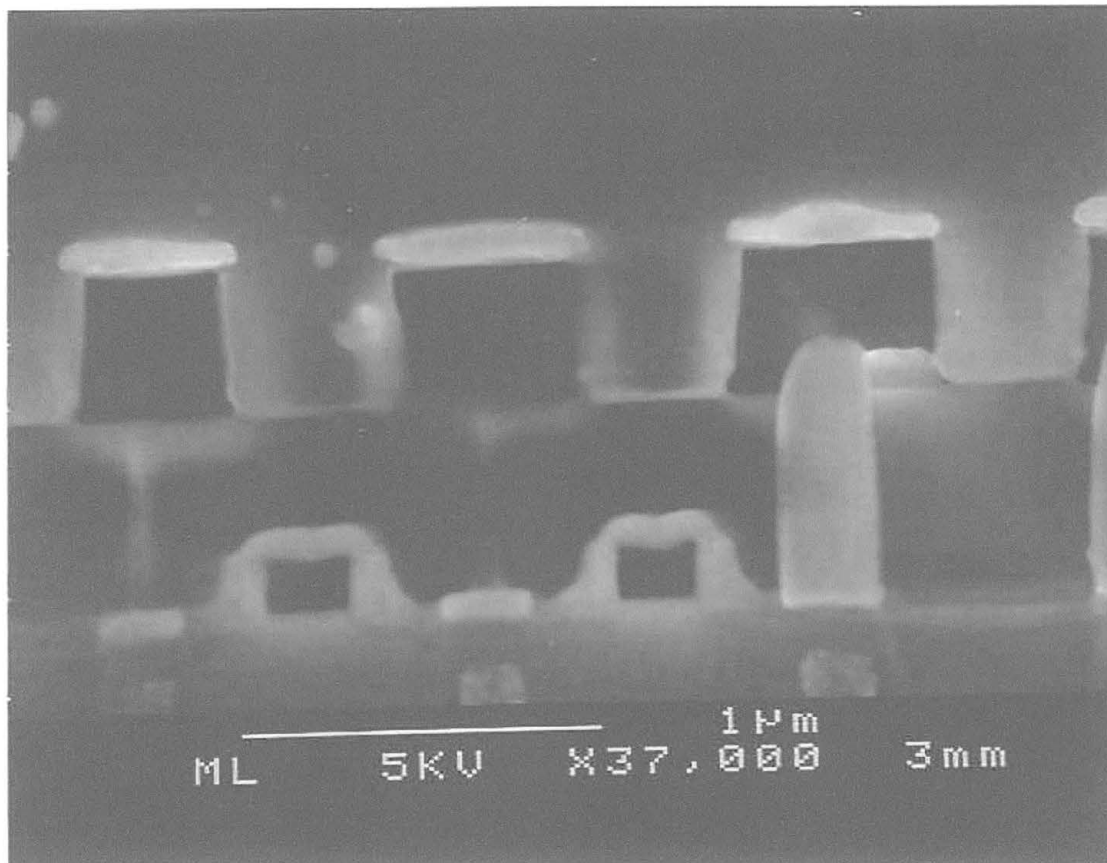


Figure 4.31 SEM image of a defective contact protruding up into the metal 1 line. The Ti/TiN cap over the metal lines can be clearly seen.

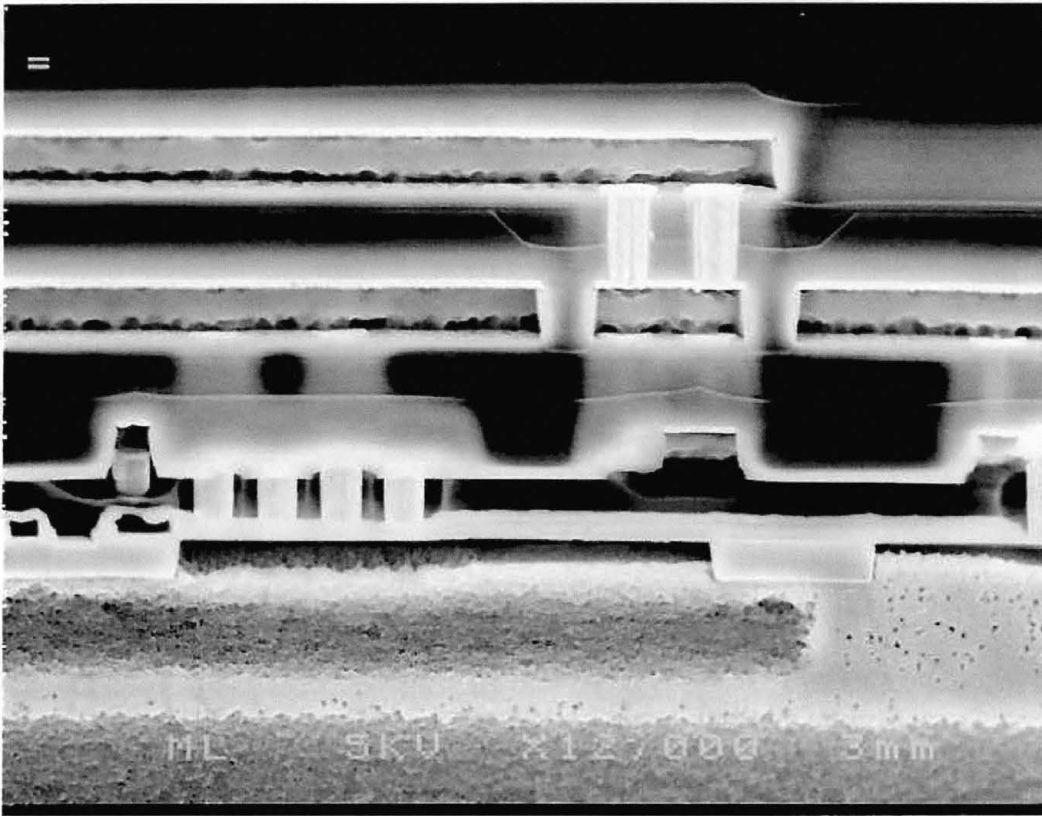


Figure 4.32 SEM image of a construction analysis cross-section of a 3 layer planarized metal device. The bottom shows clearly delineated n-wells on top of a grainy looking p-tub. These areas stain differently and the graininess is due to the chrome coating used for SEM prep. Shallow trench isolation oxide appears as square pads setting on the substrate.

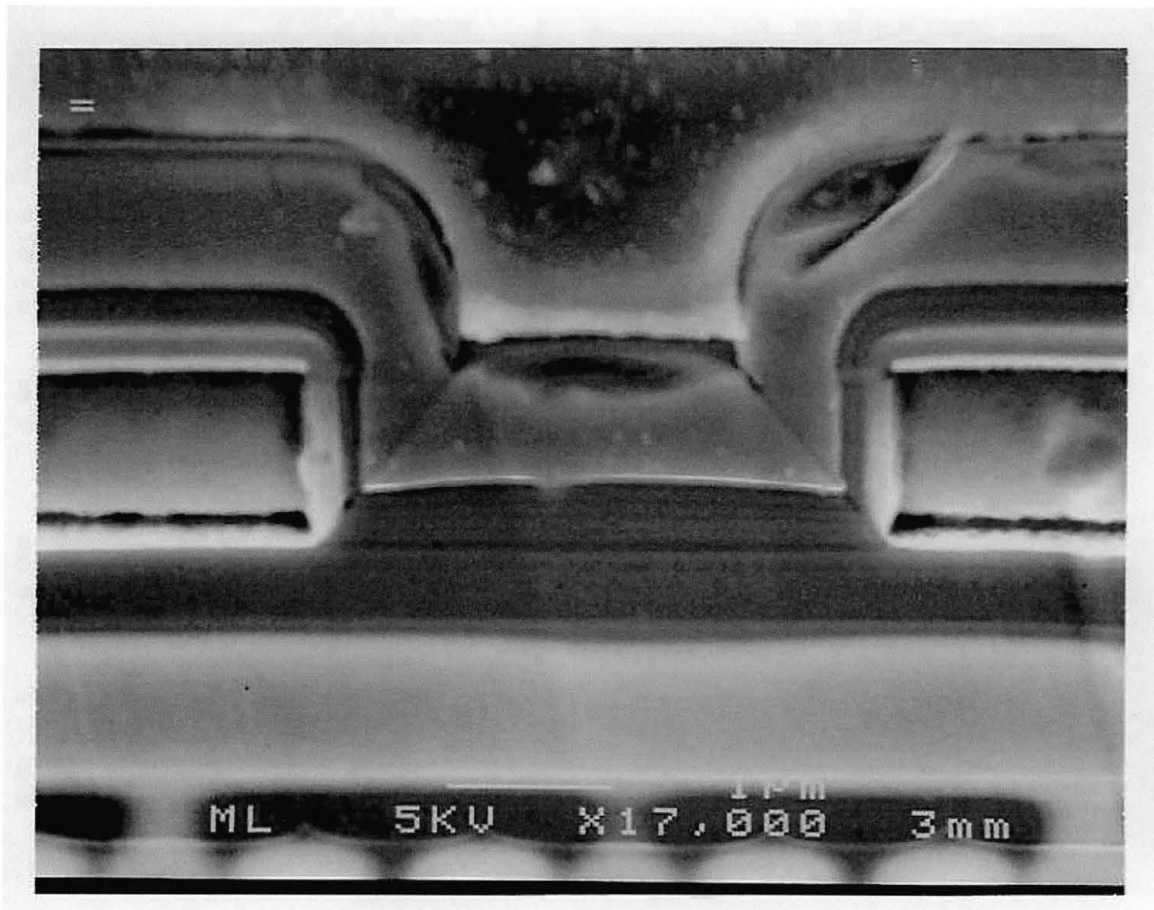


Figure 4.33 SEM image of the passivation layer over two metal 4 lines shows the conformal coverage of the CVD deposition.

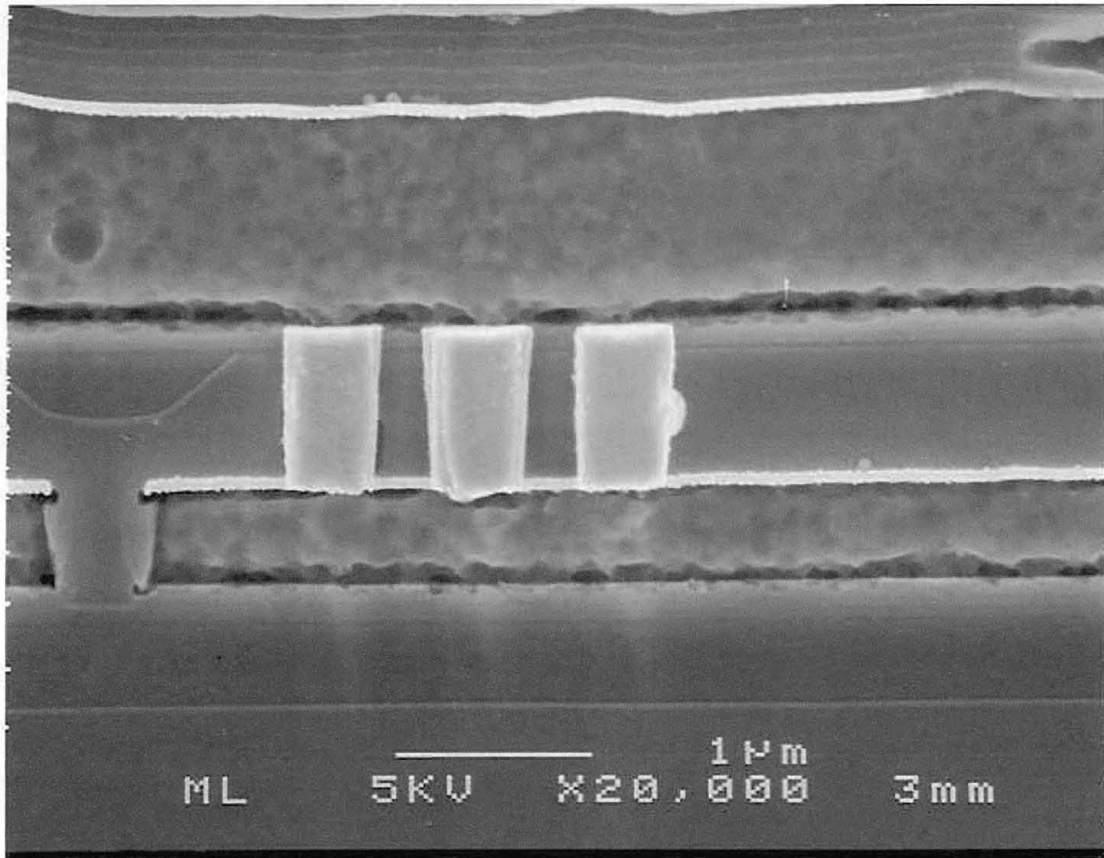


Figure 4.34 SEM image of metal 2 to metal 3 vias. The Ti underliner on the metal lines has been etched by the stain. The contrast between the Al metal lines and the W plugs is easy to see.

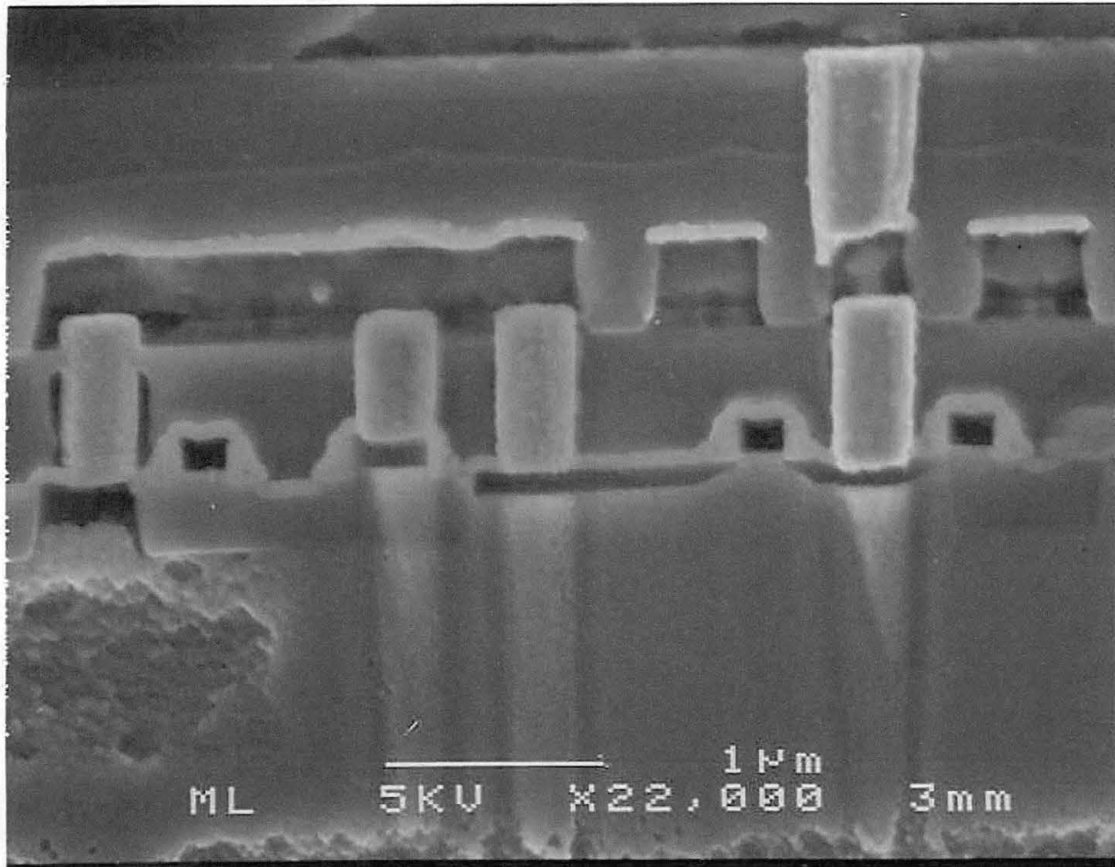


Figure 4.35 SEM image showing vertical streaks in the substrate; an artifact of polishing as tungsten is smeared in the direction of the polishing wheel rotation. Contacts to both active areas and poly (the short plug) can be seen and the lower left side shows a piece of a p-tub.

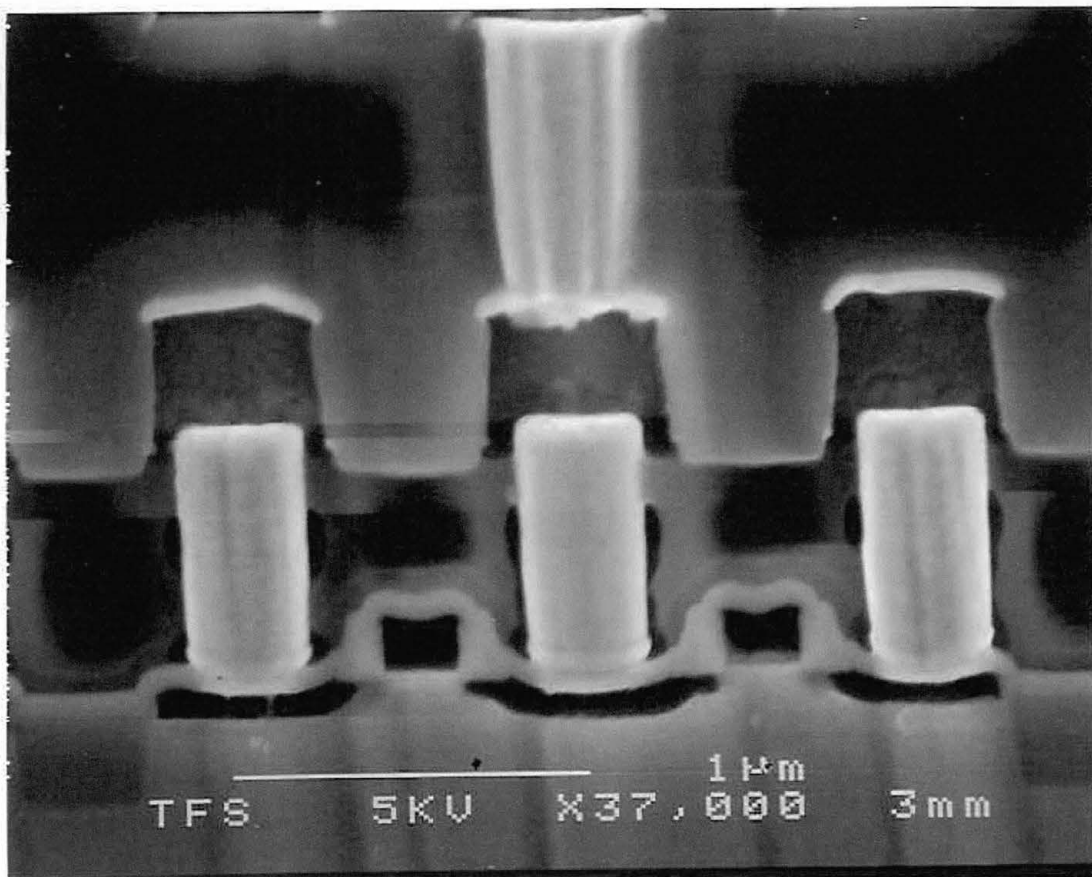


Figure 4.36 SEM image showing two transistors sharing a common drain. The gates are clearly delineated as are the nitride caps above them. The channel region under the gate is visible and the lightly doped drain (LDD) features appear as a curling up of the drain region ends. A set of stacked vias to the drain is shown as well.

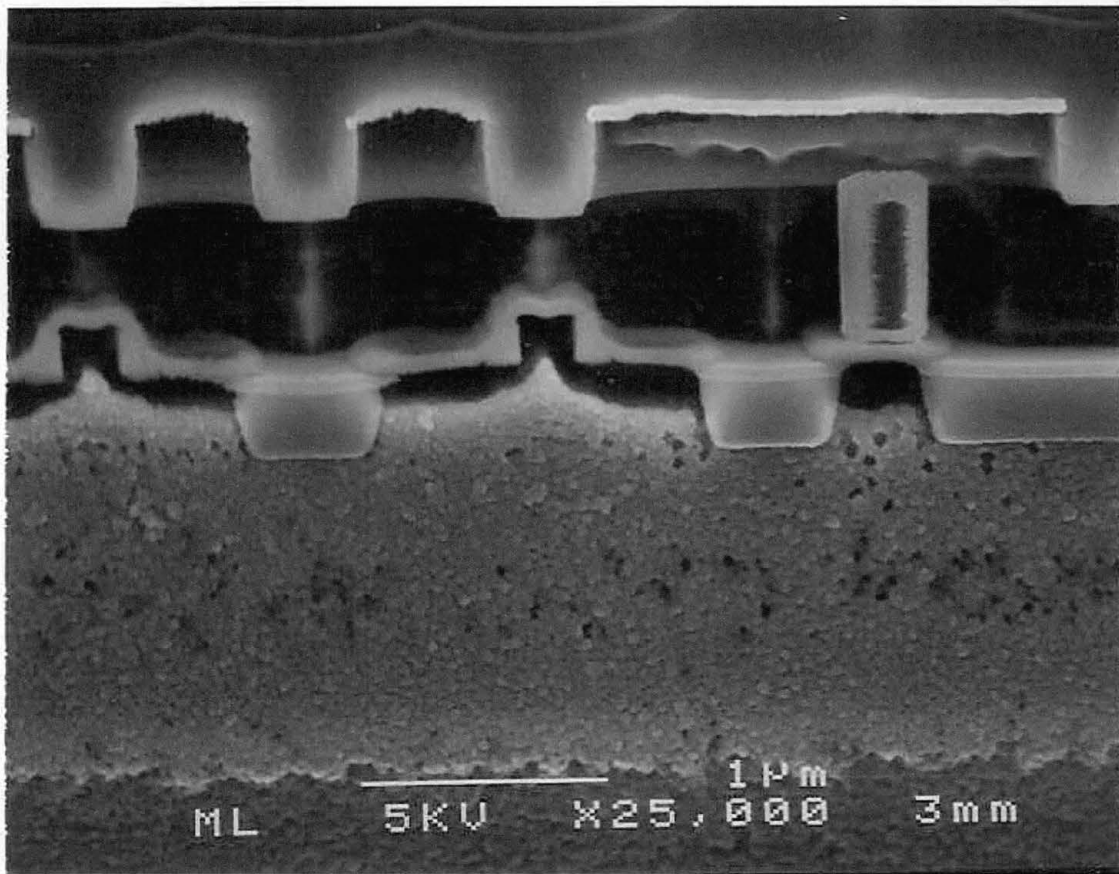


Figure 4.37 SEM image showing shallow trench isolation of a pair of transistors. Slight over-etching provides good depth perspective as the etchant is highly selective to the interlevel dielectric (ILD) used above the active areas. It is likely a doped oxide and different from the ILD above metal 1 as evidenced by the minimal etching of that layer. Near the very bottom is the epi-layer boundary between the p^+ and p^- substrate.

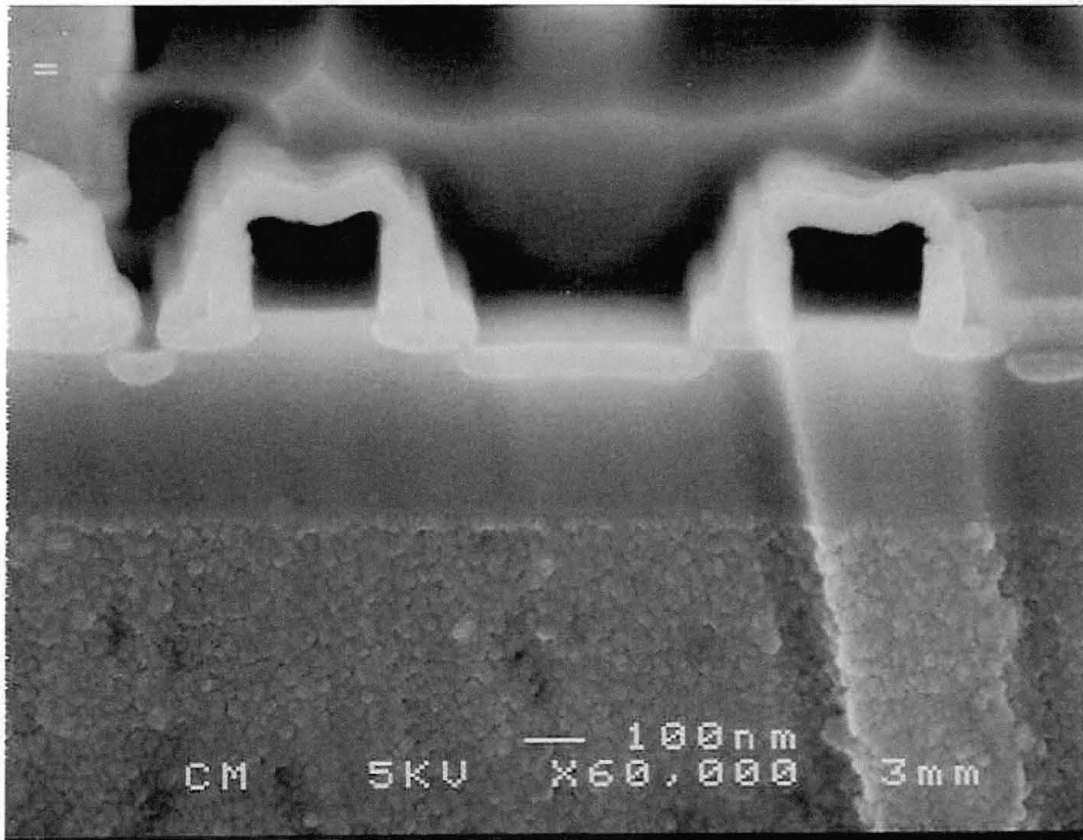


Figure 4.38 SEM image of etched area showing polysilicon lines (enclosed dark areas and the nitride caps). The nitride sidewall spacers used to mask the LDD areas during the deep drain implant are slightly visible. The poly structures are sitting on top of field oxide made using shallow trench isolation. Taken with the help of Chris Maldonado-Cirrus Logic.

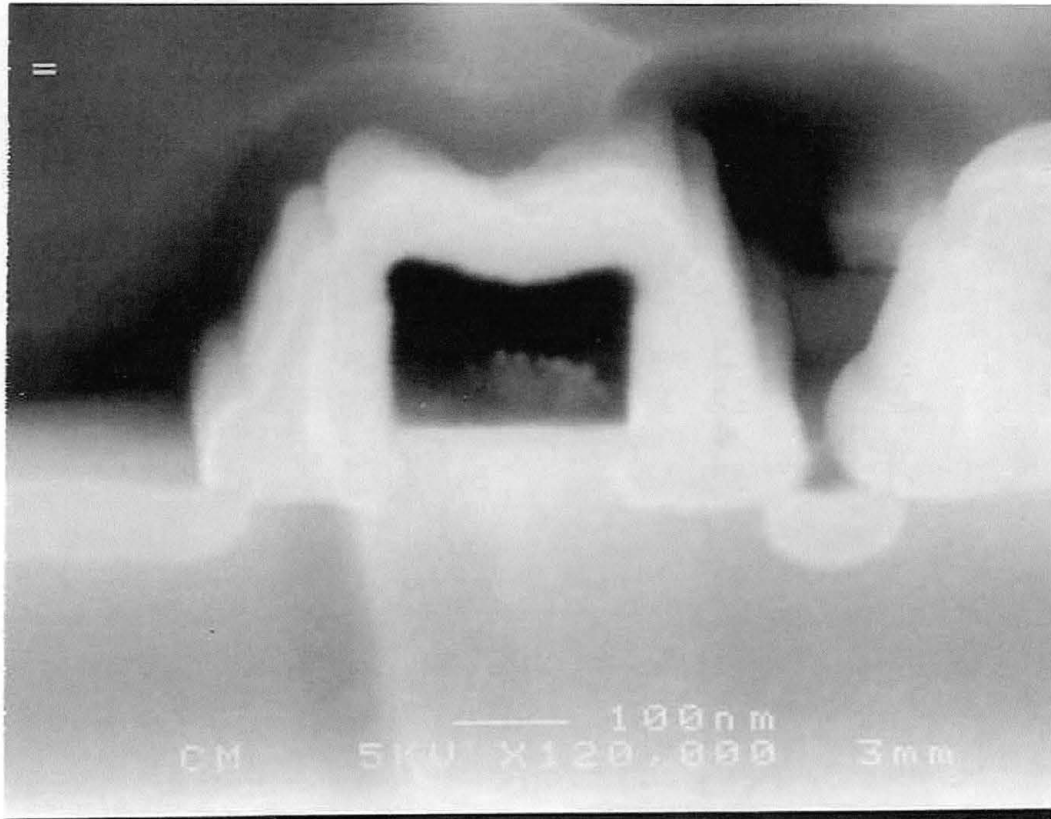


Figure 4.39 High magnification SEM image of the poly structure in figure 4.37 showing the sidewall spacers. Taken with the help of Chris Maldonado-Cirrus Logic.

CHAPTER 5

CONCLUSION

Etching processes are used repeatedly and in a variety of ways throughout the microelectronics industry. Fabrication steps rely on etching to selectively remove excess materials in the patterning of devices on a die surface while failure analysts use etching as a tool to 'reverse engineer' a failed part to determine the root cause of the failure. Both rely on combinations of chemical and physical etch processes to achieve good etch rates as well as uniform, selective and often anisotropic etch characteristics.

Specifically this work has examined the wet etching of silicon dioxide and silicon nitride blanket thin films and the results of various etch processes used in failure and constructional analysis of integrated circuits.

The wet etch research on the oxide and nitride films was designed to compare our etch rates to published data. Work on the nitride films showed favorable results for etch rates. While rates for the oxide films appear to be favorable as well, further work is required to be conclusive due to the combination of very high etch rates and film thickness limitations. Additional findings include post-clean surface contaminants

suggesting the need to establish a rigorous wafer cleaning protocol for the lab environment; evidence of masking artifacts on post-etch oxide surfaces confirming the importance of bath agitation and recirculation and; nitride etch rate variability associated with using hot phosphoric acid and the need for refluxing.

The failure and constructional analysis work was designed to provide details on the relevant wet and dry etch processes and chemistries used and to characterize the results of defect identification and constructional analysis work. Failure analysis is a critical function in the microelectronics industry as it provides a feedback mechanism for longer term device performance issues. For the engineer or analyst it provides exposure to many fab processes and forces an understanding of the individual steps as an integrative process. Constructional analysis is useful in production performance monitoring for adherence to specified design rules and in the analysis of competitor parts for assessing potential patent infringement.

Many etching protocols have been established for deprocessing, several of which were used in this work. While 'cookbook' recipes are available, their use is dictated by the specific job at hand. Determining the appropriate protocol is based on some idea about the suspected defect and what it will take to highlight it. Even then there may be a number of acceptable ways to deprocess the part and the one selected is

dependent on the skill level of the analyst, available equipment and time constraints.

Throughout the etching process there must be some means of monitoring effectiveness. This may include highly sophisticated methods such as endpoint detection and advanced film thickness measurement systems used in production environments or visual inspection via optical scopes and SEM's in FA labs. In any case the successful implementation of etch methodologies relies on good characterization methods and an effective feedback loop designed to insure maximum yields and expedient identification of failure modes.

APPENDIX A

Operating Procedures for the Nanospec AFT 210

This procedure describes the basic power-up procedures and the steps required for taking a measurement on an unpatterned wafer. For more comprehensive procedures please refer to the Operations Manual.

1. Turn the black box power “on”.
2. Turn the red lamp switch “on”.
3. Turn the computer and monitor on.
4. Let equipment warm up for ~30 minutes.
5. Select “no” to “Enable Datalink”
6. Make sure wavelength is set to 480nm on the spectrophotometer head at the prompt. If not press “no” and adjust accordingly.
7. Select “no” for “Refractive Index Option”.
8. Select “no” for “Enable Printer”.
9. Place the silicon reference film under the 5X objective and focus the light to a sharp octagon.
10. At the window prompt adjust the gain control to between 65.0 and 67.0.
11. Press enter to set the substrate reference.
12. At the Programs Available screen select the one appropriate to the film being measured.
13. Enter the 5X objective at the prompt.
14. Next set the film reference by placing the appropriate standard film under the objective, focusing and pressing “measure”. For example if you are measuring an oxide sample, use the oxide standard to reference here.
15. At the prompt enter the sample ID or name you wish to call it.
16. Place sample on the stage and focus as described above.
17. Press “measure”.

18. At the measurement result screen you may accept or reject the measurement. Reject if you know there is some error in the value. Rejection will not include that measurement in any statistical calculations.
19. Take as many measurements on the sample as required.
20. For multiple measurements requiring statistical analysis press “Display Stat” to view the mean and standard deviation.
21. To measure a new sample press “New Test”. Note that all previous measurement data is then excluded from the new statistical calculations.

APPENDIX B

Proposed Experimental Protocol

I. Wafer Preparation

A. Cut samples to approximately 15mm x 15mm and scribe the back of each with date, etch duration and type

B. Clean 5 samples as follows

- 1) Place the samples in fluoroware basket and place in beaker of 2% Micro and place on stirrer for 5 minutes at room temperature.
- 2) Remove from micro and rinse with 18 M Ω deionized water.
- 3) Rinse with 2-propanol.
- 4) Dry with N₂ gas.
- 5) Place samples in acetone sonic 5 minutes.
- 6) Remove from acetone and dip directly into beaker of 2-propanol.
- 7) Repeat propanol rinse again.
- 8) Repeat step 7 and dry with N₂ gas.

C. Nanospec sample sets to determine potential reactive chemistries between Micro and film material. Modify cleaning process accordingly.

D. Prepare for etching noting the following precautions:

- 1) Wear full face shield, safety glasses/goggles, acid gown and gloves.
- 2) Make sure hood exhaust blower is on and have eyewash and chemical spill items available.
- 3) Post appropriate safety signs (for HF or H₃PO₄).
- 4) Conduct HF work in the presence of other qualified personnel.

II. Silicon Dioxide Etch

A. Measure ~300 ml of 10:1 buffered oxide etch in a Teflon or Nalgene graduated cylinder and pour into a Teflon or Nalgene beaker.

- B. Place beaker into water bath maintained at 25° C until etchant temperature stabilizes.
- C. Place the first sample into fluoroware basket then into the etchant for 1 minute.
- D. Remove and quench with 18 MΩ deionized water for 1 minute.
- E. Rinse with 18 MΩ deionized water.
- F. Dry with N₂ gas.
- G. Place in plastic storage box and put in dessicator.
- H. Repeat steps A through E for the 2, 3, 4 and 5 minute etches using the same etching solution but replacing quenching bath each time.
- I. Place used etchant and water quenches in HF approved waste container and record appropriately.
- J. Characterize as soon as possible to determine etch rate.

III. Silicon Nitride Etch

- A. Measure ~150 ml of 85% phosphoric acid into a clean (overnight nitric acid soak/dei water rinse) 600ml Pyrex beaker.
- B. Place in DC 704 oil bath (pre-heated to 153 C on hot plate) until solution temperature stabilizes.
- C. Place the first sample into fluoroware basket then into the etchant for two minutes.
- D. Remove and quench with 18 MΩ deionized water for 1 minute.
- E. Rinse with 18 MΩ deionized water.
- F. Dip in beaker of 2-propanol.
- G. Dry with N₂ gas.
- H. Place in plastic storage box and put in dessicator.
- I. Repeat steps A through E for the 4 and 6, minute etches using the same etching solution but replacing quenching bath each time.
- J. Repeat steps A through E for an 8 minute etch using the fresh etching solution and quenching bath.
- K. Repeat steps A through E for a 10 minute etch using the fresh etching solution and quenching bath.
- L. Modify etch bath refresh protocol as needed.

- M. Place used etchant and water quenches in approved waste container and record appropriately.
- N. Characterize as soon as possible

APPENDIX C

Wet Etch Recipes For Failure Analysis¹³

Plastic Etchants

Etchant	Composition & Prep	Usage
Nitric acid (HNO ₃)	Clear (68-70% HNO ₃)	Etches plastic and exposed metalization very fast and is not recommended for plastic decap. Used mainly to make 10:1:7 etch and other etchants requiring HNO ₃ .
	Yellow fuming (80-92% HNO ₃)	Attacks plastic very fast, especially if heated (~80°C). Used to remove plastic packaging and to decap plastic parts.
	Red fuming (98% HNO ₃)	Similar to yellow fuming, but not used in the lab for safety reasons.
Buffered Nitric	1 part fuming H ₂ SO ₄ 3 parts fuming red nitric.	Typically used for plastic devices with copper lead frames. Etches plastic and exposed metalization very fast. Mix before each use.
Sulfuric acid (H ₂ SO ₄)	Dilute (10% H ₂ SO ₄)	Attacks plastic and metalization very fast and not recommended for decap.
	Fuming (85-98%)	Similar to dilute H ₂ SO ₄ .

Metal Etchants

Etchant	Composition & Prep	Usage
Metal etch (or Aluminum etch)	16 parts H ₃ PO ₄ 1 part HNO ₃ 1 part acetic acid 2 parts deionized water	Etches aluminum moderately slow at room temperature with very slow undercutting. Metal layers are removed by heating device to 80°C and etching for ~2 minutes.
Hydrogen peroxide (H ₂ O ₂)	30% H ₂ O ₂	Etches TiW moderately fast at room temperature. Used to remove barrier metal (TiW). Heat to 70–80°C to increase etch rate.
Hydrochloric acid (HCl)	38% HCl	Etches aluminum very fast with lots of undercutting. Heat at 70°C for 10-30 seconds.
Aqua regia	3-4 parts HCl (38%) 1 part HNO ₃ (90%)	Etches gold, aluminum and platinum fast. Mix before each use. Used to remove gold bonds (1–5 minutes).
Phosphoric acid (H ₃ PO ₄)	85% (H ₃ PO ₄)	Etches aluminum moderately slow at room temperature. Used for double level metal since undercutting action is slow.

Oxide and Passivation Etchants

Etchant	Composition & Prep	Usage
Standard oxide etch (SOE)	75 mL 1M NH_4F 205 mL DI H_2O 250 mL glacial acetic acid	Etches oxides slowly with minimum damage to metal (provided metal has not been exposed) and W plugs. It is mainly used to keep the W plugs intact. Etch for 3 minute intervals.
Doped oxide etch (DOE)		Etches doped oxides moderately fast and, when used in conjunction with Pad etch, it can speed up the removal of ILD. It seems to etch polysilicide slowly. Typically, 4 minute intervals are used.
Buffered oxide etch (BOE) 6 parts NH_4F 1 part HF (49%)	A mixture of NH_4F and HF in various ratios. The etch rate is dependent on the ratio: 5:1 ~ 1200Å /min 10:1 ~ 550 Å/min	Etches oxides moderately fast. Commonly used to remove oxide without damaging metal. It also strips passivation and delineates titanium nitride. It will attack metal and lift poly if overexposed. Etch for 40 seconds then inspect. Repeat until all oxide is removed.
Hydrofluoric acid (HF)	49% HF	Etches oxide and poly very fast. Typically used to strip device to substrate. Also used to make other etchants.
	10% (1 part HF, 49% and 10 parts DI water)	Etches oxides moderately fast. Etches doped and deposited oxides faster than undoped and thermal oxides.
Pad etch w/surfactant	33% glacial acetic acid 13.5% NH_4F -from Ashland Chemical	Etches oxides and stressed areas moderately fast with minimal damage to Al and poly. It characteristically etches around the metal to reveal the side walls. It etches marginally slower than BOE, but it is ideal for removing oxide over M2 and M1 for SEM inspection.
Potassium hydroxide (KOH)	45% KOH	Delineates pinholes in passivation. Used as a passivation integrity test. Device is immersed for 20 minutes and then examined.

Silicon Stains and Etchants

Etchant	Composition & Prep	Usage
Standard 10:1 (or 10:1:7)	10 parts (70% HNO ₃) 1 part HF (49%) 7 parts glacial acetic acid (99%)	Used to stain cross sections (2-5 seconds). Etches N type moderately fast and P type moderately slow. Undoped Si and oxides etch very slowly. Mix fresh. ***** This etch can also be used to stain top-down. First, coat the back of the chip with Au (1 minute in the Anatech), the n etch for 50s in 10:1:7. This procedure has been used to stain N wells.
Buffered 10:1	10 parts (70% HNO ₃) 1 part HF (49%) 14 parts glacial acetic acid (99%)	Similar to Standard 10:1, but slower etch rates (5-10 sec).
Dilute poly etch	20 parts acetic acid (99%) 1 part HF (49%) 8 parts HNO ₃ (90%)	Etches polysilicon moderately fast and oxides very slowly. All oxide must be removed prior to use. Mix fresh as it weakens within 15 minutes.
White etch	4 parts HNO ₃ (70%) 1 part HF (49%)	Basic recipe for Si etch formulations. Si removal rate is nonlinear with time as the solution warms. It is extremely corrosive and dangerous. Reaction with Si is exothermic and effervescent with the release of red fumes (NO ₂).

APPENDIX D

CHEMICAL SAFETY CONSIDERATIONS

Etching processes rely on the use of chemicals on a regular basis. Some are relatively safe to use while others may be toxic, highly volatile and even explosive. Care should be taken whenever handling chemicals and one should be aware of the properties of the chemicals they are using. Materials Safety Data Sheets (MSDS) sheets are available for all chemicals through the vendor and provide several important pieces of information including toxicity, health hazards, explosion hazards, reactivity data and physical/chemical characteristics. They also provide information on treatment protocols for various exposure types. In a lab or fab environment you will encounter different classes of chemicals including:

- Acids and other corrosives
- Solvents
- Oxidizing agents
- Inert gases

Be sure to wear the proper protective gear as called for with any particular chemical. This can be found on the MSDS sheets and may include the use of:

- Chemical resistant gloves
- Protective eyewear
- Full face shield

- Respirator
- Chemical resistant gown

A commonly used acid for etching is hydrofluoric acid (HF) which must be handled extremely carefully. It is very dangerous since skin contact may not be realized for several hours. It DOES NOT burn when you touch it. However skin exposure of greater than two square inches can be lethal. It is imperative that all personnel be properly trained in the use and handling of HF and the appropriate response in case of accidental exposure. For minimal contact, calcium gluconate gel should be applied immediately and medical help sought immediately.

Greater exposures should be handled in accordance with specific guidelines of the company's safety program, which at a minimum should include an HF safety protocol. Efforts to coordinate these programs with local emergency response agencies may be required.

Certain other chemicals are also particularly onerous such as chlorine, silane and arsine, though since they are gases, they are much more highly controlled at the source and less likely to result in accidental exposure.

BIBLIOGRAPHY

- ¹ Chang, C. Y., and S. M. Sze, eds. ULSI Technology. New York: McGraw-Hill, 1996.
- ² Barrett, Craig R., From Sand to Silicon: Manufacturing and Integrated Circuit. Scientific American, Special Issue, January 1998.
- ³ Jaeger, Richard C., eds. Introduction to Microelectronic Fabrication. Reading, MA: Addison-Wesley, 1993.
- ⁴ Campbell, Stephen. The Science and Engineering of Microelectronic Fabrication. New York: Oxford University Press, 1996.
- ⁵ Atkins, Peter. Physical Chemistry 5th ed. New York: Oxford University Press., 1994.
- ⁶ Whitten, Kenneth W., Kenneth D. Gailey, and Raymond E. Davis. General Chemistry. Fort Worth: Saunders College Publishing, 1992.
- ⁷ Ohring, Milton. The Materials Science of Thin Films. San Diego: Academic Press, 1992.
- ⁸ Quirk, Michael, and Julian Serda. Semiconductor Manufacturing Technology. New Jersey: Prentice-Hall, 2001.
- ⁹ Micrion Corporation. Micrion 2100 Focused Ion Beam System Operator's Reference Manual. Peabody MA: Micrion Corporation, 1995.
- ¹⁰ Clark, Scott. Chemical Etching of Silicon Nitride with Hot Phosphoric Acid. Bold Technologies. <http://www.boldtech1.com>.
- ¹¹ Clark, Scott. Etching Silicon Dioxide with Aqueous HF Solutions. Bold Technologies. <http://www.boldtech1.com>.
- ¹² Beck, Friedrich, Stephen S. Wilson, translator. Integrated Circuit Failure Analysis. New York, John Wiley and Sons, 1998.
- ¹³ Cirrus Logic Corporation. Failure Analysis Lab Manual. Austin: Cirrus Logic Inc, 1999.

¹⁴ About Thin Film. Filmetrics, Inc., San Diego: <http://www.filmetrics.com>.

¹⁵ Nanometrics Incorporated. *Nanometrics AFT210 Operations Manual*. Milpitas, CA

VITA

Matthew L. Langendorf was born February 28, 1957 in St. Louis, Missouri, to Lewis and Virginia Langendorf. In 1975 he enrolled at St. Louis Community College and in 1981 he earned his B.S.B.A. concentrating in accounting from the University of Missouri-St. Louis. Moving to Austin, Texas in 1982 he spent fifteen years working in finance and administration positions with the Capital Metropolitan Transportation Authority. In 1997 he enrolled in the Graduate School of Southwest Texas State University, San Marcos, Texas. He contributed on an article in 1998 entitled *Spectroscopic Observation of Isomerization Kinetics in Isotopically Labeled (Benzene)₁₃*, *Journal of Physical Chemistry A*, 102(49), 10032-10040, Easter et al.,. He is currently a device physics engineer with Cirrus Logic Inc. in Austin, Texas.

Permanent Address: 9002 Queenswood Dr.
Austin, Texas 78748

This thesis was typed by Matthew L. Langendorf, Stasi Gaveras and Carolynne Knox.